(12) INTERNATIONAL APPLICATION PUBLISHED UNDER THE PATENT COOPERATION TREATY (PCT)

(19) World Intellectual Property Organization
International Bureau

(43) International Publication Date
30 August 2018 (30.08.2018)

WIPO | PCT

(10) International Publication Number
WO 2018/153226 A1

(51) International Patent Classification:
E21B 1/00 (2006.01)

(21) International Application Number:
PCT/CN2018/074644

(22) International Filing Date:
31 January 2018 (31.01.2018)

(25) Filing Language: English

(26) Publication Language: English

(30) Priority Data:
62/462,795 23 February 2017 (23.02.2017) US

(71) Applicant: **THE HONGKONG POLYTECHNIC UNIVERSITY** [CN/CN]; Hung Hom, Kowloon, Hongkong (CN).

(72) Inventor: **JING, Xingjian**; c/o THE HONGKONG POLYTECHNIC UNIVERSITY, Hung Hom, Kowloon, Hong Kong (CN).

(74) Agent: **SHANGHAI DANRONG & ZONGDE INTELLECTUAL PROPERTY AGENCY CO., LTD.**; YU, Danrong, Room 1708-1709, 2nd Building, NO. 335 Guoding Road, Yangpu District, Shanghai 200433 (CN).

(81) Designated States *(unless otherwise indicated, for every kind of national protection available)*: AE, AG, AL, AM, AO, AT, AU, AZ, BA, BB, BG, BH, BN, BR, BW, BY, BZ, CA, CH, CL, CN, CO, CR, CU, CZ, DE, DJ, DK, DM, DO, DZ, EC, EE, EG, ES, FI, GB, GD, GE, GH, GM, GT, HN, HR, HU, ID, IL, IN, IR, IS, JO, JP, KE, KG, KH, KN, KP, KR, KW, KZ, LA, LC, LK, LR, LS, LU, LY, MA, MD, ME, MG, MK, MN, MW, MX, MY, MZ, NA, NG, NI, NO, NZ, OM, PA, PE, PG, PH, PL, PT, QA, RO, RS, RU, RW, SA,

WO 2018/153226 A1

(54) Title: IMPROVED PASSIVE VIBRATION REDUCING APPARATUS

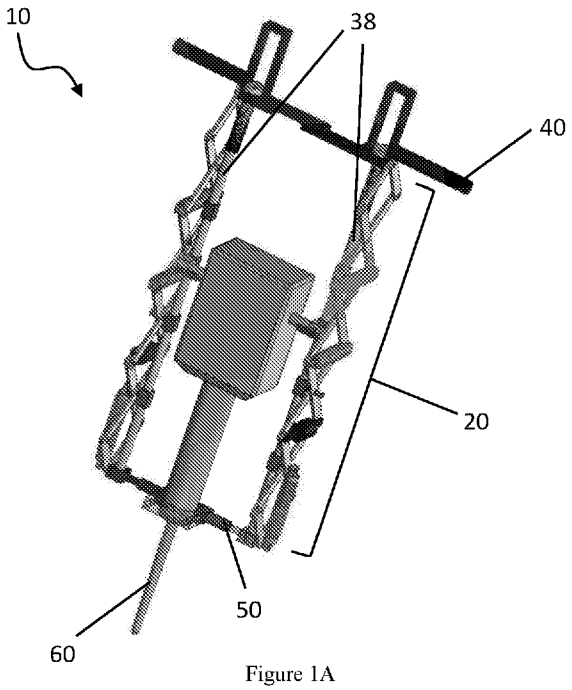

Figure 1A

(57) Abstract: There is provided a vibration reducing apparatus (10) for a percussive tool (60) having an axis of reciprocation. The apparatus comprises, a guide frame (38,38a,38b) and at least one member (50) extending across the axis of reciprocation. An assembly (20) extending in a direction of along the axis of reciprocation comprises at least two layers (26,28,30,32) and each layer comprises four interconnected elongate members (27a,27b,29a,29b,31a,31b) pivotally attached and rotatable with respect to each other to define a polygon; and the assembly has at least one biasing means (24a,24b). A handle (40) is movably coupled to the guide frame and supported on the assembly. The apparatus provides decreasing stiffness with increasing compression of the assembly under an operator applied load to the handle for reducing vibration in a predetermined frequency range.

[Continued on next page]

SC, SD, SE, SG, SK, SL, SM, ST, SV, SY, TH, TJ, TM, TN, TR, TT, TZ, UA, UG, US, UZ, VC, VN, ZA, ZM, ZW.

(84) Designated States *(unless otherwise indicated, for every kind of regional protection available)*: ARIPO (BW, GH, GM, KE, LR, LS, MW, MZ, NA, RW, SD, SL, ST, SZ, TZ, UG, ZM, ZW), Eurasian (AM, AZ, BY, KG, KZ, RU, TJ, TM), European (AL, AT, BE, BG, CH, CY, CZ, DE, DK, EE, ES, FI, FR, GB, GR, HR, HU, IE, IS, IT, LT, LU, LV, MC, MK, MT, NL, NO, PL, PT, RO, RS, SE, SI, SK, SM, TR), OAPI (BF, BJ, CF, CG, CI, CM, GA, GN, GQ, GW, KM, ML, MR, NE, SN, TD, TG).

Declarations under Rule 4.17:

— *as to the identity of the inventor (Rule 4.17(i))*

Published:

— *with international search report (Art. 21(3))*

IMPROVED PASSIVE VIBRATION REDUCING APPARATUS

FIELD

The present disclosure relates to an improved passive vibration reducing apparatus and system, particularly suited to suppressing vibration emitted by a reciprocating tool.

BACKGROUND

Vibration is a type of oscillation characterised by small, limited oscillations in a system in a near balanced state. In most aspects of engineering, because mechanical vibration affects mechanical properties, aggravates fatigue and wear, and can even cause the destruction of structures, such vibration is regarded as a negative factor which needs to be controlled.

Vibration transmitted to construction workers from the operation of various powered tools such as rammers, rock drills, demolition hammers, road breakers, hammer drills, chipping hammers or saws is an area where vibration has a significant health impact directly on the operators of the powered tools. It is known in the art that the vibration frequency range that humans perceive is from 1 to 1000Hz, with humans most sensitive to vibration of 1-80Hz. In particular, the most harmful vibration is in the frequency range between 6 Hz and 20 Hz. When construction workers firmly grasp the handles of powered tools for increased control and efficiency of such devices, local vibration is transmitted to the hands and arms of the user, as well throughout their body.

Local vibration can result in finger arterial contraction and reduction in grasping ability, with prolonged exposure to high levels of vibration by operating hand-held machines causing issues with normal circulation as well to nervous and musculoskeletal systems. A long period of high level vibration can serious damage to the human body, cause considerable pain and even result in permanent disability with frequency and intensity of vibration key contributing factors. This leads to a practical limit as to how long an operator can safely operate the equipment, which in turn has implications for the resources required to be allocated to specific tasks.

Vibration also affects the operation of large scale (often vehicle mounted) systems such as rock breakers. As is known by persons skilled in the art, the driving pistons of such machines are fired by nitrogen gas, hydraulic oil or a combination to strike the working tool which does the shattering, cracking or splitting of the material at the work site. Excessive vibration potentially impacts the operational life of components in such systems, and can lead to break down and decreased performance.

Typical traditional dampers have the same damping coefficient for all frequencies; with a higher damper having a smaller resonant peak; and a worse vibration amplitude at high frequencies; since the damper has very stiff and sticky for small vibration displacement. To properly provide vibration suppression; high damping is needed at the resonant frequency of the system; but a lower damping at other frequencies.

Particularly in the case of hand held machines, active damping mechanisms exist which include sensors for monitoring vibrations from a source, with some arrangement to generate an opposing force with the proper phase and amplitude sufficient to attenuate the vibration. However, most active damping mechanisms dramatically increase cost and weight and can affect overall performance of tools in which they are included.

Unfortunately, most traditional passive vibration dampening systems using traditional springs or dampers (particularly for hand held tools) do not suppress vibration as (1) the worker needs to press down to hold the machine tightly in order for high operational efficiency and (2) with more compression of traditional springs or materials, there is dramatically increasing stiffness and consequently significant reduction in the amount of vibration suppression provided.

SUMMARY

Features and advantages of the disclosure will be set forth in the description which follows, and in part will be obvious from the description, or can be learned by practice of the herein disclosed principles. The features and advantages of the disclosure can be realized and obtained by means of the instruments and combinations particularly pointed out in the appended claims.

In accordance with a first aspect of the present disclosure, there is provided a vibration reducing apparatus for a percussive tool having a working member which reciprocates along an axis of reciprocation, the apparatus comprising:

a guide frame configured for retaining the percussive tool, the guide frame comprising at least two elements extending along and at least one member extending across the axis of reciprocation when the percussive tool is retained therein,

an assembly extending in a direction of along the axis of reciprocation wherein said assembly comprises at least two layers, each layer comprising four interconnected elongate members pivotally attached and rotatable with respect to each other to define a polygon; wherein the assembly has at least one biasing means extending between the ends of at least one pair of elongate interconnected members of a layer and is displaceable in the direction of along the axis of reciprocation;

a handle movably coupled to the guide frame and supported on the assembly for transmission of an operator applied load down and along the assembly;

wherein the arrangement of the at least one biasing means relative to the elongate members provides decreasing stiffness with increasing compression of the assembly under an operator applied load to the handle for reducing vibration thereof in a predetermined frequency range.

The vibration reducing apparatus may comprise one or more further assemblies spaced apart from the assembly, wherein each assembly is attached at one end thereof to the at least one member extending across the axis of reciprocation.

One or more parameters of the or each assembly may be modified for achieving one or more of a lower natural resonance frequency relative to a percussive tool without the vibration reducing apparatus; increased loading capacity; a predetermined displacement distance of the at least one or more further assemblies along the axis of reciprocation and size of the at least one or more further assemblies in an unloaded state.

One or more of the modified parameters of the or each assembly may be selected from the group comprising spring stiffness, the angle between elongate members, the material of the elongate members, the ratio of lengths of elongate members to each other, and the number of layers.

The stiffness of the at least one biasing means may be adjustable for changing the resonant frequency of the apparatus.

The stiffness of the at least one biasing means may be adjusted by substitution with one or more biasing means having a different stiffness to the at least one biasing means.

The stiffness of the at least one biasing means may be adjusted by the addition or removal of one or more biasing means.

The angle between adjacent elongate members may be adjustable so as to modify the vibration suppression provided by the or each assembly.

The material of the elongate members may be selected so as to have a reduced stiffness relative to steel.

The material of the elongate members may be aluminium or magnesium.

Two or more elongate members of the apparatus have a first length; and the other elongate members of the apparatus have a second length; and the relative ratio of the first length to the second length may be selected to provide vibration suppression in the apparatus in the predetermined frequency range of 6-20 Hz.

The angle between the elongate members and/or the stiffness of biasing means may be adjustable so as to maintain the physical size of the apparatus with an increase in the operator applied load.

The elongate member angle and number of layers in the or each assembly may be adjusted so as to modify the possible amount of displacement of the or each assembly in the direction of along the axis of reciprocation.

The or each assembly may be attached to the guide frame at one or more regions distal to the ends of the guide frame for resisting non-vertical deformation under load.

The or each assembly may be configured to reduce vibration transmission from a percussive tool receivable therein in the predetermined frequency range of 6 - 20 Hz.

At least two of the elongate members may be pivotally interconnected with each other at a location distal from the ends thereof.

The maximum travel of the movably supported handle on the guide member may be fixed by stops on the guide frame.

The handle and at least one member extending across the frame may be adjustable so as to increase the distance between the at least one or more further assemblies and the at least one assembly.

The handle may be supported on the frame by a biasing means arranged to extend in a direction of along the axis of reciprocation of the working member of the tool.

The at least one member extending across the axis of reciprocation for retaining the powered percussive tool in the guide frame may be an adjustable clamp.

The lengths of elongate members may be substantially the same.

At least one pair of intersecting elongate members may be arranged asymmetrically about the axis of reciprocation.

The tool selected for retention in the guide frame may be selected from a group of percussive tools comprising a jackhammer, road breaker and hammer drill.

In accordance with a second aspect of the present disclosure, there is provided a vibration assembly of a vibration reducing apparatus for a percussive tool having an axis of reciprocation, the vibration assembly comprising:

at least two layers, each layer comprising four interconnected elongate members pivotally attached and rotatable with respect to each other to define a closed loop; the assembly being displaceable in the direction of along the axis of reciprocation and wherein the at least one assembly has at least one biasing means extending between the ends of at least one pair of elongate interconnected members of a layer;

wherein the assembly is configured for engagement with one element of a guide frame comprising at least two elements extending along the axis of reciprocation of the tool and at least one member extending across the axis of reciprocation wherein said at least one member is configured to retain the powered percussive tool in the guide frame;

wherein the assembly is configured for supporting at least one part of a handle movably coupled to the guide frame for transmission of force to the percussive tool and wherein the arrangement of the at least one biasing means relative to the elongate members provides decreasing stiffness with increasing compression of the assembly under an operator applied load to the handle for reducing vibration thereof in a predetermined frequency range.

In accordance with a third aspect of the present disclosure, there is provided a method of using the vibration reducing apparatus according to the first aspect with a tool selected from the group of percussive tools comprising a jackhammer, road breaker and hammer drill.

BRIEF DESCRIPTION OF THE DRAWINGS

In order to describe the manner in which the above-recited and other advantages and features of the disclosure can be obtained, a more particular description of the principles briefly described above will be rendered by reference to specific embodiments thereof which are illustrated in the appended drawings. Understanding that these drawings depict only exemplary embodiments of the disclosure and are not therefore to be considered to be limiting of its scope, the principles herein are described and explained with additional specificity and detail through the use of the accompanying drawings.

Preferred embodiments of the present disclosure will be explained in further detail below by way of examples and with reference to the accompanying drawings, in which:-

Figure 1A shows a schematic representation of an embodiment of assemblies according to the present disclosure in which a jackhammer or road breaker is retained in the assembly.

Figure 1B depicts a further embodiment when a hammer drill is retained in the assembly.

Figure 2A depicts exemplary axes of reference included in the embodiment of disclosure depicted in Figure 1A.

Figure 2B depicts a schematic simplified system of one assembly of the exemplary embodiment depicted in Figure 2B.

Figure 2C depicts a schematic simplified system of a further single symmetric assembly having two layers.

Figure 2D depicts a schematic simplified n-layered asymmetric assembly.

Figure 2E depicts a schematic simplified three layered asymmetric assembly under central loading.

Figure 2F depicts a schematic simplified two layered asymmetric assembly under off-centre loading conditions.

Figure 2G depicts a schematic simplified two layered asymmetric assembly under off-centre loading conditions.

Figure 2H depicts an exemplary mathematical coordinate system for motion of one elongate connecting member.

Figure 3A depicts the displacement transmissibility with different spring stiffness.

Figure 3B depicts the static stiffness of the system in compression.

Figure 3C depicts displacement transmissibility of different M_1.

Figure 3D depicts the displacement transmissibility of different elongate member assembly angle.

Figure 3E depicts the displacement transmissibility of different damping.

Figure 4A depicts the acceleration transmissibility with different spring stiffness.

Figure 4B depicts the acceleration transmissibility with different M_1.

Figure 4C depicts the acceleration transmissibility with different elongate member assembly angle.

Figure 4D depicts the acceleration transmissibility with different damping.

Figure 4E depicts the acceleration transmissibility of different elongate member material.

Figure 4F depicts the acceleration transmissibility with different L_1/L_2.

Figure 4G depicts the acceleration transmissibility of different layer n .

Figure 5 depicts a comparison of the performance of the initial design and optimised design obtained by changing parameters.

Figure 6A depicts a modal analysis of the simplified model with one vibration reducing assembly

Figure 6B depicts a modal analysis of the complete model with two vibration reducing assemblies

Figure 7 depicts a simulation result of 30 *Hz* Single-Frequency Excitation

Figure 8A depicts an experimental prototype in laboratory

Figure 8B depicts an experimental prototype in an onsite experiment.

Figure 9 depicts time and frequency responses in typical laboratory testing (Z1 is the vibration on the percussive breaker and Z2 is the vibration on the handle of the vibration reducing apparatus)

Figure 10A depicts acceleration signals in time and frequency domains for a traditional breaker on direction Z;

Figure 10B depicts acceleration signals in time and frequency domains for the bottom of an apparatus of the present disclosure with a breaker on direction Z;

Figure 10C depicts acceleration signals in time and frequency domains for the top of the apparatus on direction Z;

Figure 10D depicts acceleration signals in time and frequency domains for the handle of the apparatus on direction Z;

Figure 11A depicts the schematic representation of Figure 1A in expanded form with the jackhammer removed for the purposes of clarity, showing an optional adjustable width frame for engaging different jackhammer models.

Figure 11B depicts an exemplary schematic representation of an enlarged view of one exemplary embodiment of the engagement of the jackhammer with the frame.

Figure 11C depicts another exemplary embodiment showing further optional features for restricting possible motion.

Figure 11D depicts an expanded view of the handles in the embodiment depicted in Figure 11C.

DETAILED DESCRIPTION OF THE PREFERRED EMBODIMENTS

Various embodiments of the disclosure are discussed in detail below. While specific implementations are discussed, it should be understood that this is done for illustration purposes only. A person skilled in the relevant art will recognize that other components and configurations may be used without departing from the scope of the disclosure.

The disclosed technology addresses the need in the art for improved passive vibration apparatus, particularly suitable for use in reciprocating tools which are physically stabilised and maintained in the desired orientation for performing work by the grip of a construction worker.

In an aspect of the disclosure there is provided a frame having a pair of vibration reducing assemblies arranged in parallel; configured to provide beneficial nonlinear stiffness under compressive load for a vibration generating tool such as a jackhammer or road breaker supported within the frame. When the operator presses down the handles of the frame, more downward forces are added to the tool to increase operational efficiency. However, because of the beneficial vibration reducing characteristics of the vibration reducing assemblies, vibration is not transmitted to the hands of the operator. This can be compared to the nonlinear stiffness which would be provided if a vertically extending spring only was used; wherein increased downward pressure for efficiency in demolition or other operation would lead to more compression of the installed springs; and hence decreased vibration damping.

Referring to Figure 1A, there is depicted an exemplary vibration reducing apparatus **10** according to an embodiment of the present disclosure.

The vibration reducing apparatus **10** comprises a pair of vibration reducing assemblies **20** which support a handle **40** which is movable on a frame **38**.

A member **50** extends across the frame **38** for supporting the lower portion of a percussive tool such as a jackhammer, road breaker, hammer drill or the like. The percussive tool has an axis of reciprocation along which the reciprocating member (e.g. the drill bit of the hammer drill, or the chisel of a jackhammer) moves back and forth.

Referring to Figure 1B, there is depicted a further exemplary vibration reducing apparatus **10b** according to a further embodiment of the present disclosure when a hammer drill **60b** is connected to a frame **38b** of the vibration reducing apparatus **10b**.

The vibration reducing apparatus **10b** comprises a pair of vibration reducing assemblies **20b** which support a handle **40b** which is movable on the frame **38b**.

A member **50b** extends across the frame **38b** for supporting the lower portion of the hammer drill **60b**. The hammer drill **60b** has an axis of reciprocation along which the drill bit of the hammer drill **60b** moves back and forth.

Mathematical Theoretical Modelling

Referring to Figure 2A- Figure 2G, various exemplary embodiments of the vibration reducing apparatus is shown. (In the embodiment depicted for the purposes of clarity there are no vertical aligned damping springs included, the handle has been omitted, and there is no depiction of the sliding attachment between the frame and the vibration assemblies.)

In the simplified version of the embodiment depicted in Figure 2A, 4 “layers” 26, 28, 30,32 are shown.

Two elongate members 29a,29b of a predetermined length L2 intersect and are pivotally connected to elongate members having the same predetermined length 31a, 31b at a location other than the ends. Advantageously, the length of the elongate members 29a,29b are twice the length of the 27a, 27b of the other members enabling springs to be installed more easily as shown.

For modelling purposes, the breaker is considered as a rigid body M_2 and the two parallel vibration reducing structures are simplified into one for simplification purposes as depicted in Figure 3B.

The vibration is exerted upward at the bottom of M_2.

The upper mass M_1 is to act as the added pushing-down force provided by the operator's hands. The elongate member weight of the vibration reducing structure can also be considered equivalently in the upper mass M_1.

Preferably the spring used is a standard linear spring with a stiffness K (or K_n as the case may be).

L_1 is the elongate member length of the small elongate members, and L_2 is the length of large ones in Figure 2B, 2D.In the embodiment of Fig 2C shown the members have the same length and are denoted by l. In Figures 2E, 2F, the members form a part of the specified layer as denoted by the subscripts e.g. L_{31} is Layer 3 small member 1.

The assembly angle of elongate members with respect to the horizon line is represented by θ (see also Figure 3C). The air damping effect is denoted by D with the corresponding damping coefficient is C. The involved parameters are listed in Table 1.

Symbol	Structural Parameters	Unit
M_1	Mass of Isolation Object	*kg*
M_2	Mass of Vibration Source	*kg*
M_x	Mass of each 100*mm* Elongate member	*kg*
L_1	Side Length of Small Structure	*mm*
L_2	Side Length of Large Structure	*mm*
R_L	Ratio of L_2/L_1	/
n	Number of Layer	/
θ	Assembly Angle of Elongate member	*rad*
φ	Rotational Motion	*rad*
y	Absolute Motion of Isolation Mass	*mm*
$\hat{y}$	Relative Motion of Isolation Mass and Vibration Source	*mm*
z	Bottom Excitation	*mm*
a	Amplitude of Relative Motion $\hat{y}$	*mm*
z_0	Amplitude of Bottom Excitation z	*mm*
ϕ	Phase of Relative Motion $\hat{y}$	*rad*
ω_0	Frequency of Bottom Excitation z	*rad/s*
T_d	Displacement Transmissibility	/
T_a	Acceleration Transmissibility	/
K	Spring Stiffness	*N/mm*
c	Damping Coefficient	/
D	Damping	/
f	Natural Frequency	*Hz*

The absolute motion of the mass M_1 is denoted by y , the base excitation z , the rotation angle of each connecting elongate member φ , and the horizontal motion of the rotation joint in each layer of the smaller elongate member length is x . The positive direction of the motion y is in the upward direction. The length of the small elongate members L_1 is chosen as l and the length of the large elongate members L_2 is $2l$ as those in the real case.

The rotation motion of each elongate member φ is shown in Figure 3C. The elongate members can be designed to be much lighter in weight compared with the isolation mass, sufficiently short in length and strong in stiffness (via choosing materials, e.g., steel or aluminium alloy etc.) to reduce potential inertia or flexibility influence in dynamic response.

It can be seen that the rotational motion φ and horizontal motion x can be expressed by relative motion $\hat{y}$. The ratio of L_2/L_1 is chosen as 2. The geometrical relation can be obtained as

$$\left(l\cos(\theta)-x\right)^2+\left(l\sin(\theta)+\frac{\hat{y}}{2(n+1)}\right)^2=l^2 \tag{1}$$

$$\tan(\theta+\varphi)=\frac{\frac{\hat{y}}{2(n+1)}+l\sin(\theta)}{l\cos(\theta)-x} \tag{2}$$

$$\hat{y}=y-z \tag{3}$$

The transport motion φ and x are expressed as

$$\varphi=\arctan\left(\frac{\frac{\hat{y}}{2(n+1)}+l\sin(\theta)}{l\cos(\theta)-x}\right)-\theta \tag{4}$$

$$x=l\cos(\theta)-\sqrt{l^2-\left(l\sin(\theta)+\frac{\hat{y}}{2(n+1)}\right)^2} \tag{5}$$

For convenience in discussion and for understanding dominant dynamic response of the system, the mass of the connecting elongate members are not considered in system modelling of this study.

The kinetic energy can be written as

$$T=\frac{1}{2}M_1\dot{y}^2+\frac{1}{2}M_2\dot{z}^2 \quad (6)$$

The potential energy as

$$V=\frac{1}{2}k_l(4x)^2 \quad (7)$$

Lagrange function expressed as

$$L=T-V=\frac{1}{2}M_1\dot{y}^2+\frac{1}{2}M_2\dot{z}^2-\frac{1}{2}k_l(4x)^2 \quad (8)$$

The Lagrange principle is

$$\begin{cases}\frac{\mathrm{d}}{\mathrm{d}t}(\frac{\partial L}{\partial \dot{y}})-\frac{\partial L}{\partial y}=-D\\ \frac{\mathrm{d}}{\mathrm{d}t}(\frac{\partial L}{\partial \dot{z}})-\frac{\partial L}{\partial z}=F_0\cos(\omega t)-D\end{cases} \quad (9)$$

where L is the Lagrange function expressed as $L=T-V$, D the dissipated energy for air damping. It can be obtained that

$$D=c(\dot{y}-\dot{z}) \quad (10)$$

where C is the damping coefficient of the X-shaped structure.

By substituting kinetic energy, potential energy and transport motion into the Lagrange principle, the dynamic equation can be obtained as

$$\begin{cases}M_1\ddot{y}+16k_lx\frac{\partial x}{\partial \hat{y}}\frac{\partial \hat{y}}{\partial y}=-c(\dot{y}-\dot{z})\\ M_2\ddot{z}+16k_lx\frac{\partial x}{\partial \hat{y}}\frac{\partial \hat{y}}{\partial z}=F_0\cos(\omega t)-c(\dot{y}-\dot{z})\end{cases} \quad (11)$$

Define

$$f_1(\hat{y})=16k_lx\frac{\partial x}{\partial \hat{y}}\frac{\partial \hat{y}}{\partial y} \quad (12)$$

$$f_2(\hat{y}) = 16k_l x \frac{\partial x}{\partial \hat{y}} \frac{\partial \hat{y}}{\partial z} \tag{13}$$

where

$$\begin{aligned} \frac{\partial x}{\partial \hat{y}} &= \frac{\partial [l\cos(\theta) - \sqrt{l^2 - \left(l\sin(\theta) + \frac{\hat{y}}{2(n+1)}\right)^2}\,]}{\partial \hat{y}} \\ &= \frac{\hat{y} + 2(n+1)l\sin(\theta)}{4(n+1)^2\sqrt{l^2 - \left(l\sin(\theta) + \frac{\hat{y}}{2(n+1)}\right)^2}} \end{aligned} \tag{14}$$

$$\frac{\partial \hat{y}}{\partial y} = \frac{y-z}{\partial y} = 1 \tag{15}$$

$$\frac{\partial \hat{y}}{\partial z} = \frac{y-z}{\partial z} = -1 \tag{16}$$

Substituting (12) and (13) into (11)

$$f_1(\hat{y}) = 4k_l x \frac{\hat{y} + 2(n+1)l\sin(\theta)}{(n+1)^2\sqrt{l^2 - \left(l\sin(\theta) + \frac{\hat{y}}{2(n+1)}\right)^2}} \tag{16}$$

$$f_2(\hat{y}) = -4k_l x \frac{\hat{y} + 2(n+1)l\sin(\theta)}{(n+1)^2\sqrt{l^2 - \left(l\sin(\theta) + \frac{\hat{y}}{2(n+1)}\right)^2}} \tag{17}$$

(16) and (17) can be expanded by Taylor series at zero equilibrium as

$$\begin{aligned} F_1(\hat{y}) &= \frac{f_1(0)}{0!} + \frac{f_1'(0)}{1!}\hat{y} + \frac{f_1''(0)}{2!}\hat{y}^2 + \frac{f_1'''(0)}{3!}\hat{y}^3 + \frac{f_1''''(0)}{4!}\hat{y}^4 + o \\ &= \beta_1\hat{y} + \beta_2\hat{y}^2 + \beta_3\hat{y}^3 + \beta_4\hat{y}^4 \end{aligned} \tag{18}$$

$$\begin{aligned} F_2(\hat{y}) &= \frac{f_2(0)}{0!} + \frac{f_2'(0)}{1!}\hat{y} + \frac{f_2''(0)}{2!}\hat{y}^2 + \frac{f_2'''(0)}{3!}\hat{y}^3 + \frac{f_2''''(0)}{4!}\hat{y}^4 + o \\ &= \alpha_1\hat{y} + \alpha_2\hat{y}^2 + \alpha_3\hat{y}^3 + \alpha_4\hat{y}^4 \end{aligned} \tag{19}$$

where

$$\beta_1 = \frac{4k_l \tan^2(\theta)}{(n+1)^2} \tag{20}$$

$$\beta_1 = \frac{3k_t \sin(\theta)}{l(n+1)^3 \cos^4(\theta)} \tag{21}$$

$$\beta_3 = -\frac{k_t(4\cos^2(\theta)-5)}{2l^2(n+1)^4 \cos^6(\theta)} \tag{22}$$

$$\beta_4 = -\frac{5k_t(4\cos^2(\theta)-7)\sin(\theta)}{16l^3(n+1)^5 \cos^8(\theta)} \tag{23}$$

$$\alpha_1 = -\frac{4k_t \tan^2(\theta)}{(n+1)^2} \tag{24}$$

$$\alpha_1 = -\frac{3k_t \sin(\theta)}{l(n+1)^3 \cos^4(\theta)} \tag{25}$$

$$\alpha_3 = \frac{k_t(4\cos^2(\theta)-5)}{2l^2(n+1)^4 \cos^6(\theta)} \tag{26}$$

$$\alpha_4 = \frac{5k_t(4\cos^2(\theta)-7)\sin(\theta)}{16l^3(n+1)^5 \cos^8(\theta)} \tag{27}$$

Substituting the Taylor series expansion (16)–(19) into (15) as

$$\begin{cases} M_1\ddot{\hat{y}} + c\dot{\hat{y}} + M_1\ddot{z} + \beta_1\hat{y} + \beta_2\hat{y}^2 + \beta_3\hat{y}^3 + \beta_4\hat{y}^4 = 0 \\ M_2\ddot{z} + c\dot{\hat{y}} + \alpha_1\hat{y} + \alpha_2\hat{y}^2 + \alpha_3\hat{y}^3 + \alpha_4\hat{y}^4 - F_0\cos(\omega t) = 0 \end{cases} \tag{28}$$

where $\ddot{y} = \ddot{\hat{y}} + \ddot{z}$.

Using the Harmonic Balance Method (HBM) for theoretical results. The solution of (21) can be set as

$$\begin{aligned} \hat{y} &= a_0 + a\cos(\omega t + \varphi_1) \\ z &= b_0 + b\cos(\omega t + \varphi_2) \end{aligned} \tag{29}$$

where a_0 and b_0 is the bias term, a and b is the amplitude of harmonic terms.

$$\begin{cases} a_0^3\alpha_3+\frac{1}{2}a^2\alpha_2+a_0\alpha_1+\frac{3}{8}a^4\alpha_4+a_0^4\alpha_4+\frac{3a^2a_0\alpha_3}{2}+3a^2a_0^2\alpha_4+a_0^2\alpha_2=0 \\ (-3aa_0^{\ 2}\alpha_3-a\alpha_1-\frac{3}{4}a^3\alpha_3-4aa_0^{\ 3}\alpha_4-2aa_0\alpha_2-3a^3a_0\alpha_4-ca\omega)sin(\varphi_1)+M_2b\omega^2sin(\varphi_2)=0 \\ (a\alpha_1+\frac{3}{4}a^3\alpha_3+4aa_0^{\ 3}\alpha_4+2aa_0\alpha_2+3a^3a_0\alpha_4+3aa_0^{\ 2}\alpha_3-ca\omega)cos(\varphi_1)-M_2b\omega^2cos(\varphi_2)-F_0=0 \\ a_0^3\beta_3+\frac{1}{2}a^2\beta_2+a_0\beta_1++\frac{3}{8}a^4\beta_4+a_0^4\beta_4+\frac{3a^2a_0\beta_3}{2}+3a^2a_0^2\beta_4+a_0^2\beta_2=0 \\ (-4aa_0^{\ 3}\beta_4-2aa_0\beta_2-3aa_0^{\ 2}\beta_3+M_1a\omega^2-\frac{3}{4}a^3\beta_3-a\beta_1-3a^3a_0\beta_4-ca\omega)sin(\varphi_1)+M_1b\omega^2sin(\varphi_2)=0 \\ (-M_1a\omega^2+\frac{3}{4}a^3\beta_3+a\beta_1+3a^3a_0\beta_4+4aa_0^{\ 3}\beta_4+2aa_0\beta_2+3aa_0^{\ 2}\beta_3-ca\omega)cos(\varphi_1)-M_1b\omega^2cos(\varphi_2)=0 \end{cases} \quad (30)$$

The displacement transmissibility T_d can be obtained as

$$T_d=\left|\frac{\sqrt{a^2+b^2+2ab\cos\varphi_1}}{b}\right| \quad (31)$$

The structural parameters of the system can be designed for different vibration isolation performance. In the theoretical calculations shown the parameters including spring stiffness, mass of isolation object, assembly angle of elongate members and the damping ratio are considered as structural parameters for different vibration isolation performance, with the elongate members mass being neglected.

The displacement transmissibility and the natural frequency calculated according to equation 31 demonstrates the vibration isolation effect with a series of different structural parameters.

It would be appreciated that similar analyses could be conducted of the systems depicted in Figures 2C (two layer symmetric structure), Figure 2D (n layer asymmetric structure), Figure 2E (thee layer asymmetric structure having a first form), Figure 2F (two layer asymmetric structure having a second form), Figure 2G (two layer asymmetric structure having a third form).

In Figures 2C- 2G, “o” represents a rotation joint. K, k_1,k_2,k_v and k_h are stiffness coefficients of corresponding springs. C, c_1, and c_2 are damping coefficents of corresponding dampers

As can be seen with reference to these figures in particular, the springs could be vertically installed between the two joints which are used supplementary for removing negative stiffness within the system, which can be seen in Figure 1A.

However, the springs are innovatively used in horizontal ways as shown, which provide the main spring force. The dampers are mainly installed horizontally to create the claimed desired nonlinear damping and vertical dampers are not needed but can be used for increasing damping in case that it needed. Both linear and nonlinear springs and dampers of any appropriate type can be used with similar performance.

As is discussed further in more detail there are no specific requirements on the number of sections/layers. Generally, more layers leads to smaller dynamic stiffness, smaller damping effect and more linear effect both in equivalent stiffness and damping. Conversely, with fewer layers, this will lead to a larger dynamic stiffness, larger damping effect and more non-linear effect both in equivalent stiffness and damping.

The length of a section/layer is determined by the member length, while a longer member length leads to smaller and more linear damping effect and has a mild effect on stiffness. A bigger assembly angle leads to larger loading capacity and bigger dynamic stiffness and vice versa. (see Figure 2C).

The rod length of the same layer or different layer can be different to produce asymmetric shaped structure, as shown in Fig 2C - 2G with similar or even better performance in stiffness and damping effects.

As for the springs, a bigger spring constant leads to larger loading capacity and bigger stiffness with respect to the same compression or extension. Importantly, the springs can be any type (air springs, coil springs, materials or others), and linear or nonlinear, which are used to provide elastic force, but mainly installed in the horizontal way with a vertical supplement (as shown in Figure 1) to remove negative stiffness.

The detailed spring constants are determined such that after installation the working position should optimally have a 90 degree at the middle of the X-shaped structures, as is analysed in more detail below.

Further to the above, the following parameters are considered, especially in relation to the embodiment depicted in Figures 2A, 2B and the geometric parameters of Figures 2H.

(a) Effect of spring stiffness K

Figure 4a shows that the vibration isolation effect is influenced by the spring stiffness. It can be seen that decreasing the spring stiffness can reduce the peak value of the displacement transmissibility and the resonant frequency of the system.

When the spring stiffness decreases from 100 to 10, the resonant frequency decreases from 6.8 Hz to 1.2 Hz. This relationship demonstrates that reducing the spring stiffness improves the vibration suppression performance.

With the same springs to support the same mass M_1 without the X-shaped structure, it has been calculated that the resonant frequencies would be 5.1 Hz, 11.3 Hz, and 16.1 Hz respectively.

This may be compared with the resonance frequencies obtained when the system includes the X-shaped structures (1.2 Hz, 2.8 Hz, and 6.8 Hz), demonstrating mathematically that the resonant frequencies are significantly reduced, clearly showing the advantageous quasi-zero-stiffness property of the X-shaped structure in dynamic vibration isolation as compared to that provided by traditional spring arrangements.

To have more understanding, the static stiffness of the structure is developed as follows and shown in Figure 4B with different stiffness value for K.

Considering the given initial mass M_1, the structure is at equilibrium with initial spring force $F_0 = \frac{M_1 g}{5\tan\theta}$ and then a force F is applied downward,

$$F = 5\left(F_0 + Kx\right)\tan(\theta - \varphi) - Mg \tag{32a}$$

Considering the relationship between x and relative displacement $\hat{y}$,

$$F = 5\left(\frac{M_1 g}{5\tan\theta_0} + K\left[l\cos(\theta) - \sqrt{l^2 - \left(l\sin(\theta) + \frac{\hat{y}}{10}\right)^2}\right]\right)\frac{l\sin\theta - \frac{\hat{y}}{5}}{2l\cos\theta - \sqrt{l^2 - \left(l\sin(\theta) + \frac{\hat{y}}{10}\right)^2}} - M_1 g \tag{32b}$$

It can be seen clearly from Figure 4b that the stiffness of the structure actually decreases as the suppression of the structure (i.e., the absolute relative displacement between M_1 and M_2 is increased).

This shows that when more downward force is applied to the handles:

- the working position for the operator is lower;
- there is more compression of the frame structure;

- the structure has a decreasing dynamic stiffness, which is very beneficial to vibration control.

- there is a higher demolition efficiency as the operator is applying more force.

This again demonstrate the unique nonlinear advantages of the structure compared with all other traditional vibration suppression systems.

(b) Effect of increased mass M_1

With other parameters set to L_1=100, L_2=200, M_2=19.68, K=100, $\theta = \pi/4$, and the same elongate member material, the upper mass M_1 can be changed to different values to examine how the downward force at the vibration reducing apparatus handles can affect the vibration transmission. The curves of displacement transmissibility T_d are shown in Figure 4c, where it can be seen that increasing the mass M_1 can decrease the resonant frequency, while at the same time providing a reduced peak value.

It should be emphasized that for a pure linear system, when increasing the mass but maintaining the same spring stiffness, the resonant frequency would be decreased as

$$\sqrt{\frac{K}{20}} \Big/ \sqrt{\frac{K}{10}} \approx 0.7$$

However, with the vibration reducing apparatus of the present disclosure, the resonance frequencies are decreased as 3.5/6.8≈0.5, which is much smaller than compared to a pure linear system.

This once again proves that the vibration reducing apparatus has beneficial nonlinear stiffness property which offers a smaller stiffness with increase of the downward force (the latter leads to more compression of the structure).

(c) Effect of elongate member assembly angle θ

The other parameters are set to the same as L_1=100, L_2=200, M_1=9.85, M_2=19.68, K=100, while the elongate member assembly angle is considered as $\pi/6$, $\pi/4$ and $\pi/3$. The displacement transmissibilities T_d are shown in Figure 4d.

We can see from Figure 4c that, the resonant frequency becomes smaller when the assembly angle changes from 60° to 30°. It demonstrates again that the vibration isolation performance becomes better with more compression within the structure, i.e. the decrease of angle θ , tending to be a quasi-zero-stiffness property.

Therefore, assembly angle of the elongate members is a critical parameter to reduce the vibration transmission from the percussive tool to operators' hands and arms

(d) Effect of damping *c*

With the same parameter setting as before but $\theta = \pi/4$ and different damping coefficient *c*, the transmissibilities are shown in Figure 4E which shows that the peak value is decreased with an increase of the damping coefficient.

FEM analysis of the dynamic response of the structure

FEM analysis was performed to understand more about the structural dynamics of the structure with respect to each critical parameter. In the finite element analysis, some parameters are fixed as M_2 =19.68, M_x =0.03 (elongate member mass of L_1-type), D=0.01 (equivalent damping), L_1=100, L_2=200, M_1=9.85, $\theta = \pi/4$, and the elongate member material is structural steel.

The input excitation can adopt a force of sweeping frequency and with amplitude 1000N exerted at the bottom of the mass M_2 which is similar to the real working situation of a road breaker. It is easy to obtain the acceleration transmissibility T_a of the response of the structure together with the road breaker to reflect the vibration isolation effect with different structural parameters.

(a) Effect of spring stiffness *K*

With the structural parameters mentioned above, and choosing different spring stiffness, the curves of acceleration transmissibility T_a are shown in Figure 5A.

It can be seen that whatever the spring stiffness is, the curves of acceleration transmissibility are similar to the result of theoretical calculation.

The vibration isolation effect of the system is obviously influenced by the spring stiffness, which is consistent with the theoretical analysis in Figure 4A. For example, in Figure 5A, for K =100, the resonant frequency is 5.9 Hz, but for K =50, it reduces to 4.5 Hz.

This shows that reducing the spring stiffness is effective to reduce the resonant frequency and thus improve the vibration suppression performance. Moreover, all transmissibility curves have a second peak at around 104.6 Hz due to the resonant frequency of the mass M_2, i.e., the road breaker itself. This is consistent with the actual experimental results later, also corresponding to the second mode frequency of the structure.

(b) Effect of mass M_1

It should be noted that the Mass M_1 is used to simulate the downward force exerted on the structure handle. The bigger the mass M_1, the more downward force and thus more compression on the structure. With the same structural parameters as before, the mass M_1 is chosen as 15.7 and 9.85 respectively and the curves of acceleration transmissibility T_a are shown in Figure 5B.

It can be seen that increasing the mass M_1 decreases the peak frequency which is particularly important to the vibration suppression at the structures' handles; however, the second peak is basically not changed since it is only dependent on the materials and structures of the road breaker. This is consistent with the theoretical analysis before in Figure 4C.

Therefore, the downward force on the structure is critical for vibration suppression. As discussed before, the downward force would lead to the increase of the stiffness in traditional spring systems resulting in **worse** vibration suppression. However, the structure of the present disclosure provides an excellent nonlinear stiffness property which can present higher vibration suppression and higher demolition efficiency due to the increased downward force simultaneously.

(c) Effect of elongate member assembly angle θ

With the other parameters the same as before and tuning the assembly angle θ the curves of T_a for different assembly angle are shown in Figure 5C.

It can be seen that the frequencies of the two peaks both become smaller when reducing the assembly angle; due to the decrease of the structural stiffness of the structure.

It demonstrates that the vibration isolation performance becomes better with the decrease of angle θ tending to become a quasi-zero-stiffness property as discussed. This is consistent with the theoretical analysis in Figure 4D.

Hence, the assembly angle of the elongate members in the structure is a critical parameter to reduce vibration frequencies with between 20-30 degrees determined to provide good vibration suppression performance.

(d) Effect of damping *D*

With the same parameter setting but different damping D, the transmissibility curves are shown in Figure 5D.

Increase of the damping can effectively reduce the resonant peak values. This is similar to the results in the theoretical analysis in Figure 4C. However, increasing the damping ratio will also increase the amplitude of acceleration transmissibility in the frequency range between 10 Hz and 100 Hz.

(e) Effect of elongate member material

The elongate member materials can be chosen to see potential influence in the FEM analysis. With the same parameter setting but choosing different material for all elongate members, the curves of acceleration transmissibility are shown in Figure 5E.

It is seen that changing materials can affect the curves of vibration transmissibility, and especially for high frequency vibration the aluminium or magnesium elongate member has much smaller transmissibility than that of steel elongate members, due to the smaller stiffness of the materials. This is an important design factor since different materials will also influence the overall weight of the structure and its handling comfort in practice.

(f) Effect of ratio L_1/L_2

Different elongate member length ratio can be freely changed in the FEM analysis, which would create different asymmetric structure. With the same parameter setting but L_1=100mm and different ratio of L_1/L_2, the curves of T_a are shown in Figure 5F.

It can be seen that with the decrease of the ratio from 1.5 to 0.25, the first resonant frequency is increasing continuously while the second resonant frequency is decreasing accordingly. Considering that the sensitive vibration to hands and arms are the frequency from 6Hz to 20 Hz a larger elongate member length ratio is obviously better than a smaller elongate member length ratio.

(g) Effect of layer number *n*

With the other parameters set to the same as before but changing different *n*, the curves of acceleration transmissibility are shown in Figure 5G.

It is clear that the layer number is also an important factor for the vibration isolation effect, and both the two resonant frequencies are decreasing with increasing the layer number, which is very helpful for the vibration isolation performance.

Therefore, we can improve the vibration isolation effect though increasing the number of layers, but an increasing layer number leads to a bigger size of the structure.

Refining design of structural parameters

It can be seen above that different structural parameters affect the vibration suppression effect of the vibration reducing assemblies of the present disclosure. Therefore, it is important to refine the parameters to improve performance for specific size, weight, and vibration frequency of a percussive tool.

In practice, there are usually not too many choices for the size and materials of the apparatus/system of the present disclosure since the size of the specific percussive tools is generally consistent in the market with similar weight and vibration frequency. However, some parameters of the vibration reducing assembly such as the spring stiffness, the working angle θ , and materials etc. could be modified.

Therefore, in this section, based on the comparison analysis of different parameters in the previous sections, a relatively better parameter setting is determined for a system, which can achieve much better vibration suppression effect considering the sensitive frequency range 6-20 Hz.

Selection of Appropriate Parameters

Considering that the first two resonant frequencies are critical to the vibration suppression performance in the frequency range 6-20 Hz, a summary of the influence of various parameters in relation to vibration suppression performance is given below.

Table 2. A summary of influence arising from adjustment of parameters

	The 1st resonance		The 2nd resonance		Transmissibility in 6-20 Hz
	frequency	peak	frequency	peak	
M_1 ↑	↓↓	--	=	=	↓↓
Stiffness K ↑	↑↑	↑	=	=	↑↑
Assembly angle θ ↑	↑↑	↑	↑	--	↑↑
Length ratio (L_1/L_2) ↑ with fixed L_1=100mm	↓↓	--	↑↑	↓	↓↓
Layer number n ↑	↓↓	↓	↓↓	↓	↓↓
Damping effect ↑	=	↓	=	↓	↑
Materials from steel, to aluminium to magnesium	↓	↓	↓	↓	↓

From Table 2, the following points can be concluded.

(a) In general, all structural parameters present a monotonic influence on the transmissibility in the frequency range between 6 Hz and 20 Hz (the sensitive frequency range for vibration transmission to hands and arms of the operator);

(b) The influence of length ratio L_1/L_2 is different with respect to the first and second resonant frequencies, and two small length ratios is good for a more compact structure but will result in the two resonant peaks to be closer to 20 Hz leading to a worse vibration suppression in the sensitive frequency range;

(c) The bigger mass M1, smaller stiffness K, smaller assembly angle θ , and bigger layer number n will all monotonically lead to a smaller resonant frequency and thus better vibration suppression in the sensitive frequency range (6-20Hz);

(d) Flexural material such as plastic seems better for vibration suppression but lateral stiffness would be worse to the handling capability of breakers. Therefore, lightweight aluminum seems a better choice in practice.

With the results above, it can be seen that the structure can be designed by adjusting several structural parameters to achieve good vibration suppression performance with a lower natural frequency, considering high loading capacity, large displacement motion, and avoiding the stability problem.

For example,

- to increase the loading capacity without changing the size of the existing device, the assembly angle of elongate members and the stiffness of springs should be increased;

- to increase the compression working range, the elongate member assembly angle and the layer number of the vibration reducing assembly structure should be increased;

- to reduce the natural frequency of the structure, the length ratio L_1/L_2, the mass M_1 and the layer number of the vibration reducing assembly structure should be increased; or the spring stiffness should be reduced and the elongate member assembly angle should be reduced.

It would also be appreciated that although the examples depicted include two vibration reducing assemblies, one, two or three assemblies could be used without departing from the scope of the present disclosure.

Overall, there are redundant structure parameters which can be employed to tune the vibration suppression performance to practical application, presenting excellent flexibility for achieving a range of outcomes.

Example:

Based on a simple optimization to minimize the weighted transmissibility in the critical range a vibration reducing apparatus with initial parameter settings was proposed as follows:

$L_1=100mm$, $L_2=200mm$, $M_1=10kg$, $M_2=20kg$, $\theta=\pi/4$, $K=100N/mm$, $D=0.01$ and the elongate member material is structural steel.

To optimise the parameters of this apparatus, the following parameters were selected:

$L_1=100mm$, $L_2=200mm$, $M_1=15kg$, $M_2=20kg$, $\theta=\pi/6$, $K=100N/mm$, $D=0.1$ and the elongate member material is aluminium alloy.

The results are shown in Figure 5, which indicates the comparison of acceleration transmissibility curves between the refined or optimized design and the initial design.

It can be seen that all the resonant frequencies (the first frequency is 3 Hz) and peak values with the optimized parameter setting are smaller than those initially (the first frequency is 6 Hz).

This is especially the case in the sensitive frequency range of vibration transmission. Specifically the maximum reduction of the transmissibility at around 6 Hz is an impressive approximately 40 dB.

Comparing the two parameter settings, it can be seen that the mass M_1 (i.e., the downward pushing force) and assembly angle are two critical design parameters for this performance improvement.

However, both parameters do not relate to structural size but are factors which can be controlled by operators in practice. Both parameters are related to the compression of the vibration reducing assemblies in the apparatus.

Simulation results of refined design for a complete model

Modal analysis of the complete model of the structure is undertaken to provide an insight into the structural dynamics in real application.

For comparison, the simplified model of one vibration reducing assembly depicted in Figure 2B is analyzed first, and the modal analysis results are shown in Figure 6A. Modal analysis of the complete model of the structure shown in Figure 2A, with two parallel vibration reducing assemblies using the optimised parameters discussed above is then undertaken.

In Figure 6A, it can be seen that the frequency of the first-order mode is only 3 Hz. The inherent vibration mode is an up and down motion. The angles of the elongate members are changed, but the elongate members are not deformed. It corresponds to the first peak of the acceleration transmissibility curve for the refined design in Figure 4G or Figure 5. The second mode (39 Hz) is not considered since the frame in the vertical direction restricts the motion. The third mode has a frequency around 48 Hz which produces deformation of the shaped structure horizontally. Making the elongate member length L_2 smaller to be equal to L_1, will address this problem.

For all the other higher vibration modes, the influence on the handles of the structure would be very small since the frequencies are around or more than 50 Hz and the vibration amplitude would be very small.

Referring now to Figure 6B, there is shown the first 3 vibration modes of the complete model of the structure shown in Figure 2A (including two vibration reducing assemblies). The modal results are basically the same as the modal results in Figure 6A for the simplified model. The vibration mode within the system/apparatus of the present system for the mode 2 still has bending deformation horizontally as in the exemplary structure shown it is not fixed to the guide frame.

From the modal analysis above, it can be seen that (a) the mode frequencies obtained are basically consistent with the theoretical analysis of the resonant frequencies of the system; (b)

the mode frequencies below 50 Hz should be considered in the parameter selection; however, due to the excellent quasi-zero stiffness of the X-shaped structure, all higher frequency vibration more than 5 Hz would be significantly suppressed; (c) There are no special low frequency mode frequencies in the sensitive frequency range 6-20 Hz for the designed system, which is very good for the predicted overall vibration suppression performance.

Finite Element Model Analysis

Considering the real percussive tool such as a road breaker working usually at a constant frequency such as 30 Hz in demolition, investigation is performed of the dynamic response of the system subject to a single-frequency excitation but with different input amplitude with a finite element model.

All structure parameters are basically the same as the real prototype (introduced later). Note that the stiffness system is nonlinear (Section 3) and thus nonlinear response would be expected to see when the excitation amplitude is large enough. This single-frequency excitation is important to understanding of the real experimental data later.

Figures 7A- C show the time domain and corresponding frequency domain output responses of the BIAVE system under 30*Hz* single-frequency excitation with different input force 2*KN, 6KN* and 10*KN*.

In Figures 7A-C it can be seen clearly that

(a) The vibration suppression performance is apparent with a vibration reduction in energy of approximately 80-90%; which is consistent with the theoretical and simulation results of the previous sections;

(b) When the excitation amplitude is large enough up to 6 KN, the output response is obviously complicated with more frequency components observed instead of a single frequency peak at 30 Hz, due to the nonlinear dynamics in the system;

(c) With increasing excitation amplitude, super-harmonic response at the frequencies (60 Hz) of two times bigger than the input frequency (30 Hz) appears and then output response tends to more complicated; For example, under the 10KN excitation, besides the output response at 30 Hz, there are some other frequency components including the one around 60 Hz, a smaller one at around 45 Hz, and another obvious one at 15 Hz, which are corresponding to super-harmonic response, inter-modulation response and sub-harmonic response respectively; and the sub-harmonic response at 15 Hz is very strong.

Therefore, almost all nonlinear dynamics due to a single-tone excitation can be observed with a very strong sub-harmonic response, indicating that potential response of real percussive tools could be very complicated in strong excitation environments.

It should be noted that the sub-harmonic response peak at 15 Hz is exactly located within the sensitive frequency range (6-20Hz) for a human operator and therefore a vibration suppression system of ultra-low resonant frequency is really needed for isolating this harmful vibration.

The quasi-zero stiffness of the vibration reducing assemblies of the present disclosure exactly meets this challenging requirement with a very low resonant frequency around 3 Hz and which can effectively suppress the vibration peak shown.

Measured Characteristics of an Actual Experimental Prototype

The refined parameter setting is used for the prototype as discussed above. That is, $L_1 = 100mm$, $L_2 = 200mm$, $M_1 = 15kg$, $M_2 = 20kg$, $\theta = \pi/6$, $K = 100N/mm$, $D = 0.1$ and the elongate member material is aluminium alloy . Note that M_1 is the downward pushing force. T

That is once the percussive tool (breaker) is in operation the handle of the prototype structure would be pushed down to the desired position, which is equivalent to the mass M_1, with an assembly angle $\theta = \pi/6$. The mass M_2 is exactly the mass of the percussive breaker used in experiments.

The whole structure is about one meter tall.

In the specific prototype produced according to the disclosure of the present disclosure there are two 4-layer X-shaped vibration suppression structures arranged in parallel (Figure 2A), although it would be appreciated that other arrangements with different numbers of layers would be possible as previously discussed.

Both vibration suppression structures have 1-layer large elongate members and 3-layer small elongate members joined by corresponding rotating joints. The mass of the connecting rods is around 0.3*kg* per 100*mm*. The overall downward force on the handle which used to make the structure to work at the desired assembly angle is 15k*N*, which follows the parameter setting used in theoretical calculation and FEM analysis. The breaker used in the prototype is 20*kg*, with an impact frequency of 1800*times/min*, i.e., 30*Hz*.

Once the breaker is actuated, hitting the concrete or rubber generates a single-frequency excitation to the system vertically, which has a main frequency around 30 Hz on rubber or 20 Hz on concrete. The vibration acceleration signals on the breaker and on the handle of the prototype structure both can be measured for further analysis, which are referred to as Z-down and Z-up respectively.

To evaluate the vibration level, the ISO5349 standard calculation for hands and arms vibration is adopts, which is a frequency-weighted acceleration energy as shown in (33).

$$a_{hw} = \sqrt{\sum_{i=1}^{n} (K_i a_{hi})^2} \tag{33}$$

where:

n is the total number of frequency band.

K_i is the weighting coefficient of No. *i* frequency band, the value is shown in Table 3.

a_{hi} is the acceleration RMS value, the formula is as follows:

$$a_{hi} = \sqrt{\frac{1}{T}\int_0^T a^2(t)dt} = \frac{a_0}{\sqrt{2}} \tag{34}$$

where:

T is the recording time.

a_0 is the maximum value of vibration acceleration.

ISO 5349 proposes the frequency range including octave bands, its center frequency is from 8 to 1000*Hz*, 1/3 octave bands, its center frequency is from 6.3 to 1250*Hz*. The weight coefficient are shown in Table 3.

Centre Frequency (*Hz*)	K_i	Centre Frequency (*Hz*)	K_i
6.3	1.0	100	0.16
8.0	1.0	125	0.125
10.0	1.0	160	0.1
12.5	1.0	200	0.08
16	1.0	250	0.063
20	0.8	315	0.05
25	0.63	400	0.04
31.5	0.5	500	0.03
40	0.4	630	0.025
50	0.3	800	0.2
63	0.25	1000	0.016
80	0.2	1250	0.0125

Table 3. Weighting coefficient of weighted acceleration under 1/3 octave bands

Based on the calculation method above, the measured data from several experimental testing in laboratory with the breaker hitting on rubber materials are summarized in Table 4.

Vibration on the breaker--*Down*		Vibration on the prototype structure	T_a=Vibration_up /Vibration_down	Working Condition
Only Z-direction	14.014	4.665	0.332898	3 spring full
	13.852	*5.13896*	*0.370988*	*4 spring no*
	15.469	6.111534	0.395072	4 spring full
	13.875	*4.306374*	*0.310350*	*5 spring no*
	16.619	5.460997	0.328589	5 spring full
Overall X+Y+Z 3 direction	15.580	7.38699961	0.474128835	3 spring full
	15.253	*8.10176862*	*0.53114292*	*4 spring no*
	16.791	8.29026793	0.493730044	4 spring full
	14.713	*7.61053066*	*0.517235251*	*5 spring no*
	17.623	8.24978376	0.468108553	5 spring full

Table 4. Frequency-weighted acceleration of the prototype structure in laboratory testing

In Table 4, the following parameters should be considered

- different springs have different stiffness coefficients (K);
- no loading means that the pushing down force is the weight of the prototype structure itself;
- full loading means that the ideal 15kg downward force is applied.

The following points can be drawn from Table 4:

(i) The vibration on the breakers is about 14 m/s^2, while on the handles it is only about 5 m/s^2. The vibration reduction is very significant (up to 70%), and the suppressed vibration level means that the workers can continuously work up to 5 or 8 hours in comparison to the situation without the structure where the workers can only work about 30 mins.

(ii) When more downward pushing force is applied, the vibration on the breaker is much higher indicating more powerful demolition; but the vibration level on the prototype handles are maintained at a relatively reasonably healthy level with a similar reduction in the overall vibration (there is no significant apparent increase in this despite the increased downward force).

(iii) The addition of more springs in the prototype system can enable more downward pushing force with the same compression level, although the corresponding vibration level on the handles increases (not uniformly due to variation in the hitting surface during testing).

(iv) The overall vibration of all 3 directions has no significant difference from and follows a similar trend to the vibration in the Z-direction since the vibration in the Z-direction dominates. It is much clearer that more springs lead to more vibration energy absorbed from the breaker while lower vibration transmissibilities can be seen in each case comparing the full-loading and no-loading cases, showing again the unique nonlinear stiffness property of the disclosed structures.

Table 5 summarizes the different testing results by calculating the root-mean-square of the measured vibration signals.

Z Down	*Z* Up	T_a=Z_up/Z_down	Working Condition
279.0656823	45.36138	0.16254736	3 spring full loading
275.711242	57.50320	*0.20856314*	*4 spring no loading*
313.633182	64.42959	0.20542979	4 spring full loading
275.2987827	39.62296	*0.14392714*	*5 spring no loading*
334.0796643	52.88027	0.15828642	5 spring full loading

Table 5. RMS of acceleration signals in laboratory testing

Table 5 summarises the overall vibration suppression in terms of vibration energy transmitted from the breaker to the prototype handles.

It can be clearly seen that up to 80% or more vibration energy is suppressed in all cases, and more springs lead to more vibration energy on the breaker which is helpful for demolition

efficiency, while similar vibration transmissibilities can be seen in each case comparing the full-loading and no-loading cases. This clearly shows that the unique nonlinear quasi-zero stiffness of the system of the present disclosure.

Figure 9 shows some time and frequency response for the above test results.

The results are summarized or shown in Table 6 and Figure 9.

It can be seen that the main excitation comes from the vibration frequency of the breaker (around 30 Hz), and there is an obvious vibration peak around 30 Hz. The vibration suppression between 6 Hz and 20 Hz is very good in each test case.

Complicated nonlinear dynamic response can be seen exactly as the analytical analysis before, including super-harmonics, sub-harmonics and intermodulation.

In some cases, the sub-harmonic response is very strong (around 15 Hz) which can be seen both on the breaker and the handles of the structure of the present disclosure due to the coupling dynamics between the structure and the breaker, but still has obvious suppression.

It can be seen that with the apparatus, the vibration on the breaker (Z_1) is higher than that without the apparatus (improved up to 75% in terms of overall vibration energy or 30% for the weighted vibration). This would be understood by a person skilled in the art to reflect improved demolition efficiency.

However, it can also be seen that with the apparatus/structure of the disclosure, the vibration at the handle (Z_2) is suppressed significantly as compared to the traditional breaker Z to a much healthier level according to the ISO hand-arm vibration standard.

	Apparatus+breaker Z_1	Apparatus Handle	Traditional Road
Frequency-weighted acceleration	17.7296±0.5651	6.8486±0.4495	13.6950±0.2414
Root mean square	1072.035±11.4868	416.7246±28.4300	612.856±88.0166

Table 6. On-site vibration testing of the disclosed structure and Traditional Breaker

Figure 10-A-D shows one typical testing result, where "traditional Z" refers to the vibration on the traditional percussive tool (in this case a road breaker) without the disclosed apparatus and system, while the "down, up and hand" refer to the vibration on the tool body, apparatus and system handle and operator hand with the apparatus and system, respectively. As can be seen from these figures, the vibration suppression performance provided by the apparatus and system is very significant, in terms of the overall vibration energy and the vibration within the sensitive frequency range 6-20 Hz.

The nonlinear stiffness of the vibration reduction assembles enables a purely passive vibration reducing apparatus and system. Mathematical modelling, FEM analysis and experimental validation shows this is very effective for vibration suppression up to 70% or above and can significantly reduce the vibration transmitted from percussive tools to operator handles. The system and apparatus of the present disclosure successfully solves vibration issues caused by manually manipulating various construction tools for many years.

The nonlinear stiffness characteristics is very beneficial for passive vibration control, including the following several unique features simultaneously: (1) quasi-zero stiffness, (2) high loading capacity, (3) decreasing stiffness with increasing compression of the structure, (4) flexible & easy to implement, and (5) adjustable structural parameters.

These features enable the apparatus/system to be very effective and efficient in suppression of excessive vibration transmitted to operator hands during manipulating various percussive demolition tools in the construction field, without affecting the handling comfort. At the same time, as significantly reducing the vibration transmission to operators (up to 70% or 90% in different cases), the system can improve the demolition efficiency (up to 30% in terms of weighted vibration energy).

Referring now to Figure 11A, there is depicted an exploded view of the vibration reducing apparatus showing in Figure 1A. In this embodiment, the handle **40** is formed in two pieces **40a** and **40b**, allowing for adjustment of the spacing between the guide members **48a, 48b** of the frame **38**. Similarly, the bottom member which receives the jackhammer or reciprocating tool **60** is comprised of a plurality of length adjustable member **58a** and **58b** together with a central receiving portion **52**. Referring now to Figure 11B, it can be seen that this Figure depicts an exploded view of the transversely extending member **50** which maintains the guide rods **38a**, **38b** in a spaced apart orientation.

The member **50** advantageously is comprised of attachment members **50a** and **50b** which are

attached to the guide means **38a, 38b** and the vibration reducing assemblies **20**. The centre portion of the transversely extending member **50** is advantageously comprised of a clamp, formed by clamping component **52a** and **52b**. These clamping components receive a reciprocating tool such as a jackhammer or road breaker or hammer drill. It would be appreciated that the arrangement depicted is merely exemplary, and other arrangements would maintain the percussive reciprocating tool in the desired orientation would be possible. As shown, there may also be engagement means which slidably attach the vibration assemblies at one or more points along the guide frame.

Referring now to Figure 11C, there is depicted a further embodiment of the vibration reducing apparatus of Figure 1A. Advantageously, it can be seen that the handle **40** is comprised of components **40a** and **40b** which are movable with respect to each other to adjust the spacing between the guide members **38a** and **38b**. The handle is supported on the guide member **38a** such that it can move on the guide members on a biasing means or spring **39**. The spring is supported on the stop **41** which defines the maximum amount of travel permitted for the handle **40**.

Advantageously for safety reasons, the handle may be shaped as shown with an upwardly extending guide which contains the end of guide means to avoid impaling the operator.

It can be seen also that the jackhammer or road breaker **60** is attached such that the axis of reciprocation of the tool is generally aligned with the guide means **38a**, **38b**. Typically these are between 50-120 cm in length and around 30-80cm in width, although these parameters can of course be adjusted based upon the reciprocating tool which is constrained therein.

In the embodiment depicted in Figure 12C, the biasing means or spring **24a, 24b** of the vibration reducing assemblies **20** extend transversely between the ends of the elongate members. There is an additional spring **26** aligned in a direction of the axis of reciprocation which may provide some limited damping.

As would be appreciated by a person skilled in the art to operate the vibration reducing apparatus of the present disclosure, the operator would apply a load to the handle **40**. This load compresses the handle spring **39** until it reach the stop **41**. At the same time, during operation a reciprocating motion is being generated by the percussive tool (jackhammer **60** supported on the guide frame **38a** and **38b**).

The force provided by the operator is transmitted via the vibration assemblies **20** down to the end or point of the working tool **60** via the engagement with the transverse member **50.**

As has been discussed in detail in the foregoing, the non-linear stiffness characteristic of the vibration reducing apparatus under load advantageously isolates the operator's hands which have been placed on the handle from significant amount of vibration in the pre-determined vibration range, for which various parameters of the apparatus may be customised as discussed.

The above embodiments are described by way of example only. Many variations are possible without departing from the scope of the disclosure as defined in the appended claims.

CLAIMS

1. A vibration reducing apparatus for a percussive tool having a working member which reciprocates along an axis of reciprocation, the apparatus comprising:

a guide frame configured for retaining the percussive tool, the guide frame comprising at least two elements extending along and at least one member extending across the axis of reciprocation when the percussive tool is retained therein,

an assembly extending in a direction of along the axis of reciprocation wherein said assembly comprises at least two layers, each layer comprising four interconnected elongate members pivotally attached and rotatable with respect to each other to define a polygon; wherein the assembly has at least one biasing means extending between the ends of at least one pair of elongate interconnected members of a layer and wherein said assembly is displaceable in the direction of along the axis of reciprocation;

a handle movably coupled to the guide frame and supported on the assembly for transmission of an operator applied load down and along the assembly;

wherein the arrangement of the at least one biasing means relative to the elongate members provides decreasing stiffness with increasing compression of the assembly under an operator applied load to the handle for reducing vibration thereof in a predetermined frequency range.

2. The vibration reducing apparatus according to claim 1 comprising one or more further assemblies spaced apart from the assembly, wherein each assembly is attached at one end thereof to the at least one member extending across the axis of reciprocation.

3. The vibration reducing apparatus according to any one of the preceding claims wherein one or more parameters of the or each assembly are modified for achieving one or more of a lower natural resonance frequency relative to a percussive tool without the vibration reducing apparatus; increased loading capacity; a predetermined displacement distance of the at least one or more further assemblies along the axis of reciprocation and size of the at least one or more further assemblies in an unloaded state.

4. The vibration reducing apparatus according to claim 3 wherein one or more of the modified parameters of the or each assembly are selected from the group comprising spring stiffness, the angle between elongate members, the material of the elongate members, the ratio of lengths of elongate members to each other, and the number of layers.

5. The vibration reducing apparatus according to any one of the preceding claims wherein the stiffness of the at least one biasing means is adjustable for changing the resonant frequency of the apparatus.

6. The vibration reducing apparatus according to claim 5 wherein the stiffness of the at least one biasing means is adjusted by substitution with one or more biasing means having a different stiffness to the at least one biasing means.

7. The vibration reducing apparatus according to claim 5 wherein the stiffness of the at least one biasing means is adjusted by the addition or removal of one or more biasing means.

8. The vibration reducing apparatus according to any one of the preceding claims wherein the angle between adjacent elongate members is adjustable so as to modify the vibration suppression provided by the or each assembly.

9. The vibration reducing apparatus according any one of the preceding claims wherein the material of the elongate members is selected so as to have a reduced stiffness relative to steel.

10. The vibration reducing apparatus according to claim 9 wherein the material of the elongate members is aluminium or magnesium.

11. The vibration reducing apparatus according to any one of the preceding claims wherein two or more elongate members of the apparatus have a first length; and wherein the other elongate members of the apparatus have a second length; wherein the relative ratio of the first length to the second length is selected to provide vibration suppression in the apparatus in the predetermined frequency range of 6-20 Hz.

12. The vibration reducing apparatus according to any one of the preceding claims, wherein the angle between the elongate members and/or the stiffness of the at least one biasing means are adjustable so as to maintain the physical size of the apparatus with an increase in the operator applied load.

13. The vibration reducing apparatus according to any one of the preceding claims, wherein the elongate member angle and number of layers in the or each assembly is adjusted so as to modify the possible amount of displacement of the or each assembly in the direction of along the axis of reciprocation.

14. The vibration reducing apparatus according to any one of the preceding claims, wherein the or each assembly are attached to the guide frame at one or more regions distal to the ends of the guide frame for resisting non-vertical deformation under load.

15. The vibration reducing apparatus according to any one of the preceding claims, wherein the or each assembly is configured to reduce vibration transmission from a percussive tool receivable therein in the predetermined frequency range of 6 - 20 Hz.

16. The vibration reducing apparatus according to any one of the preceding claims, wherein at least two of the elongate members are pivotally interconnected with each other at a location distal from the ends thereof.

17. The vibration reducing apparatus according to any one of the preceding claims, wherein the maximum travel of the movably supported handle on the guide member is fixed by stops on the guide frame.

18. The vibration reducing apparatus according to any one of the preceding claims wherein the handle and at least one member extending across the guide frame are adjustable so as to increase the distance between the at least one or more further assemblies and the at least one assembly.

19. The vibration reducing apparatus according to any one of the preceding claims wherein the handle is supported on the frame by a biasing means arranged to extend in a direction of along the axis of reciprocation of the working member of the tool.

20. The vibration reducing apparatus according to any one of the preceding claims wherein the at least one member extending across the axis of reciprocation for retaining the powered percussive tool in the guide frame is an adjustable clamp.

21. The vibration reducing apparatus according to any one of the preceding claims wherein the lengths of elongate members are substantially the same.

22. The vibration reducing apparatus according to any one of the preceding claims wherein at least one pair of intersecting elongate members are arranged asymmetrically about the axis of reciprocation.

23. The vibration reducing apparatus according to claim wherein the tool retained in the guide frame is selected from a group of percussive tools comprising a jackhammer, road breaker and hammer drill.

24. A vibration assembly of a vibration reducing apparatus for a percussive tool having an axis of reciprocation, the vibration assembly comprising:

at least two layers, each layer comprising four interconnected elongate members pivotally attached and rotatable with respect to each other to define a closed loop; the assembly being displaceable in the direction of along the axis of reciprocation and wherein the at least one assembly has at least one biasing means extending between the ends of at least one pair of elongate interconnected members of a layer;

wherein the assembly is configured for engagement with one element of a guide frame comprising at least two elements extending along the axis of reciprocation of the tool and at least one member extending across the axis of reciprocation wherein said at least one member is configured to retain the powered percussive tool in the guide frame;

wherein the assembly is configured for supporting at least one part of a handle movably coupled to the guide frame for transmission of force to the percussive tool and wherein the arrangement of the at least one biasing means relative to the elongate members provides decreasing stiffness with increasing compression of the assembly under an operator applied load to the handle for reducing vibration thereof in a predetermined frequency range.

25. A method of using the vibration reducing apparatus according to any one of the preceding claims with a tool selected from the group of percussive tools comprising a jackhammer, road breaker and hammer drill.

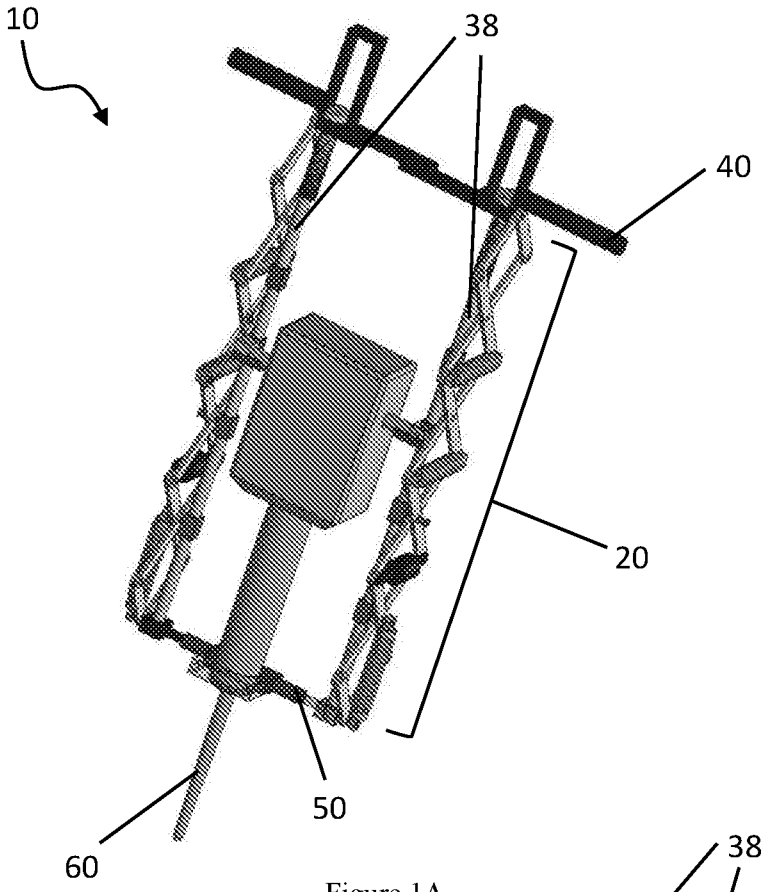

Figure 1A

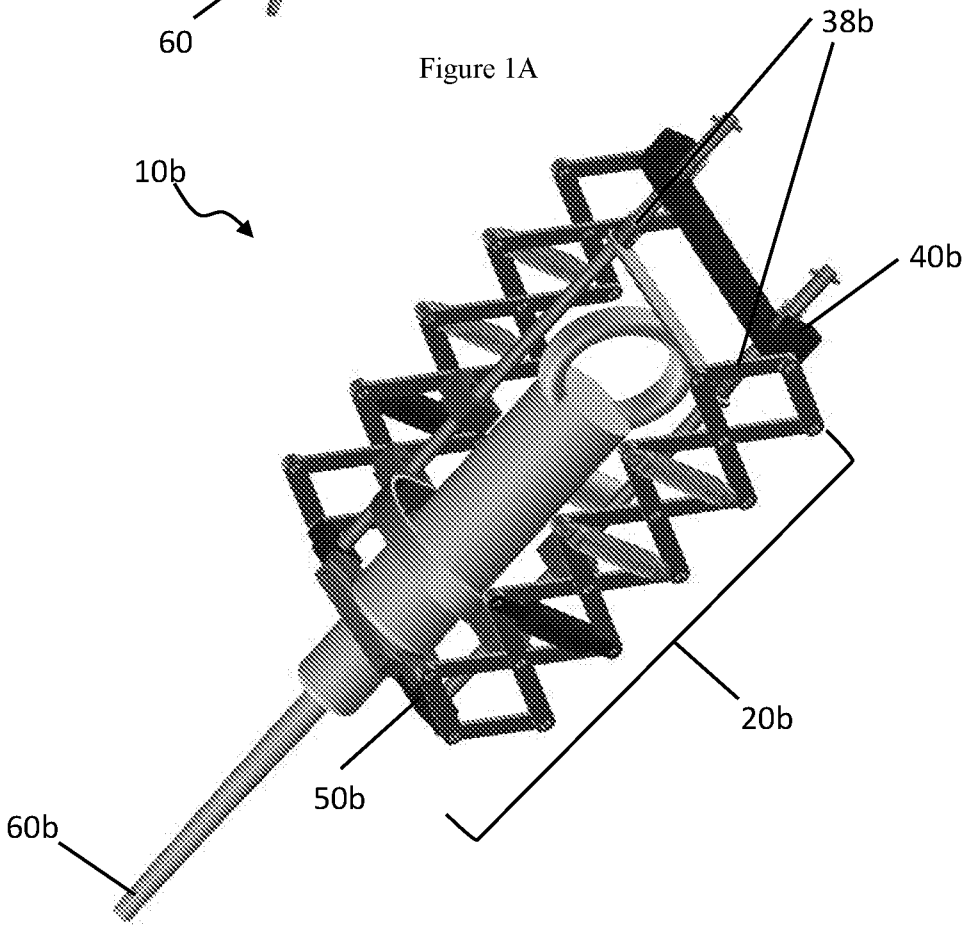

Figure 1B

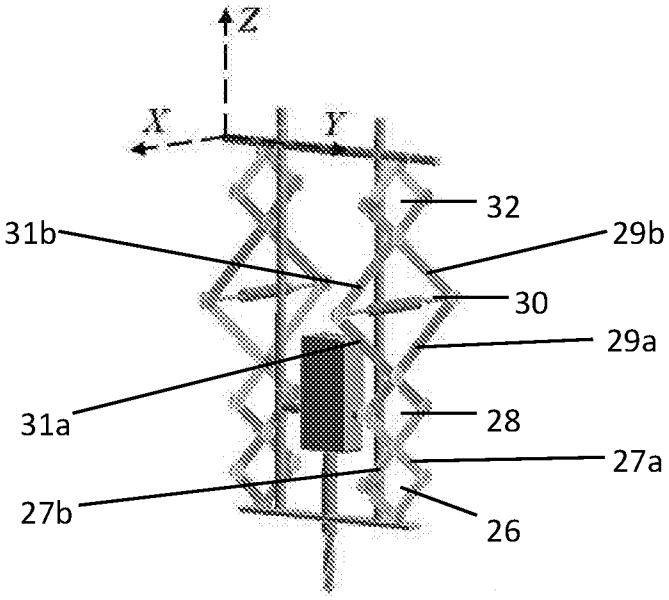

Figure 2A

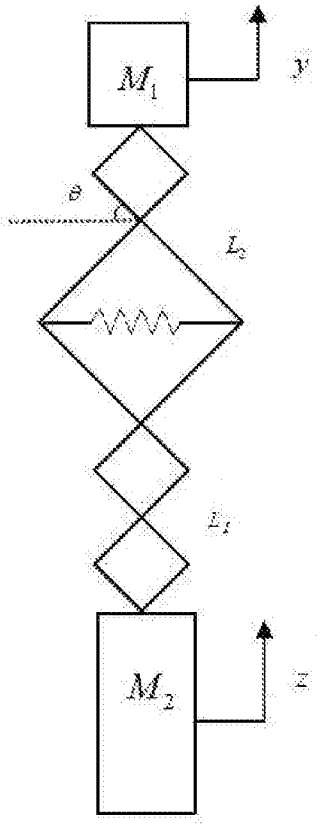

Figure 2B

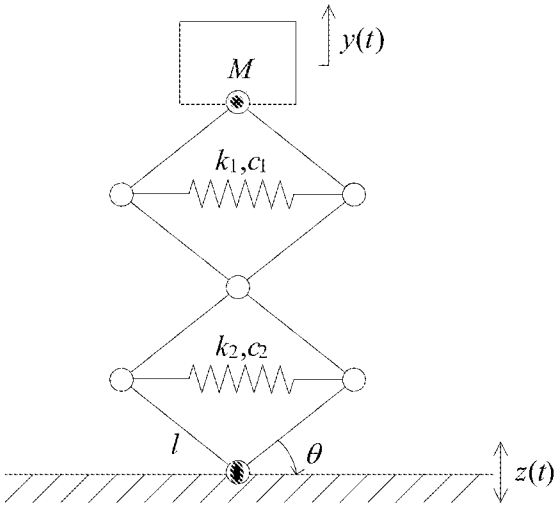

Figure 2C

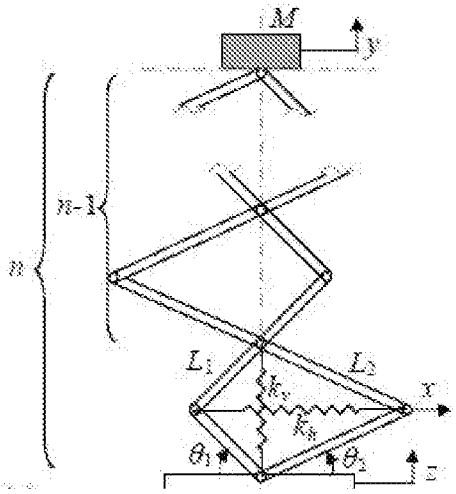

Figure 2D

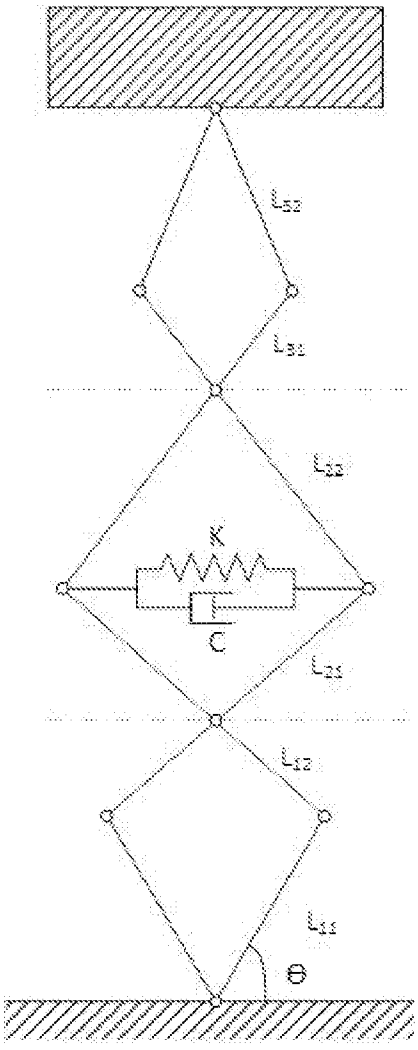

Figure 2E

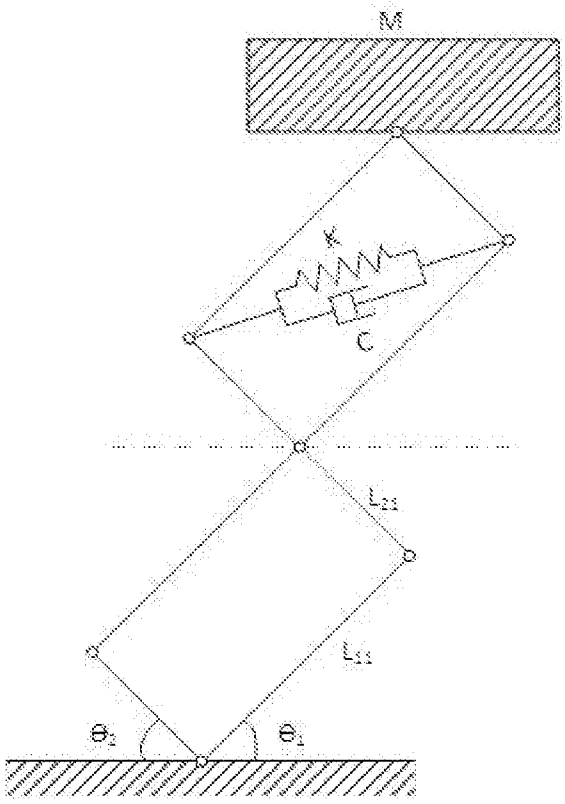

Figure 2F

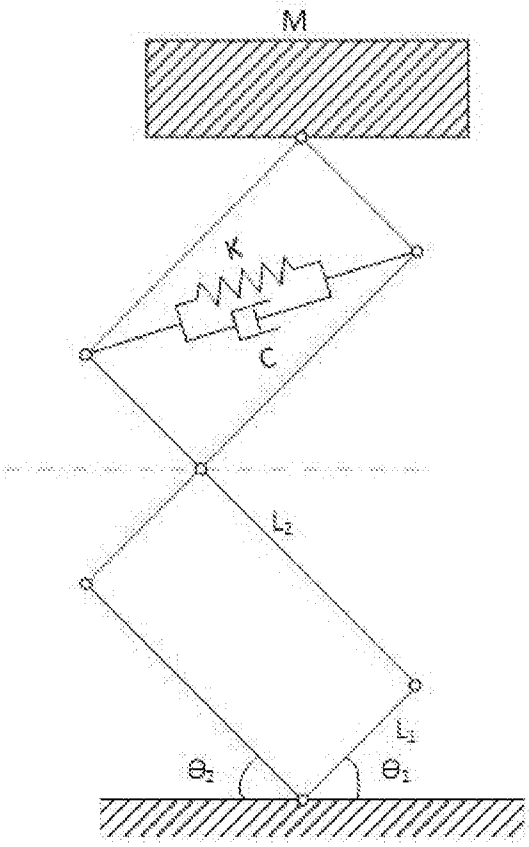

Figure 2G

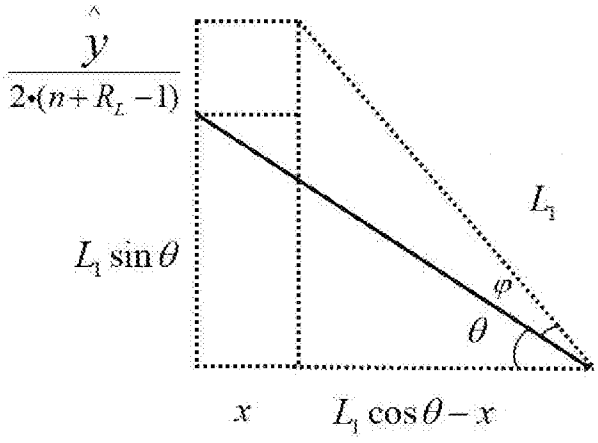

Figure 2H

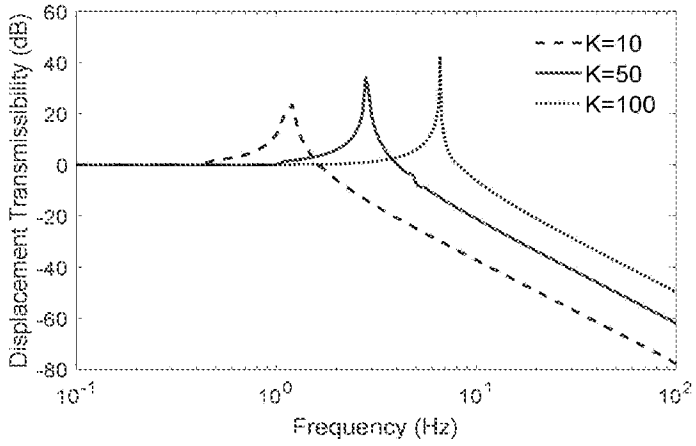

Figure 3A

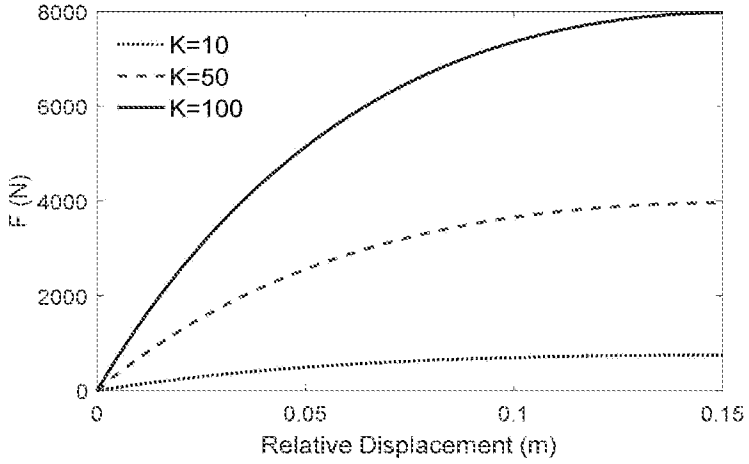

Figure 3B

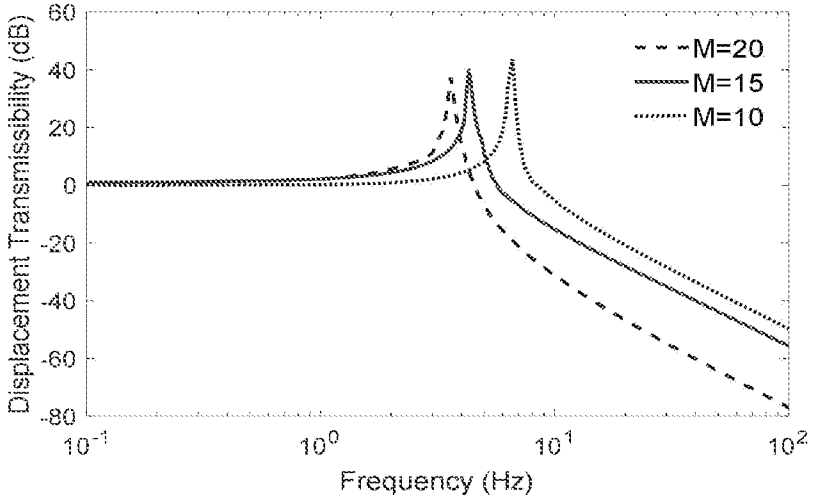

Figure 3C

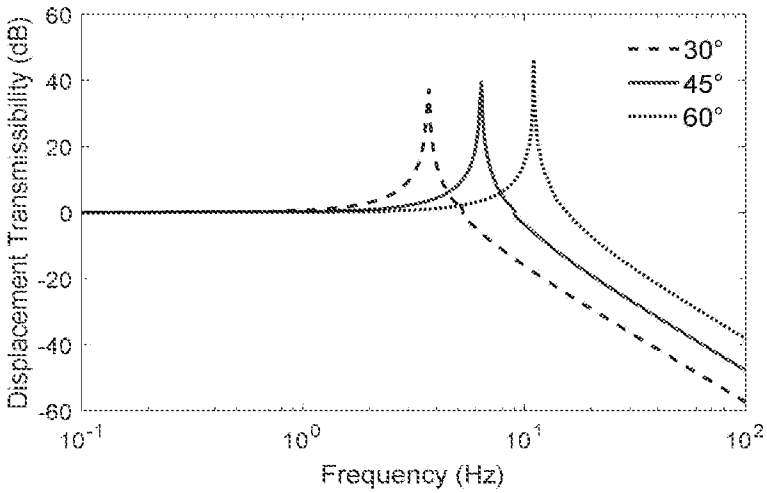

Figure 3D

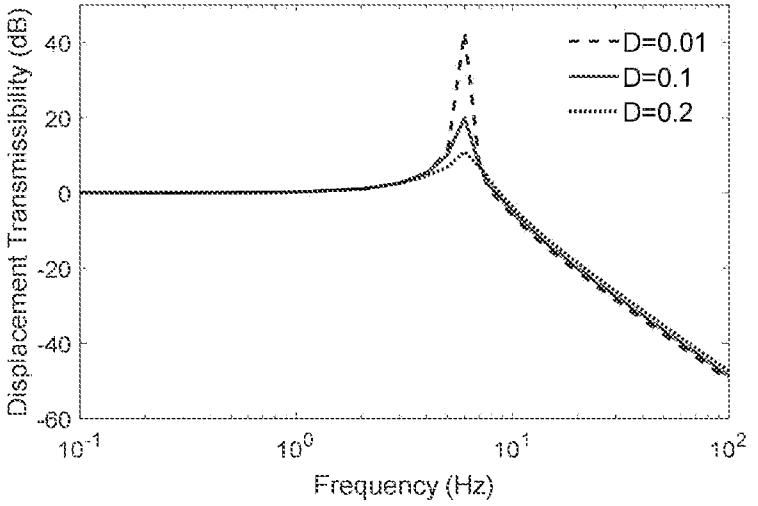

Figure 3E

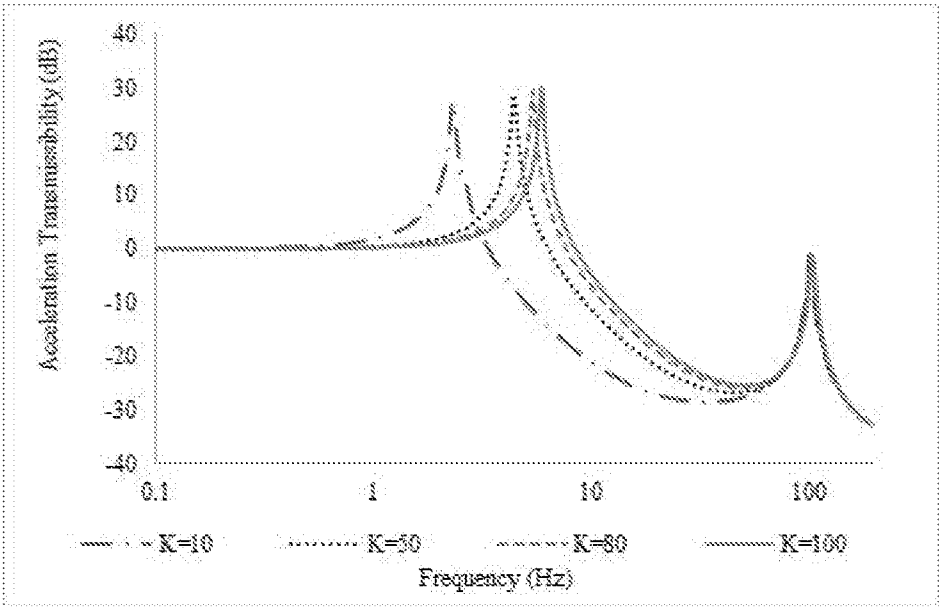

Figure 4A

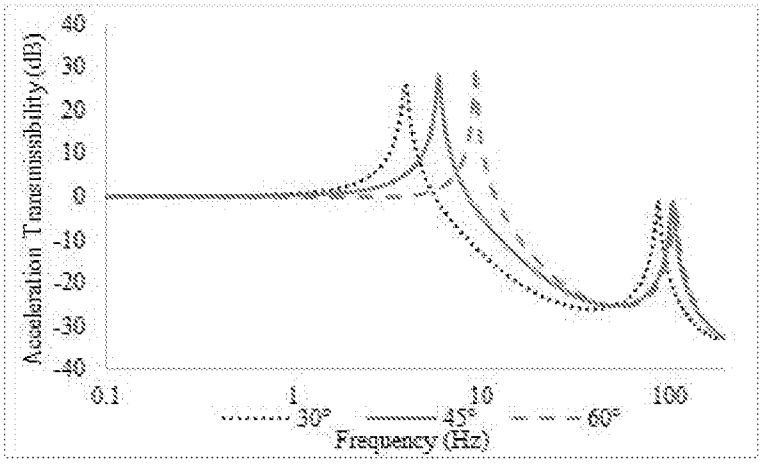

Figure 4B

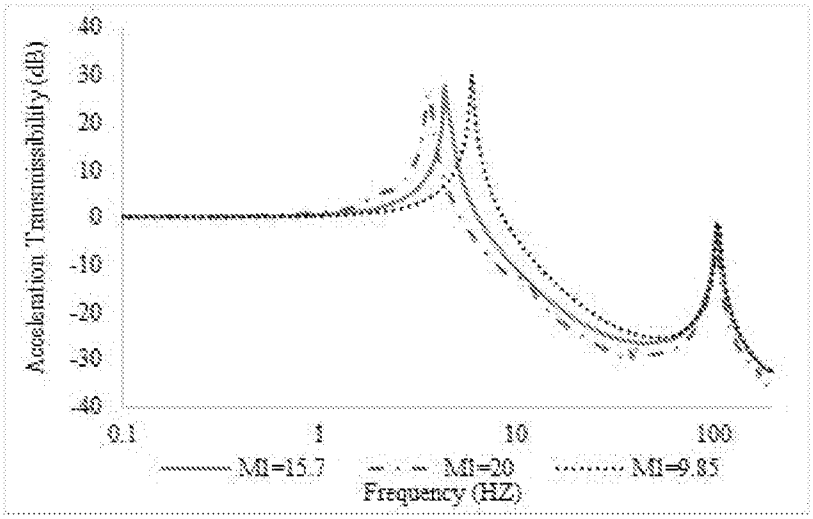

Figure 4C

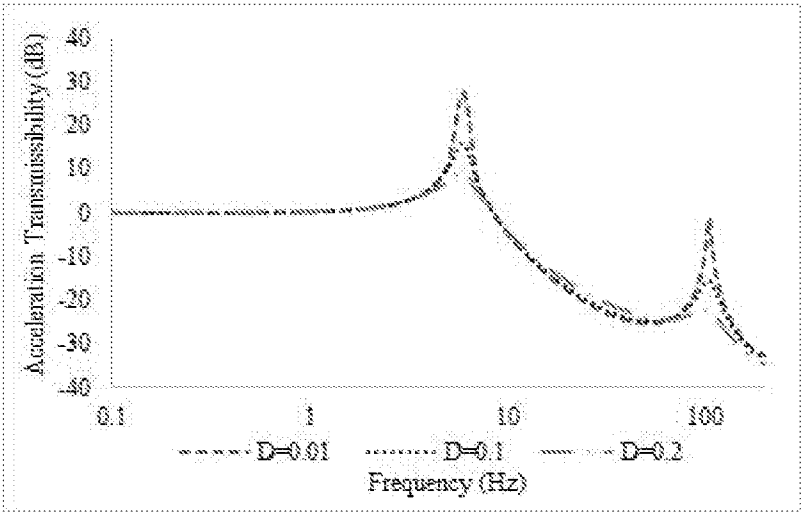

Figure 4D

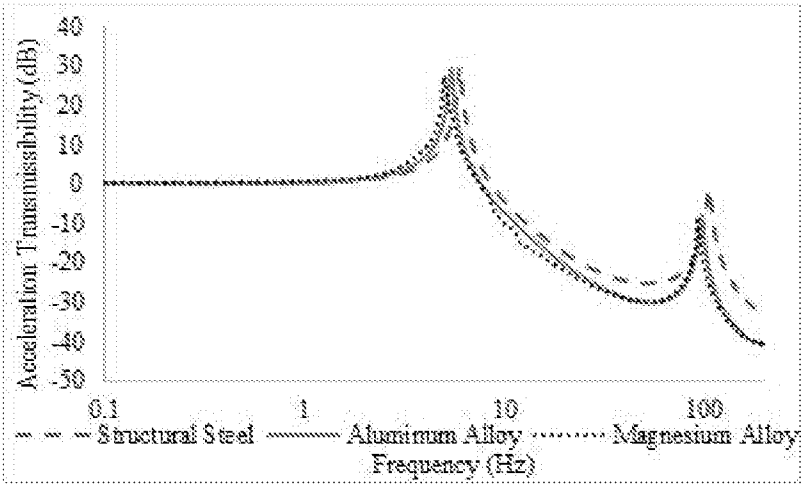

Figure 4E

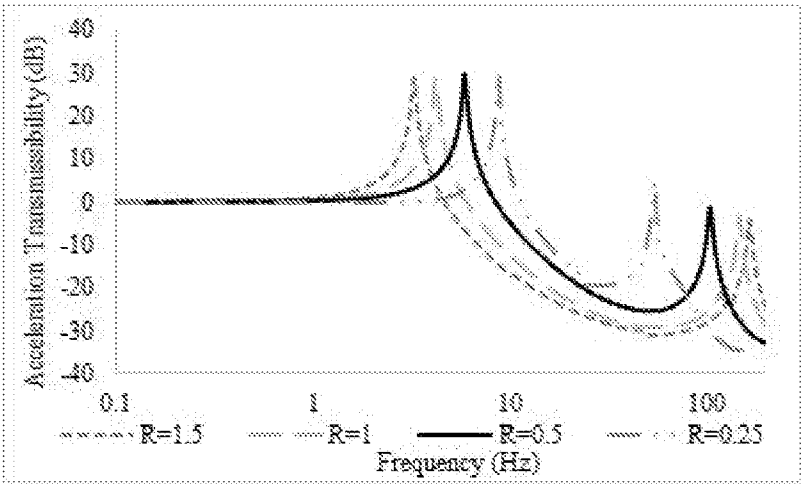

Figure 4F

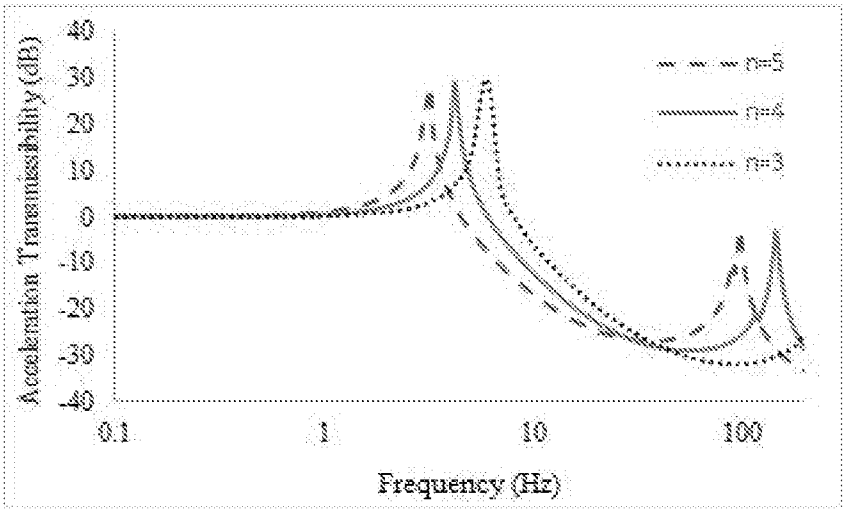

Figure 4G

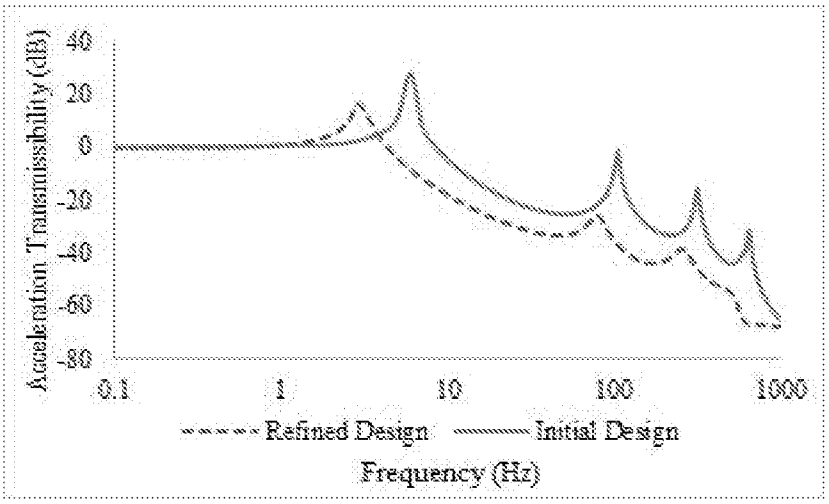

Figure 5

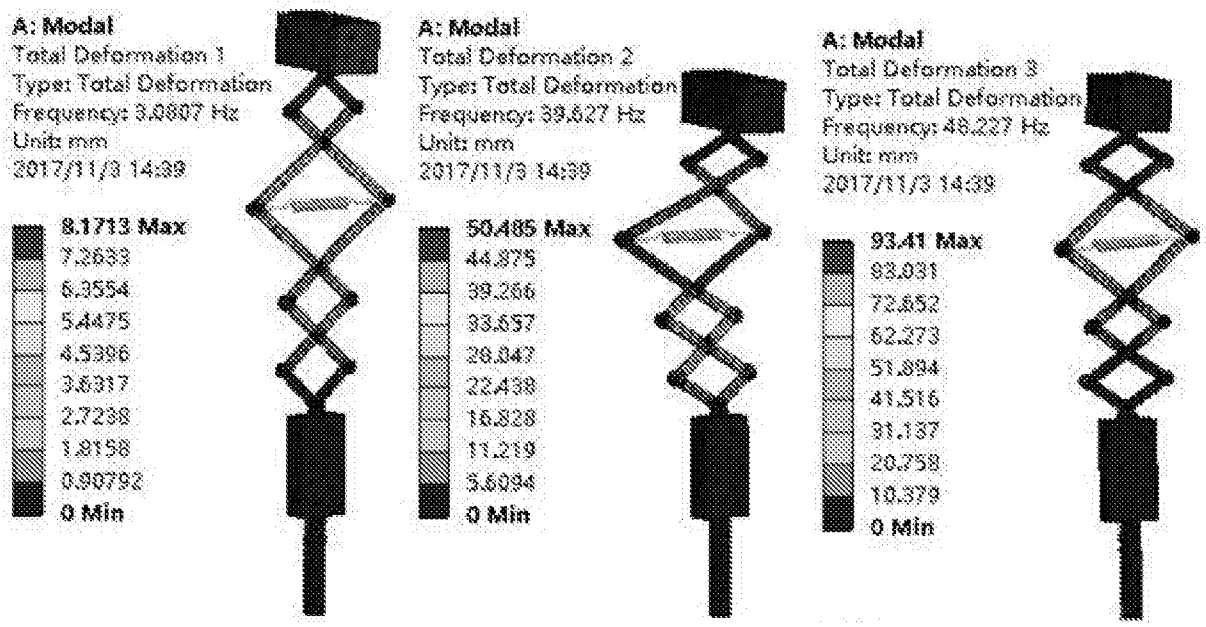

Figure 6A

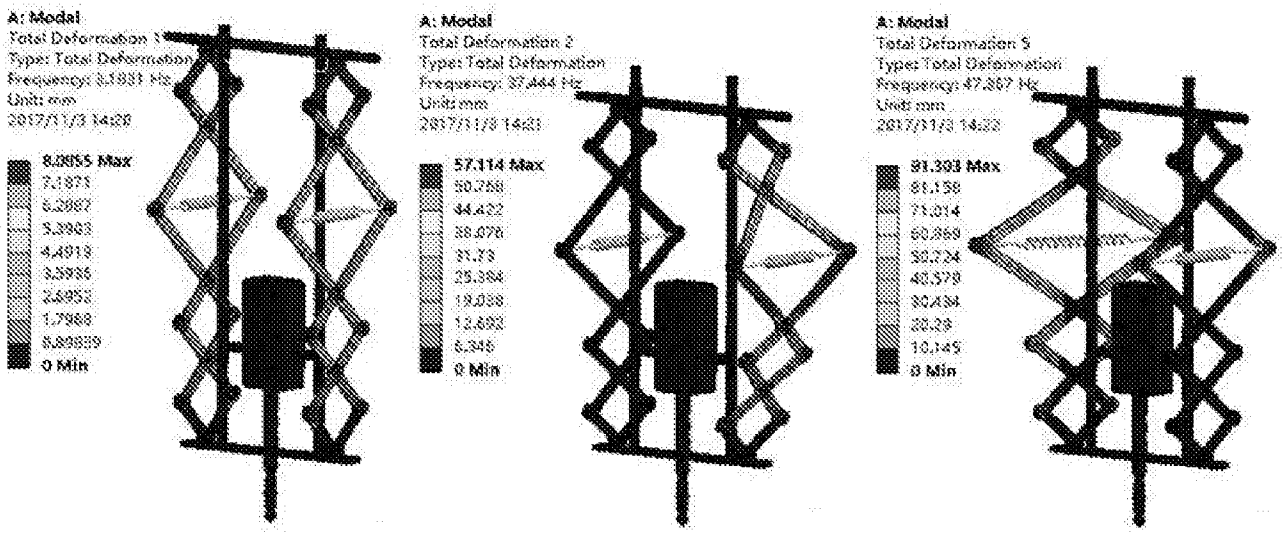

Figure 6B

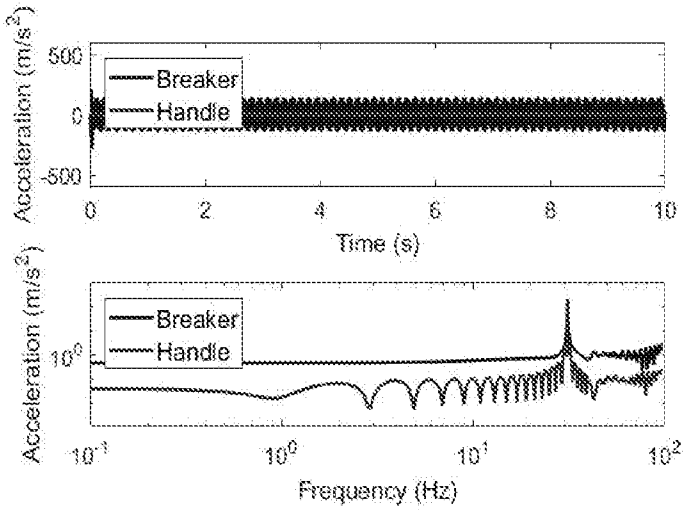

(a). 2*KN* Input Force

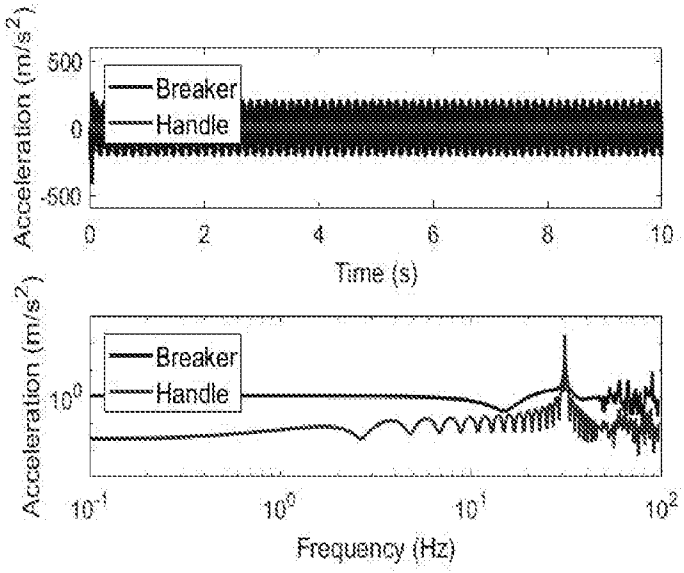

(b). 6*KN* Input Force

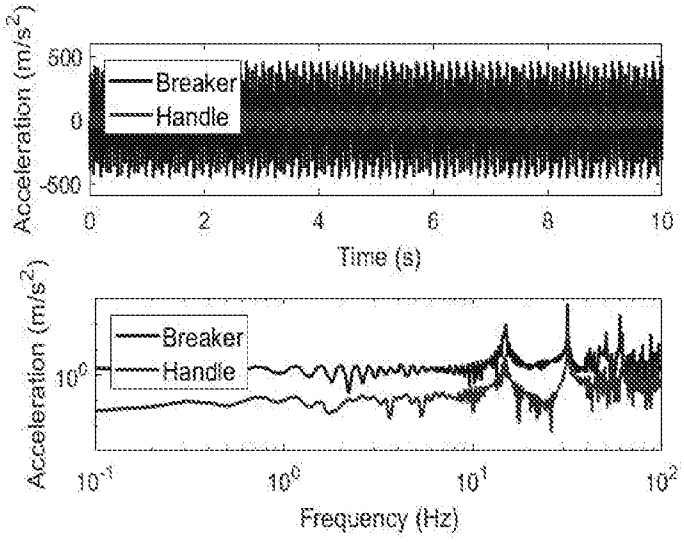

(c). 10*KN* Input Force

Figure 7

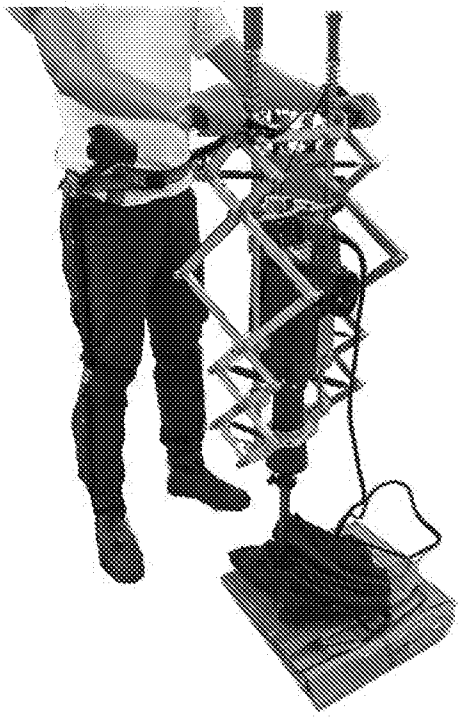

Figure 8A

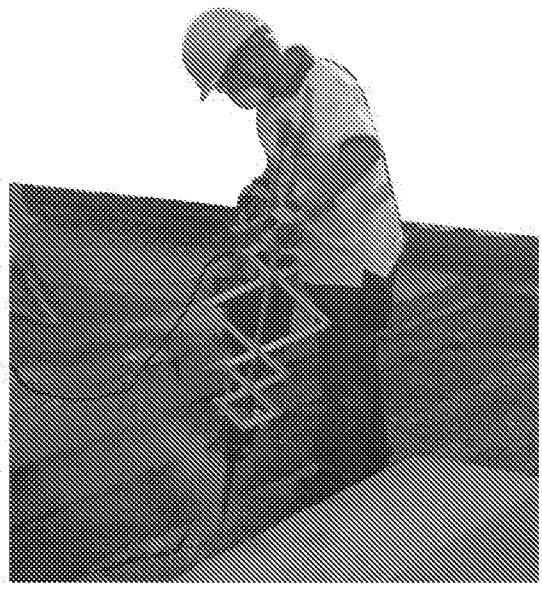

Figure 8B

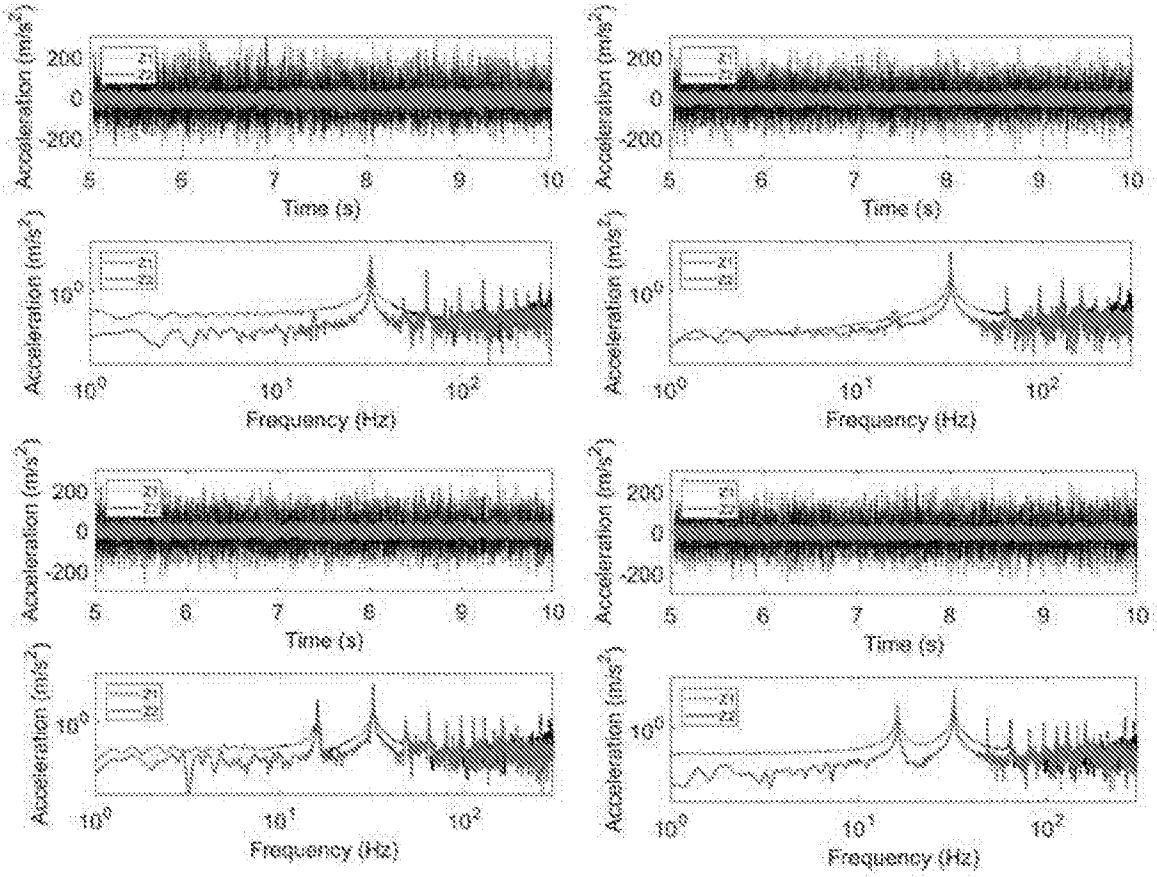

Figure 9

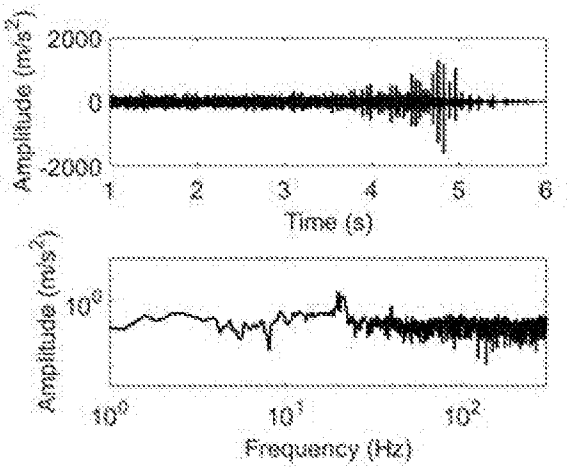

Figure 10A

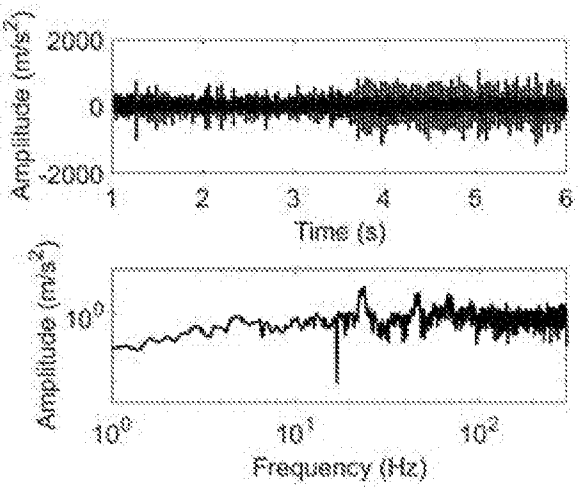

Figure 10B

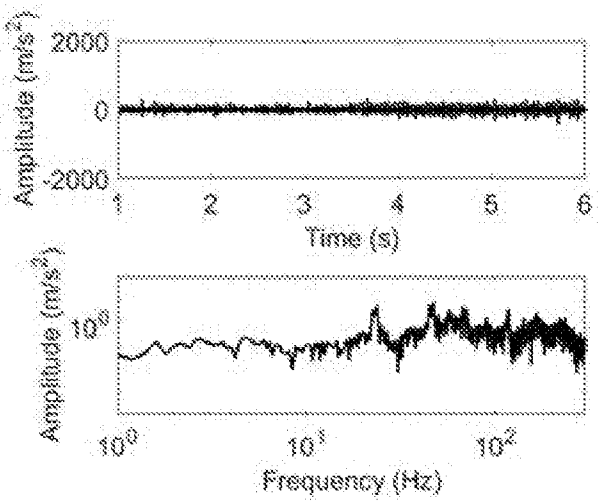

Figure 10C

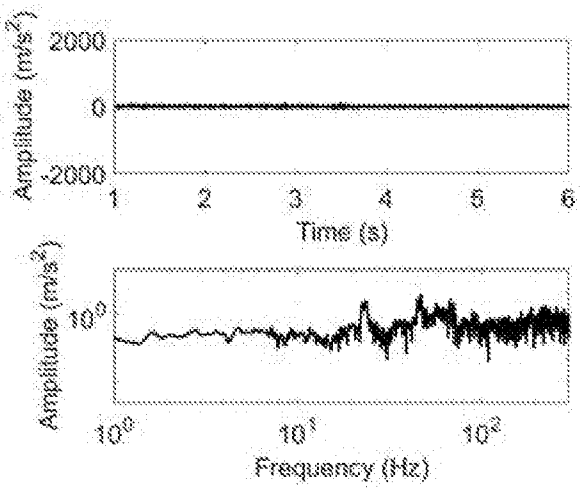

Figure 10D

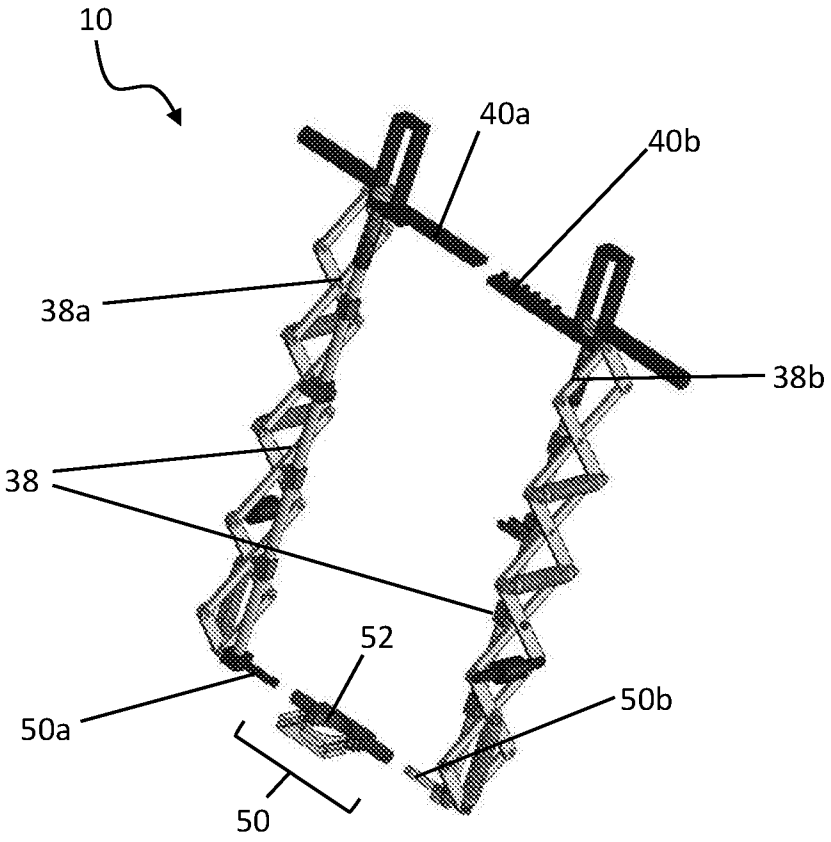

Figure 11A

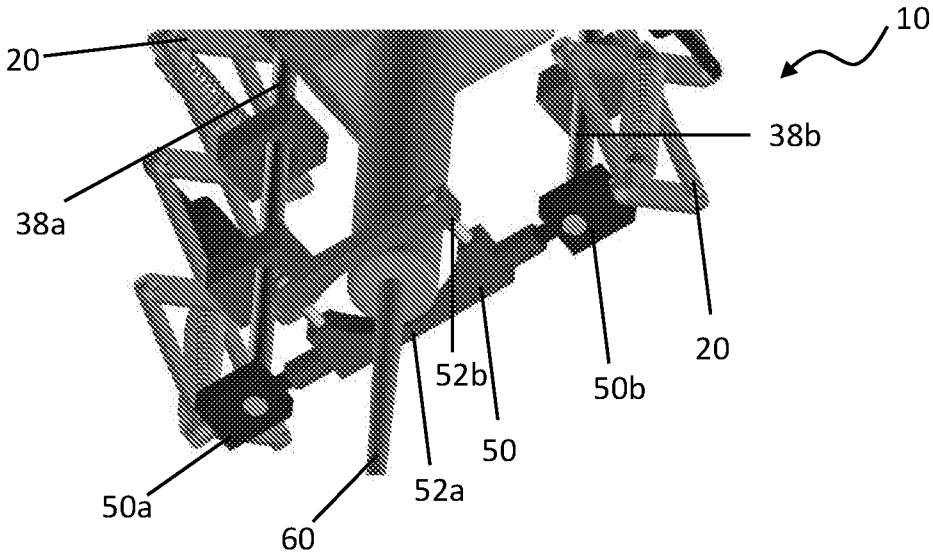

Figure 11B

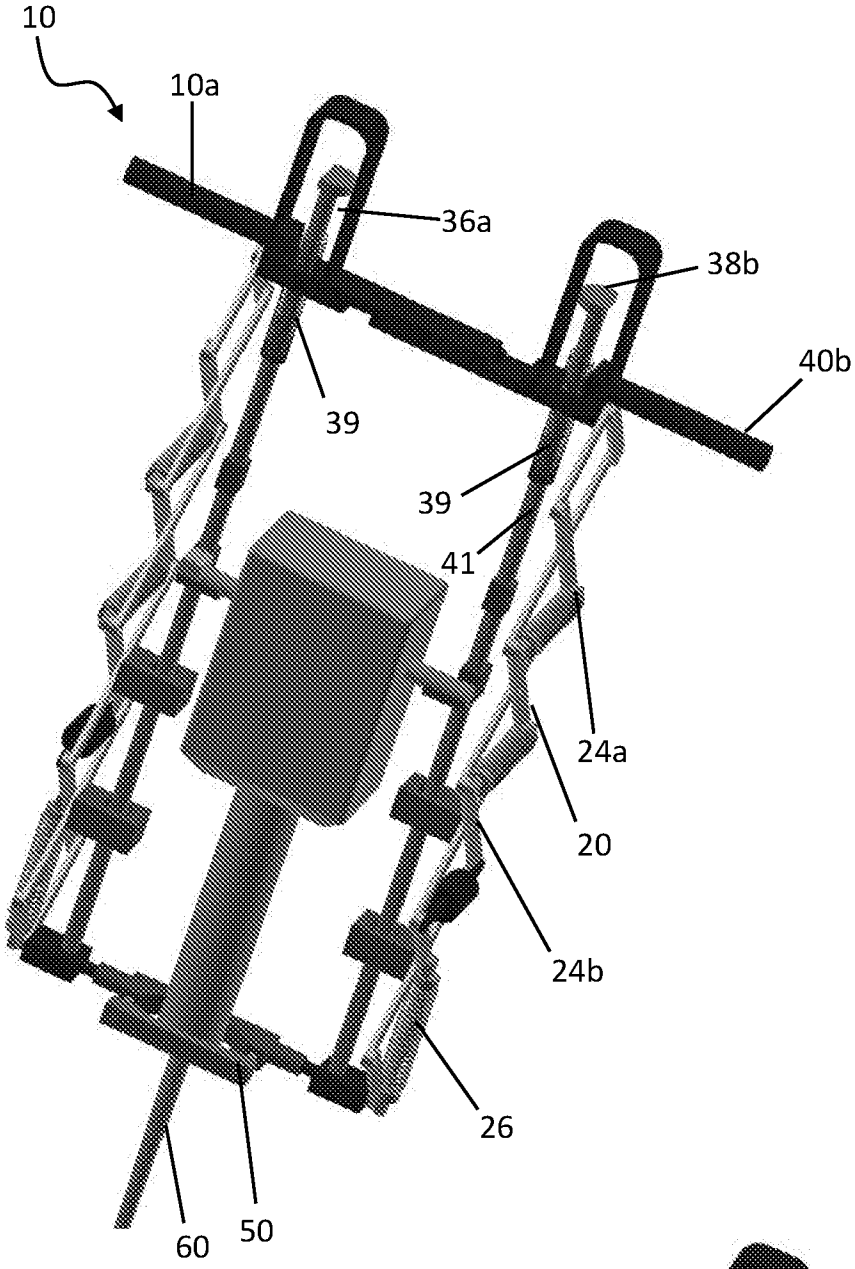

Figure 11C

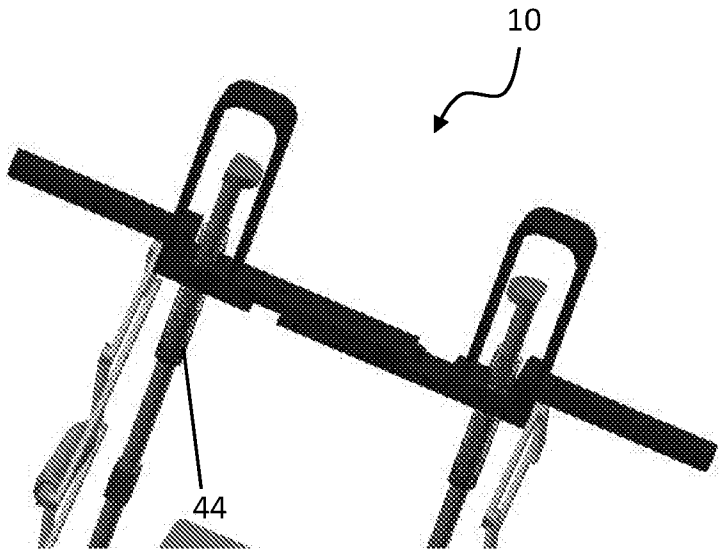

Figure 11D

INTERNATIONAL SEARCH REPORT

International application No.
PCT/CN2018/074644

A. CLASSIFICATION OF SUBJECT MATTER

E21B 1/00(2006.01)i

According to International Patent Classification (IPC) or to both national classification and IPC

B. FIELDS SEARCHED

Minimum documentation searched (classification system followed by classification symbols)

E21B; E01B

Documentation searched other than minimum documentation to the extent that such documents are included in the fields searched

Electronic data base consulted during the international search (name of data base and, where practicable, search terms used)

CNPAT,EPODOC,WPI,CNKI:impact+,percuss+,impuls+,strik+,vibrat+,reduc+,suppress+,layer?,spring?,elastic+,elongate, polygon,stiff+

C. DOCUMENTS CONSIDERED TO BE RELEVANT

Category*	Citation of document, with indication, where appropriate, of the relevant passages	Relevant to claim No.
A	CN 104264541 A (ANYANG ANZHEN HIGH TECH. INDUSTRY CO., LTD.) 07 January 2015 (2015-01-07) description, page 2, figures 1-2	1-26
A	CN 205078197 U (SHANDONG ZHONGRUI CONSTRUCTION MACHINERY CO., LTD.) 09 March 2016 (2016-03-09) the whole document	1-26
A	CN 202100211 U (SHAO, XUEZHONG) 04 January 2012 (2012-01-04) the whole document	1-26
A	CN 101906940 A (XU, YAN) 08 December 2010 (2010-12-08) the whole document	1-26
A	US 7059423 B1 (HOGGARTH, DEVERNE) 13 June 2006 (2006-06-13) the whole document	1-26
A	JP H11179680 A (FURUKAWA CO., LTD.) 06 July 1999 (1999-07-06) the whole document	1-26

☐ Further documents are listed in the continuation of Box C. ☑ See patent family annex.

* Special categories of cited documents:

"A" document defining the general state of the art which is not considered to be of particular relevance

"E" earlier application or patent but published on or after the international filing date

"L" document which may throw doubts on priority claim(s) or which is cited to establish the publication date of another citation or other special reason (as specified)

"O" document referring to an oral disclosure, use, exhibition or other means

"P" document published prior to the international filing date but later than the priority date claimed

"T" later document published after the international filing date or priority date and not in conflict with the application but cited to understand the principle or theory underlying the invention

"X" document of particular relevance; the claimed invention cannot be considered novel or cannot be considered to involve an inventive step when the document is taken alone

"Y" document of particular relevance; the claimed invention cannot be considered to involve an inventive step when the document is combined with one or more other such documents, such combination being obvious to a person skilled in the art

"&" document member of the same patent family

Date of the actual completion of the international search	Date of mailing of the international search report
02 April 2018	**26 April 2018**
Name and mailing address of the ISA/CN **STATE INTELLECTUAL PROPERTY OFFICE OF THE P.R.CHINA** **6, Xitucheng Rd., Jimen Bridge, Haidian District, Beijing 100088** **China**	Authorized officer **WANG,Hongjun**
Facsimile No. **(86-10)62019451**	Telephone No. **(86-10)010-53961019**

INTERNATIONAL SEARCH REPORT
Information on patent family members

International application No.
PCT/CN2018/074644

Patent document cited in search report			Publication date (day/month/year)	Patent family member(s)			Publication date (day/month/year)
CN	104264541	A	07 January 2015	CN	104264541	B	02 November 2016
CN	205078197	U	09 March 2016		None		
CN	202100211	U	04 January 2012		None		
CN	101906940	A	08 December 2010	CN	101906940	B	15 August 2012
US	7059423	B1	13 June 2006		None		
JP	H11179680	A	06 July 1999		None		

(19)中华人民共和国国家知识产权局

(12)发明专利申请

(10)申请公布号 CN 109312600 A
(43)申请公布日 2019.02.05

(21)申请号 201880000340.0

(22)申请日 2018.01.31

(30)优先权数据
62/462,795 2017.02.23 US

(85)PCT国际申请进入国家阶段日
2018.04.26

(86)PCT国际申请的申请数据
PCT/CN2018/074644 2018.01.31

(87)PCT国际申请的公布数据
WO2018/153226 EN 2018.08.30

(71)申请人 香港理工大学
地址 中国香港九龙红磡

(72)发明人 景兴建

(74)专利代理机构 上海德昭知识产权代理有限公司 31204
代理人 郁旦蓉

(51)Int.Cl.
E21B 1/00(2006.01)

权利要求书3页 说明书21页 附图19页

(54)发明名称

改进的被动减振设备

(57)摘要

提供了用于具有往复运动轴线的冲击工具(60)的减振设备(10)。该设备包括引导框架(38、38a、38b)和横穿往复运动轴线延伸的至少一个构件(50)。在沿着往复运动轴线的方向上延伸的组合件(20)包括至少两个层(26、28、30、32),并且每个层包括四个互连的细长构件(27a、27b、29a、29b、31a、31b),四个互连的细长构件枢转地附接并且相对于彼此可旋转以限定多边形;并且该组合件具有至少一个偏置装置(24a、24b)。手柄(40)可移动地连接到引导框架并支撑在组合件上。在操作员向手柄施加负载的情况下,该设备随着组合件增加的压缩而提供减小的刚度,以用于减小在预定频率范围内的振动。

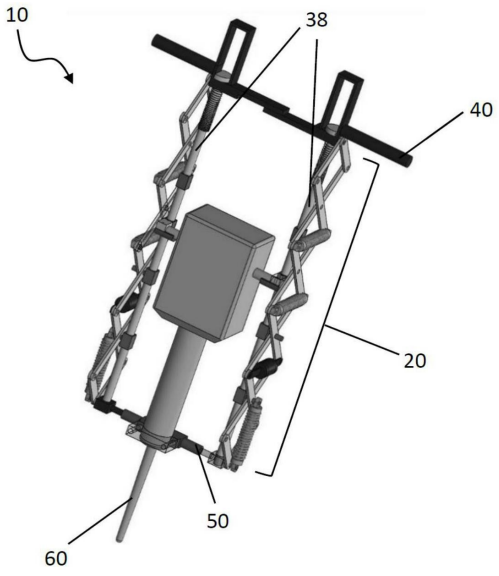

CN 109312600 A

1.一种用于冲击工具的减振设备,所述冲击工具具有沿着往复运动轴线进行往复运动的工作构件,所述设备包括:

引导框架,所述引导框架被配置用于保持所述冲击工具,所述引导框架包括沿着所述往复运动轴线延伸的至少两个元件和当所述冲击工具被保持在所述引导框架中时横穿所述往复运动轴线延伸的至少一个构件,

组合件,所述组合件在沿着所述往复运动轴线的方向上延伸,其中,所述组合件包括至少两个层,每个层包括四个互连的细长构件,四个互连的所述细长构件枢转地附接并且相对于彼此可旋转以限定多边形;其中,所述组合件具有至少一个偏置装置,所述偏置装置在层的至少一对互连的细长构件的端部之间延伸,并且其中,所述组合件可在沿着所述往复运动轴线的方向上移位;

手柄,所述手柄可移动地连接到所述引导框架并且支撑在所述组合件上,以用于向下并沿着所述组合件传递操作员施加的负载;

其中,在操作员向所述手柄施加负载的情况下,所述至少一个偏置装置相对于所述细长构件的布置随着所述组合件增加的压缩而提供减小的刚度,以用于减小所述手柄在预定频率范围内的振动。

2.根据权利要求1所述的减振设备,包括与所述组合件间隔开的一个或多个其他组合件,其中,每个组合件在其一端部处附接至横穿所述往复运动轴线延伸的所述至少一个构件。

3.根据前述权利要求中任一项所述的减振设备,其中,所述组合件或每个组合件的一个或多个参数被修改以实现以下各项中的一项或多项:相对于没有所述减振设备的冲击工具而言更低的固有谐振频率;增加的负载容量;所述至少一个或多个其他组合件沿着所述往复运动轴线的预定位移距离以及所述至少一个或多个其他组合件在无负载状态下的大小。

4.根据权利要求3所述的减振设备,其中,所述组合件或每个组合件的经修改的参数中的一个或多个参数选自包括以下各项的组:弹簧刚度、细长构件之间的角度、所述细长构件的材料、细长构件相对于彼此的长度比率,以及层数。

5.根据前述权利要求中任一项所述的减振设备,其中,所述至少一个偏置装置的刚度是可调节的,以改变所述设备的谐振频率。

6.根据权利要求5所述的减振设备,其中,所述至少一个偏置装置的刚度通过用具有与所述至少一个偏置装置不同的刚度的一个或多个偏置装置代替来调节。

7.根据权利要求5所述的减振设备,其中,所述至少一个偏置装置的刚度通过添加或移除一个或多个偏置装置来调节。

8.根据前述权利要求中任一项所述的减振设备,其中,相邻细长构件之间的角度是可调节的,以便修改由所述组合件或每个组合件提供的振动抑制。

9.根据前述权利要求中任一项所述的减振设备,其中,选择所述细长构件的材料以便具有相对于钢而言减小的刚度。

10.根据权利要求9所述的减振设备,其中,所述细长构件的材料是铝或镁。

11.根据前述权利要求中任一项所述的减振设备,其中,所述设备的两个或更多个细长构件具有第一长度;并且其中,所述设备的其他细长构件具有第二长度;其中,选择所述第

一长度与所述第二长度的相对比率以在所述设备中提供6-20Hz的预定频率范围内的振动抑制。

12.根据前述权利要求中任一项所述的减振设备，其中，所述细长构件之间的角度和/或所述至少一个偏置装置的刚度是可调节的，以便随着所述操作员施加的负载的增加而保持所述设备的所述物理大小。

13.根据前述权利要求中任一项所述的减振设备，其中，调节所述组合件或每个组合件中的所述细长构件的角度和层数，以便修改所述组合件或每个组合件在沿着所述往复运动轴线的方向上的可能位移量。

14.根据前述权利要求中任一项所述的减振设备，其中，所述组合件或每个组合件在远离所述引导框架的端部的一个或多个区域处附接至所述引导框架，以抵抗负载下的非垂直变形。

15.根据前述权利要求中任一项所述的减振设备，其中，所述组合件或每个组合件被配置用于减少来自可接纳在所述组合件中的冲击工具的在6-20Hz的预定频率范围内的振动传递。

16.根据前述权利要求中任一项所述的减振设备，其中，所述细长构件中的至少两个在远离所述细长构件的端部的位置处彼此枢转地互连。

17.根据前述权利要求中任一项所述的减振设备，其中，可移动地支撑的所述手柄在所述引导构件上的最大行程由所述引导框架上的止动件来固定。

18.根据前述权利要求中任一项所述的减振设备，其中，所述手柄和跨所述引导框架延伸的至少一个构件是可调节的，以便增加所述至少一个或多个其他组合件与所述至少一个组合件之间的距离。

19.根据前述权利要求中任一项所述的减振设备，其中，所述手柄由偏置装置支撑在所述框架上，所述偏置装置被布置用于在沿着所述工具的所述工作构件的往复运动轴线的方向上延伸。

20.根据前述权利要求中任一项所述的减振设备，其中，用于将电动的所述冲击工具保持在所述引导框架中的、横穿所述往复运动轴线延伸的所述至少一个构件可以是可调节的夹具。

21.根据前述权利要求中任一项所述的减振设备，其中，细长构件的长度是基本上相同的。

22.根据前述权利要求中任一项所述的减振设备，其中，至少一对相交的细长构件被布置成关于所述往复运动轴线不对称。

23.根据权利要求所述的减振设备，其中，保持在所述引导框架中的所述工具选自包括以下各项的一组冲击工具：手提钻、路面破碎机和冲击钻。

24.一种用于冲击工具的减振设备的振动组合件，所述冲击工具具有往复运动轴线，所述振动组合件包括：

至少两个层，每个层包括四个互连的细长构件，四个互连的所述细长构件枢转地附接并且相对于彼此可旋转以限定闭环；所述组合件可在沿着所述往复运动轴线的方向上移位，并且其中，至少一个所述组合件具有至少一个偏置装置，所述偏置装置在层的至少一对互连的细长构件的端部之间延伸；

其中，所述组合件被配置用于与引导框架的一个元件接合，所述引导框架包括沿着所述工具的所述往复运动轴线延伸的至少两个元件以及横穿所述往复运动轴线延伸的至少一个构件，其中，所述至少一个构件被配置用于将电动的所述冲击工具保持在所述引导框架中；

其中，所述组合件被配置用于支撑手柄的至少一部分，所述手柄可移动地连接到所述引导框架以将力传递到所述冲击工具，并且其中，在操作员向所述手柄施加负载的情况下，所述至少一个偏置装置相对于所述细长构件的布置随着所述组合件的增加的压缩而提供减小的刚度，以用于减小所述手柄在预定频率范围内的振动。

25.一种使用根据前述权利要求中任一项所述的减振设备的方法，其中，工具选自包括以下各项的一组冲击工具：手提钻、路面破碎机和冲击钻。

改进的被动减振设备

技术领域

[0001] 本披露涉及一种改进的被动减振设备和系统，该被动减振设备和系统特别适用于抑制由往复式工具发出的振动。

背景技术

[0002] 振动是一种振荡类型，其特征在于在近平衡态下的系统中的有限小振荡。在大多数工程方面，因为机械振动影响机械特性、加剧疲劳和磨损，并且甚至可能造成结构的破坏，所以这种振动被认为是需要被控制的负面因素。

[0003] 从各种电动工具诸如夯锤、凿岩机、电镐、路面破碎机、冲击钻、錾平锤或锯子等的操作传递给施工人员的振动是振动对电动工具的操作员直接造成严重健康影响的领域。在本领域中已知，人类感知的振动频率范围为从1至1000Hz，其中人类对1-80Hz的振动最敏感。具体地，最有害的振动在6Hz与20Hz之间的频率范围内。当施工人员牢牢抓住电动工具的手柄以提高此类装置的控制和效率时，局部振动传递到使用者的手和手臂以及他们的全身。

[0004] 局部振动可导致手指动脉收缩并降低抓握能力，其中因操作手持式机器而长期暴露于高水平的振动会导致正常循环以及神经和肌肉骨骼系统方面的问题。长期高水平的振动能够严重损害人体、造成相当大的疼痛，并且甚至造成永久性残疾，其中振动的频率和强度是关键成因。这导致了关于操作员能够安全操作设备多久的实际限制，此实际限制继而影响需要分配给特定任务的资源。

[0005] 振动也会影响大型(通常是车载式)系统诸如碎石机的操作。如本领域的技术人员所已知，这种机器的驱动活塞由氮气、液压油或其组合激发，以冲击在工地对材料进行粉碎、破裂或分割的工作工具。过度的振动潜在地影响此类系统中的部件的使用寿命，并可能导致故障以及降低性能。

[0006] 典型的传统阻尼器对于所有频率具有相同的阻尼系数；其中较高的阻尼器具有较小的谐振峰；以及在高频率时较差的振动幅值；这是因为阻尼器对于较小的振动位移来说是非常刚性和粘性的。为了适当地提供振动抑制；在系统的谐振频率下需要高阻尼；而在其他频率下需要较低的阻尼。

[0007] 特别是在手持式机器的情况下，存在主动阻尼机构，该主动阻尼机构包括用于监测来源的振动的传感器，其中一些布置用于产生足以衰减振动的具有适当相位和振幅的反作用力。然而，大多数主动阻尼机构显著地增加了成本和重量，并且可能影响包含它们的工具的整体性能。

[0008] 不幸的是，大多数使用传统弹簧或阻尼器的传统被动减振系统(特别是手持式工具)不会抑制振动，这是因为(1)工作人员需要向下按压以牢固地保持机器从而实现高操作效率；并且(2)随着传统弹簧或材料被更多地压缩，其刚性显著增加，且因此所提供的振动抑制的量显著减少。

发明内容

[0009] 本披露的特征和优点将在下面的描述中阐述，并且从所述描述来看，部分内容将是显而易见的，或者可以通过实践本文中披露的原理而习得部分内容。可以借助于在所附权利要求书中特别指出的手段和组合来实现和获得本披露的特征和优点。

[0010] 根据本披露的第一方面，提供了一种用于冲击工具的减振设备，该冲击工具具有沿着往复运动轴线进行往复运动的工作构件，该设备包括：

[0011] 引导框架，该引导框架被配置用于保持该冲击工具，该引导框架包括沿着该往复运动轴线延伸的至少两个元件和当该冲击工具被保持在该引导框架中时横穿该往复运动轴线延伸的至少一个构件，

[0012] 组合件，该组合件在沿着该往复运动轴线的方向上延伸，其中，该组合件包括至少两个层，每个层包括四个互连的细长构件，该四个互连的细长构件枢转地附接并且相对于彼此可旋转以限定多边形；其中，该组合件具有至少一个偏置装置，该偏置装置在层的至少一对互连的细长构件的端部之间延伸，并且该组合件可在沿着该往复运动轴线的方向上移位；

[0013] 手柄，该手柄可移动地连接到该引导框架并且支撑在该组合件上，以用于向下并沿着该组合件传递操作员施加的负载；

[0014] 其中，在操作员向该手柄施加负载的情况下，该至少一个偏置装置相对于该细长构件的布置随着该组合件增加的压缩而提供减小的刚度，以用于减小该手柄在预定频率范围内的振动。

[0015] 该减振设备可以包括与该组合件间隔开的一个或多个其他组合件，其中，每个组合件在其一端部处附接到横穿该往复运动轴线延伸的至少一个构件。

[0016] 该组合件或每个组合件的一个或多个参数可以被修改以实现以下各项中的一项或多项：相对于没有该减振设备的冲击工具而言更低的固有谐振频率；增加的负载容量；该至少一个或多个其他组合件沿着往复运动轴线的预定位移距离以及该至少一个或多个其他组合件在无负载状态下的大小。

[0017] 该组合件或每个组合件的经修改的参数中的一个或多个参数可以选自包括以下各项的组：弹簧刚度、细长构件之间的角度、细长构件的材料、细长构件相对于彼此的长度比率、以及层数。

[0018] 该至少一个偏置装置的刚度可以是可调节的，以改变该设备的谐振频率。

[0019] 该至少一个偏置装置的刚度可以通过用具有与该至少一个偏置装置不同的刚度的一个或多个偏置装置代替来调节。

[0020] 该至少一个偏置装置的刚度可以通过添加或移除一个或多个偏置装置来调节。

[0021] 相邻细长构件之间的角度可以是可调节的，以便修改由该组合件或每个组合件提供的振动抑制。

[0022] 可以选择细长构件的材料以便具有相对于钢而言的减小的刚度。

[0023] 该细长构件的材料可以是铝或镁。

[0024] 该设备的两个或更多个细长构件具有第一长度；并且该设备的其他细长构件具有第二长度；并且可以选择第一长度与第二长度的相对比率以在该设备中提供6-20Hz的预定频率范围内的振动抑制。

[0025] 该细长构件之间的角度和/或偏置装置的刚度可以是可调节的，以便随着操作员施加的负载的增加而保持设备的物理大小。

[0026] 可以调节该组合件或每个组合件中的细长构件的角度和层数，以便修改该组合件或每个组合件在沿着该往复运动轴线的方向上的可能位移量。

[0027] 该组合件或每个组合件可以在远离该引导框架的端部的一个或多个区域处附接至该引导框架，以抵抗负载下的非垂直变形。

[0028] 该组合件或每个组合件可以被配置用于减少来自可接纳在该组合件中的冲击工具的在6-20Hz的预定频率范围内的振动传递。

[0029] 该细长构件中的至少两个可以在远离该细长构件的端部的位置处彼此枢转地互连。

[0030] 可移动地支撑的手柄在引导构件上的最大行程可以由引导框架上的止动件来固定。

[0031] 该手柄和跨该框架延伸的至少一个构件可以是可调节的，以便增加至少一个或多个其他组合件与该至少一个组合件之间的距离。

[0032] 该手柄可以由偏置装置支撑在该框架上，该偏置装置被布置用于在沿着该工具的工作构件的往复运动轴线的方向上延伸。

[0033] 用于将电动的冲击工具保持在引导框架中的、横穿往复运动轴线延伸的至少一个构件可以是可调节的夹具。

[0034] 细长构件的长度可以是基本上相同的。

[0035] 至少一对相交的细长构件可以被布置成关于往复运动轴线不对称。

[0036] 选择用于保持在引导框架中的工具可以选自包括以下各项的一组冲击工具:手提钻、路面破碎机和冲击钻。

[0037] 根据本披露的第二方面，提供了用于冲击工具的减振设备的振动组合件，该冲击工具具有往复运动轴线，该振动组合件包括：

[0038] 至少两个层，每个层包括四个互连的细长构件，该四个互连的细长构件枢转地附接并且相对于彼此可旋转以限定闭环；该组合件可在沿着往复运动轴线的方向上移位，并且其中，至少一个组合件具有至少一个偏置装置，该偏置装置在层的至少一对互连的细长构件的端部之间延伸；

[0039] 其中，该组合件被配置用于与引导框架的一个元件接合，该引导框架包括沿着该工具的往复运动轴线延伸的至少两个元件以及横穿往复运动轴线延伸的至少一个构件，其中，至少一个构件被配置用于将电动的冲击工具保持在该引导框架中；

[0040] 其中，该组合件被配置用于支撑手柄的至少一部分，该手柄可移动地连接到该引导框架以将力传递到该冲击工具，并且其中，在操作员向该手柄施加负载的情况下，该至少一个偏置装置相对于该细长构件的布置随着该组合件的增加的压缩而提供减小的刚度，以用于减小手柄在预定频率范围内的振动。

[0041] 根据本披露的第三方面，提供了使用根据第一方面的减振设备的方法，其中工具选自包括以下各项的一组冲击工具:手提钻、路面破碎机和冲击钻。

附图说明

[0042] 为了描述可以获得本披露的上述以及其他优点和特征的方法，将通过参考在附图中示出的本披露的具体实施例来呈现对上面简要描述的原理的更具体的描述。应理解这些附图仅描绘了本披露的示例性实施例，因此，不应被认为是限制本披露的范围，将通过使用附图以附加特定性和细节来描述和阐明本文中的原理。

[0043] 下文将通过实例并参考附图来进一步详细解释本披露的优选实施例，在附图中：-

[0044] 图1A示出了根据本披露的组合件的实施例的示意图表示，其中，手提钻或路面破碎机被保持在该组合件中。

[0045] 图1B描绘了当冲击钻被保持在组合件中时的另一个实施例。

[0046] 图2A描绘了包括在图1A中所描绘的本披露的实施例中的示例性参考轴线。

[0047] 图2B描绘了图2B中所描绘的示例性实施例的一个组合件的示意性简化系统。

[0048] 图2C描绘了具有两个层的另一个单一对称组合件的示意性简化系统。

[0049] 图2D描绘了示意性的简化n层不对称组合件。

[0050] 图2E描绘了在中心负载下的示意性简化三层不对称组合件。

[0051] 图2F描绘了在偏心负载条件下的示意性简化两层不对称组合件。

[0052] 图2G描绘了在偏心负载条件下的示意性简化两层不对称组合件。

[0053] 图2H描绘了一个细长连接构件的运动的示例性数学坐标系。

[0054] 图3A描绘了具有不同弹簧刚度的位移传递率。

[0055] 图3B描绘了系统在压缩下的静态刚度。

[0056] 图3C描绘了不同M_1的位移传递率。

[0057] 图3D描绘了不同的细长构件装配角度的位移传递率。

[0058] 图3E描绘了不同阻尼的位移传递率。

[0059] 图4A描绘了具有不同弹簧刚度的加速度传递率。

[0060] 图4B描绘了具有不同M_1的加速度传递率。

[0061] 图4C描绘了具有不同的细长构件装配角度的加速度传递率。

[0062] 图4D描绘了具有不同阻尼的加速度传递率。

[0063] 图4E描绘了不同的细长构件材料的加速度传递率。

[0064] 图4F描绘了具有不同L_1/L_2的加速度传递率。

[0065] 图4G描绘了不同层n的加速度传递率。

[0066] 图5描绘了初始设计与通过改变参数获得的优化设计的性能比较。

[0067] 图6A描绘了对具有一个减振组合件的简化模型的模态分析。

[0068] 图6B描绘了对具有两个减振组合件的完整模型的模态分析。

[0069] 图7描述了30Hz单频激发的模拟结果。

[0070] 图8A描绘了实验室中的实验原型。

[0071] 图8B描绘了现场实验中的实验原型。

[0072] 图9描绘了典型实验室测试中的时间和频率响应(Z1是冲击式破碎机上的振动，而Z2是减振设备的手柄上的振动)。

[0073] 图10A描绘了传统破碎机在Z方向上的时域和频域中的加速度信号；

[0074] 图10B描绘了带有破碎机的本披露的设备的底部在Z方向上的时域和频域中的加

速度信号；

[0075] 图10C描绘了设备的顶部在Z方向上的时域和频域中的加速度信号；

[0076] 图10D描绘了设备的手柄在Z方向上的时域和频域中的加速度信号；

[0077] 图11A描绘了图1A的展开形式的示意图，其中为了清楚起见去除了手提钻，示出了用于接合不同手提钻模型的任选可调节宽度的框架。

[0078] 图11B描绘了手提钻与框架接合的一个示例性实施例的放大图的示例性示意图表示。

[0079] 图11C描绘了另一示例性实施例，示出了用于限制可能的运动的其他任选特征。

[0080] 图11D描绘了图11C中所描绘的实施例中的手柄的透视图。

具体实施方式

[0081] 下面详细讨论本披露的各种实施例。虽然讨论了具体实施方式，但应该理解这仅仅是为了说明目的而进行的。相关领域的技术人员将认识到，在不脱离本披露的范围的情况下可以使用其他部件和配置。

[0082] 所披露的技术解决了本领域中对改进的被动减振设备的需求，该改进的被动减振设备特别适用于在物理上稳定且保持在期望取向中以通过施工人员的抓握进行工作的往复式工具。

[0083] 在本披露的一个方面，提供了一种框架，该框架具有一对并行布置的减振组合件；该减振组合件被配置用于在压缩负载下向支撑于框架内的振动产生工具(诸如手提钻或路面破碎机)提供有益的非线性刚度。当操作员按下框架的手柄时，更多的向下的力被加到工具上以提高操作效率。然而，由于减振组合件的有益减振特性，振动不会传递至操作员的手上。这可以与如果仅使用竖直延伸的弹簧时将提供的非线性刚度相比较；其中，为了拆除操作或其他操作的效率而增加的向下压力将导致所安装的弹簧被更多地压缩；并因此减小振动阻尼。

[0084] 参考图1A，描绘了根据本披露的实施例的示例性减振设备10。

[0085] 减振设备10包括一对减振组合件20，该减振组合件支撑可在框架38上移动的手柄40。

[0086] 构件50跨框架38延伸以支撑冲击工具(诸如手提钻、路面破碎机、冲击钻等)的下部。该冲击工具具有往复运动轴线，往复运动构件(例如冲击钻的钻头或手提钻的凿子)沿着该往复运动轴线来回移动。

[0087] 参考图1B，描绘了当冲击钻60b连接到减振设备10b的框架38b时，根据本披露的另一实施例的另一示例性减振设备10b。

[0088] 减振设备10b包括一对减振组合件20b，该减振组合件支撑可在框架38b上移动的手柄40b。

[0089] 构件50b跨框架38b延伸以支撑冲击钻60b的下部。冲击钻60b具有往复运动轴线，冲击钻60b的钻头沿着该往复运动轴线来回移动。

[0090] 数学理论建模

[0091] 参考图2A至图2G，示出了减振设备的各种示例性实施例。(在为了清楚起见而描绘的实施例中，不包括竖直对齐的阻尼弹簧、手柄已被省略、并且未描述在框架与减振组合件

之间的滑动附接。)

[0092] 在图2A中描绘的实施例的简化版本中,示出了4个“层”26、28、30、32。

[0093] 具有预定长度L2的两个细长构件29a、29b与具有相同预定长度的多个细长构件31a、31b在除了端部之外的位置处相交且枢转地连接。有利的是,细长构件29a、29b的长度是其他构件27a、27b的长度的两倍,从而能够如图所示更容易地安装弹簧。

[0094] 为了建模目的,破碎机被视为刚性体M_2,并且为了简化目的而将两个并行的减振结构简化成一个,如图3B所示。

[0095] 在M_2的底部处向上施加振动。

[0096] 上部质量M_1用于充当由操作员的手所提供的增加的下推力。减振结构的细长构件重量也可以等同地考虑在上部质量M_1中。

[0097] 优选地,所使用的弹簧是具有刚度K(或者视情况而定可以是K_n)的标准线性弹簧。

[0098] L_1是较小细长构件的细长构件长度,并且L_2是图2B、图2D中的较大细长构件的长度。在图2C所示的实施例中,构件具有相同的长度并用1表示。在图2E、图2F中,该构件形成如由下标所示指定层的一部分,例如L_{31}是第3层较小构件1。

[0099] 细长构件相对于水平线的装配角度由θ表示(同样参见图3C)。空气阻尼效应以D表示,所具有的相应阻尼系数为c。所涉及的参数列于表1中。

[0100]

符号	结构参数	单位
M_1	隔离物体的质量	kg
M_2	振动源的质量	kg
M_x	每 100 mm 细长构件的质量	kg
L_1	较小结构的边长	mm
L_2	较大结构的边长	mm
R_L	L_2/L_1的比率	/
n	层数	/
θ	细长构件的装配角度	弧度
φ	旋转运动度	弧度
y	隔离质量的绝对运动	mm
$\hat{y}$	隔离质量与振动源的相对运动	mm
z	底部激发	mm
a	相对运动$\hat{y}$的幅值	mm

[0101]

z_0	底部激发 z 的幅值	mm
ϕ	相对运动$\hat{y}$的相位	弧度
ω_0	底部激发 z 的频率	弧度/秒
T_d	位移传递率	/
T_a	加速度传递率	/
K	弹簧刚度	N/mm
c	阻尼系数	/
D	阻尼	/
f	固有频率	Hz

[0102] 该质量M_1的绝对运动由y、底部激发z、每个连接细长构件的旋转角度φ表示，并且具有较小的细长构件长度的每个层中的旋转接头的水平运动是x。运动y的正向方向是向上方向。较小细长构件的长度L_1被选择为1，并且较大细长构件的长度L_2为21，如在实际情况中的那些一样。

[0103] 图3C中示出了每个细长构件的旋转运动度φ。细长构件可以被设计为重量比隔离质量轻许多，长度足够短并且刚性足够强(通过选择材料，例如钢或铝合金等)来减小动态响应中的潜在惯性或挠曲影响。

[0104] 可以看出，旋转运动φ和水平运动x可以用相对运动$\hat{y}$来表示。L_1/L_2的比率被选择为2。可以获得几何关系为

[0105] $$\left(l\cos(\theta)-x\right)^2+\left(l\sin(\theta)+\frac{\hat{y}}{2(n+1)}\right)^2=l^2 \quad (1)$$

[0106] $$\tan(\theta+\varphi)=\frac{\frac{\hat{y}}{2(n+1)}+l\sin(\theta)}{l\cos(\theta)-x} \quad (2)$$

[0107] $$\hat{y}=y-z \quad (3)$$

[0108] 牵连运动φ和x被表示为

[0109] $$\varphi=\arctan(\frac{\frac{\hat{y}}{2(n+1)}+l\sin(\theta)}{l\cos(\theta)-x})-\theta \quad (4)$$

[0110] $$x=l\cos(\theta)-\sqrt{l^2-\left(l\sin(\theta)+\frac{\hat{y}}{2(n+1)}\right)^2} \quad (5)$$

[0111] 为便于讨论和理解系统的主要动态响应，在本研究的系统建模中不考虑连接细长构件的质量。

[0112] 动能可被描述为

[0113] $$T=\frac{1}{2}M_1\dot{y}^2+\frac{1}{2}M_2\dot{z}^2 \quad (6)$$

[0114] 势能为

[0115] $$V=\frac{1}{2}k_l(4x)^2 \quad (7)$$

[0116] 拉格朗日函数表示为

[0117] $$L=T-V=\frac{1}{2}M_1\dot{y}^2+\frac{1}{2}M_2\dot{z}^2-\frac{1}{2}k_l(4x)^2 \quad (8)$$

[0118] 拉格朗日原理是

[0119] $$\begin{cases}\frac{\mathrm{d}}{\mathrm{d}t}(\frac{\partial L}{\partial \dot{y}})-\frac{\partial L}{\partial y}=-D\\ \frac{\mathrm{d}}{\mathrm{d}t}(\frac{\partial L}{\partial \dot{z}})-\frac{\partial L}{\partial z}=F_0\cos(\omega t)-D\end{cases} \quad (9)$$

[0120] 其中L是表示为L＝T-V的拉格朗日函数，D是空气阻尼的消耗能量。它可以获得为

[0121] $$D=c(\dot{y}-\dot{z}) \tag{10}$$

[0122] 其中c是X形结构的阻尼系数。

[0123] 通过将动能、势能和牵连运动代入拉格朗日原理，动力学方程可以获得为

[0124] $$\begin{cases} M_1\ddot{y}+16k_l x\dfrac{\partial x}{\partial \hat{y}}\dfrac{\partial \hat{y}}{\partial y}=-c(\dot{y}-\dot{z}) \\ M_2\ddot{z}+16k_l x\dfrac{\partial x}{\partial \hat{y}}\dfrac{\partial \hat{y}}{\partial z}=F_0\cos(\omega t)-c(\dot{y}-\dot{z}) \end{cases} \tag{11}$$

[0125] 定义

[0126] $$f_1(\hat{y})=16k_l x\frac{\partial x}{\partial \hat{y}}\frac{\partial \hat{y}}{\partial y} \tag{12}$$

[0127] $$f_2(\hat{y})=16k_l x\frac{\partial x}{\partial \hat{y}}\frac{\partial \hat{y}}{\partial z} \tag{13}$$

[0128] 其中

[0129] $$\frac{\partial x}{\partial \hat{y}}=\frac{\partial[l\cos(\theta)-\sqrt{l^2-\left(l\sin(\theta)+\dfrac{\hat{y}}{2(n+1)}\right)^2}\,]}{\partial \hat{y}} =\frac{\hat{y}+2(n+1)l\sin(\theta)}{4(n+1)^2\sqrt{l^2-\left(l\sin(\theta)+\dfrac{\hat{y}}{2(n+1)}\right)^2}} \tag{14}$$

[0130] $$\frac{\partial \hat{y}}{\partial y}=\frac{y-z}{\partial y}=1 \tag{15}$$

[0131] $$\frac{\partial \hat{y}}{\partial z}=\frac{y-z}{\partial z}=-1 \tag{16}$$

[0132] 将(12)和(13)代入(11)

[0133] $$f_1(\hat{y})=4k_l x\frac{\hat{y}+2(n+1)l\sin(\theta)}{(n+1)^2\sqrt{l^2-\left(l\sin(\theta)+\dfrac{\hat{y}}{2(n+1)}\right)^2}} \tag{16}$$

[0134] $$f_2(\hat{y})=-4k_l x\frac{\hat{y}+2(n+1)l\sin(\theta)}{(n+1)^2\sqrt{l^2-\left(l\sin(\theta)+\dfrac{\hat{y}}{2(n+1)}\right)^2}} \tag{17}$$

[0135] (16)和(17)可以通过泰勒级数在零平衡时展开为

[0136] $$F_1(\hat{y})=\frac{f_1(0)}{0!}+\frac{f_1'(0)}{1!}\hat{y}+\frac{f_1''(0)}{2!}\hat{y}^2+\frac{f_1'''(0)}{3!}\hat{y}^3+\frac{f_1''''(0)}{4!}\hat{y}^4+o =\beta_1\hat{y}+\beta_2\hat{y}^2+\beta_3\hat{y}^3+\beta_4\hat{y}^4 \tag{18}$$

[0137] $$F_2(\hat{y})=\frac{f_2(0)}{0!}+\frac{f_2'(0)}{1!}\hat{y}+\frac{f_2''(0)}{2!}\hat{y}^2+\frac{f_2'''(0)}{3!}\hat{y}^3+\frac{f_2''''(0)}{4!}\hat{y}^4+o =\alpha_1\hat{y}+\alpha_2\hat{y}^2+\alpha_3\hat{y}^3+\alpha_4\hat{y}^4 \tag{19}$$

[0138] 其中

[0139] $$\beta_1=\frac{4k_l\tan^2(\theta)}{(n+1)^2} \quad (20)$$

[0140] $$\beta_1=\frac{3k_l\sin(\theta)}{l(n+1)^3\cos^4(\theta)} \quad (21)$$

[0141] $$\beta_3=-\frac{k_l(4\cos^2(\theta)-5)}{2l^2(n+1)^4\cos^6(\theta)} \quad (22)$$

[0142] $$\beta_4=-\frac{5k_l(4\cos^2(\theta)-7)\sin(\theta)}{16l^3(n+1)^5\cos^8(\theta)} \quad (23)$$

[0143] $$\alpha_1=-\frac{4k_l\tan^2(\theta)}{(n+1)^2} \quad (24)$$

[0144] $$\alpha_1=-\frac{3k_l\sin(\theta)}{l(n+1)^3\cos^4(\theta)} \quad (25)$$

[0145] $$\alpha_3=\frac{k_l(4\cos^2(\theta)-5)}{2l^2(n+1)^4\cos^6(\theta)} \quad (26)$$

[0146] $$\alpha_4=\frac{5k_l(4\cos^2(\theta)-7)\sin(\theta)}{16l^3(n+1)^5\cos^8(\theta)} \quad (27)$$

[0147] 将泰勒级数展开式(16)-(19)代入(15)而成为

[0148] $$\begin{cases}M_1\ddot{\hat{y}}+c\dot{\hat{y}}+M_1\ddot{z}+\beta_1\hat{y}+\beta_2\hat{y}^2+\beta_3\hat{y}^3+\beta_4\hat{y}^4=0\\ M_2\ddot{z}+c\dot{\hat{y}}+\alpha_1\hat{y}+\alpha_2\hat{y}^2+\alpha_3\hat{y}^3+\alpha_4\hat{y}^4-F_0\cos(\omega t)=0\end{cases} \quad (28)$$

[0149] 其中 $\ddot{y}=\ddot{\hat{y}}+\ddot{z}$ 。

[0150] 使用谐波平衡法(HBM)获得理论结果。(21)的解可以设置为

[0151] $$\hat{y}=a_0+a\cos(\omega t+\varphi_1)$$

[0152] $$z=b_0+b\cos(\omega t+\varphi_2) \quad (29)$$

[0153] 其中a_0和b_0是偏项,a和b是谐波项的幅值。

[0154] $$\begin{cases}a_0^3\alpha_3+\frac{1}{2}a^2\alpha_2+a_0\alpha_1+\frac{3}{8}a^4\alpha_4+a_0^4\alpha_4+\frac{3a^2a_0\alpha_3}{2}+3a^2a_0^2\alpha_4+a_0^2\alpha_2=0\\ (-3aa_0^2\alpha_3-a\alpha_1-\frac{3}{4}a^3\alpha_3-4aa_0^3\alpha_4-2aa_0\alpha_2-3a^3a_0\alpha_4-ca\omega)sin(\varphi_1)+M_2b\omega^2sin(\varphi_2)=0\\ (a\alpha_1+\frac{3}{4}a^3\alpha_3+4aa_0^3\alpha_4+2aa_0\alpha_2+3a^3a_0\alpha_4+3aa_0^2\alpha_3-ca\omega)cos(\varphi_1)-M_2b\omega^2cos(\varphi_2)-F_0=0\\ a_0^3\beta_3+\frac{1}{2}a^2\beta_2+a_0\beta_1++\frac{3}{8}a^4\beta_4+a_0^4\beta_4+\frac{3a^2a_0\beta_3}{2}+3a^2a_0^2\beta_4+a_0^2\beta_2=0\\ (-4aa_0^3\beta_4-2aa_0\beta_2-3aa_0^2\beta_3+M_1a\omega^2-\frac{3}{4}a^3\beta_3-a\beta_1-3a^3a_0\beta_4-ca\omega)sin(\varphi_1)+M_1b\omega^2sin(\varphi_2)=0\\ (-M_1a\omega^2+\frac{3}{4}a^3\beta_3+a\beta_1+3a^3a_0\beta_4+4aa_0^3\beta_4+2aa_0\beta_2+3aa_0^2\beta_3-ca\omega)cos(\varphi_1)-M_1b\omega^2cos(\varphi_2)=0\end{cases} \quad (30)$$

[0155] 位移传递率T_d可以被获得为

[0156] $$T_d=\left|\frac{\sqrt{a^2+b^2+2ab\cos\varphi_1}}{b}\right| \quad (31)$$

[0157] 可以针对不同的隔振性能来设计系统的结构参数。在示出的理论计算中,包括弹簧刚度、隔振物体质量、细长构件的装配角度和阻尼比率的参数被视为不同隔振性能的结

构参数,其中忽略了细长构件的质量。

[0158] 根据等式31计算的位移传递率和固有频率表明了具有一系列不同结构参数的隔振效应。

[0159] 应理解的是,可以对图2C(两层对称结构)、图2D(n层不对称结构)、图2E(具有第一形式的三层不对称结构)、图2F(具有第二形式的两层不对称结构)、图2G(具有第三形式的两层不对称结构)中所描绘的系统进行类似的分析。

[0160] 在图2C至图2G中,“o”表示旋转接头。K、k_1、k_2、k_v和k_h是相应弹簧的刚度系数。C、c_1和c_2是相应阻尼器的阻尼系数。

[0161] 如具体参照这些图可以看出,弹簧可以垂直安装在两个接头之间,该接头补偿地用于消除系统内的负刚度,如在图1A中可以看出的。

[0162] 然而,弹簧如所示出的以水平方式创新性地使用,这提供了主要的弹簧力。阻尼器主要水平地安装以产生所要求保护的希望的非线性阻尼,并且不需要垂直阻尼器,但垂直阻尼器可用于在需要时增加阻尼。可以使用具有类似性能的任何适当类型的线性和非线性弹簧以及阻尼器。

[0163] 如进一步详细讨论的那样,对区段/层的数量没有特定的要求。一般来说,在等效刚度和阻尼两者中,越多的层导致越小的动态刚度、越小的阻尼效应和越多的线性效应。相反,在层数较少的情况下,这将导致在等效刚度和阻尼两者中更大的动态刚度、更大的阻尼效应和更多的非线性效应。

[0164] 区段/层的长度由构件的长度决定,而越长的构件长度导致越小和越线性的阻尼效应,并且对刚度具有轻微影响。越大的装配角度导致越大的负载容量和越大的动态刚度,反之亦然。(参见图2C)。

[0165] 相同层或不同层的杆长度可以是不同的以产生不对称形状的结构,如图2C至图2G所示的结构在刚度和阻尼效应方面具有相似或甚至更好的性能。

[0166] 关于弹簧,就相同的压缩度或延伸度而言,越大的弹簧常数导致越大的负载容量和越大的刚度。重要的是,弹簧可以是任何类型的(空气弹簧、螺旋弹簧,材料或其他类型)并且是线性或非线性的,弹簧用于提供弹力,但主要以水平方式安装,具有用于消除负刚度的垂直补充(如图1所示)。

[0167] 如下面更详细分析的,确定详细的弹簧常数从而使得在安装之后,工作位置应最优地在X形结构的中间处具有90度。

[0168] 除上述之外,还考虑以下参数,特别是关于图2A、图2B中描绘的实施例和图2H的几何参数。

[0169] (a)弹簧刚度K的影响

[0170] 图4a示出了隔振效果受弹簧刚度的影响。可以看出,减小弹簧刚度可以降低系统的位移传递率和谐振频率的峰值。

[0171] 当弹簧刚度从100减小到10时,谐振频率从6.8Hz下降到1.2Hz。这种关系表明减小弹簧刚度会提高振动抑制性能。

[0172] 通过使用相同的弹簧来支撑不具有X形结构的相同质量M_1,已经计算出谐振频率应分别为5.1Hz、11.3Hz和16.1Hz。

[0173] 这可以与当系统包括X形结构时获得的谐振频率(1.2Hz、2.8Hz和6.8Hz)进行比

较，从而在数学上证明谐振频率显著降低，这清楚地显示出了与由传统的弹簧布置所提供的结构相比，X形结构在动态隔振中的有利的准零刚度特性。

[0174] 为了得到更多的理解，结构的静态刚度发展如下且在图4B中示出，具有针对K的不同刚度值。

[0175] 考虑到给定的初始质量M_1，结构在平衡时具有初始弹簧力$F_0=\frac{M_1 g}{5\tan\theta}$，然后向下施加力F，

[0176] $$F=5\left(F_0+Kx\right)\tan(\theta-\varphi)-Mg \qquad (32a)$$

[0177] 考虑到x与相对位移$\hat{y}$之间的关系，

[0178] $$F=5\left(\frac{M_1 g}{5\tan\theta_0}+K\left[l\cos(\theta)-\sqrt{l^2-\left(l\sin(\theta)+\frac{\hat{y}}{10}\right)^2}\right]\right)\frac{l\sin\theta-\frac{\hat{y}}{5}}{2l\cos\theta-\sqrt{l^2-\left(l\sin(\theta)+\frac{\hat{y}}{10}\right)^2}}-M_1 g \qquad (32b)$$

[0179] 从图4b中可以清楚地看出，结构的刚度实际上随着对结构的抑制(即，M_1与M_2之间的绝对相对位移增加)而减小。

[0180] 这表明当更多的向下力施加到手柄时：

[0181] • 操作员的工作位置更低；

[0182] • 框架结构具有更多的压缩；

[0183] • 结构具有降低的动态刚度，这对振动控制非常有利。

[0184] • 当操作员施加越多力时，存在越高的拆除效率。

[0185] 这再次证明了与所有其他传统的振动抑制系统相比，该结构独特的非线性优势。

[0186] (b)增加的质量M_1的影响

[0187] 在其他参数设置为L_1＝100、L_2＝200、M_2＝19.68、K＝100、θ＝π/4并且使用相同的细长构件材料的情况下，可以将上部质量M_1改变为不同的值，以检查减振设备手柄处的向下力如何影响振动传递。位移传递率Td的曲线如图4c所示，其中可以看出，增加质量M1可以降低谐振频率，同时提供降低的峰值。

[0188] 应该强调的是，对于纯线性系统，当增加质量但保持相同的弹簧刚度时，谐振频率将会降低为

[0189] $$\sqrt{\frac{K}{20}}\Big/\sqrt{\frac{K}{10}}\approx 0.7$$

[0190] 然而，利用本披露的减振设备，谐振频率降低为3.5/6.8≈0.5，这比纯线性系统小得多。

[0191] 这再一次证明了该减振设备具有有益的非线性刚度特性，其随着向下力的增加而提供更小的刚度(向下力的增加导致对结构的更多压缩)。

[0192] (c)细长构件装配角度θ的影响

[0193] 其他参数同样设置为L1＝100、L2＝200、M1＝9.85、M2＝19.68、K＝100，而细长构件装配角度被认为是π/6、π/4和π/3。位移传递率Td在图4d中示出。

[0194] 我们从图4c可以看出，当装配角度从60°变为30°时，谐振频率变得更小。这再次表明，随着结构内的更多压缩，即角度θ的减小，隔振性能变得更好，趋于成为准零刚度特性。

[0195] 因此,细长构件的装配角度是用于减少从冲击工具到操作员的手和臂的振动传递的关键参数。

[0196] (d)阻尼c的影响

[0197] 在参数被设定为如之前所设定的相同的参数但是θ=π/4并且使用不同的阻尼系数c的情况下,传递率在图4E中示出,该图示出了峰值随着阻尼系数的增加而减小。

[0198] 对结构的动力响应的有限元(FEM)分析

[0199] 进行FEM分析以更多地了解结构在每个关键参数方面的结构动力学。在有限元分析中,一些参数被固定为M_2=19.68、M_x=0.03(L_1型细长构件的质量)、D=0.01(等效阻尼)、L_1=100、L_2=200、M_1=9.85、θ=π/4,并且细长构件材料是结构钢。

[0200] 输入激发可以采用在质量M_2的底部施加的具有幅值的扫频的力1000N,这与路面破碎机的实际工作情况类似。很容易获得结构与路面破碎机一起的响应的加速度传递率T_a,来反映使用不同结构参数的隔振效应。

[0201] (a)弹簧刚度K的影响

[0202] 在使用上述结构参数并选择不同弹簧刚度的情况下,加速度传递率T_a的曲线如图5A所示。

[0203] 可以看出,无论弹簧刚度如何,加速度传递率的曲线都与理论计算结果相似。

[0204] 系统的隔振效应明显受到弹簧刚度的影响,这与图4A中的理论分析一致。例如,在图5A中,对于K=100,谐振频率为5.9Hz,而对于K=50,谐振频率则降至4.5Hz。

[0205] 这表明减小弹簧刚度能够有效地减小谐振频率,并且由此提高振动抑制性能。此外,由于质量M_2(即,路面破碎机本身)的谐振频率,所有传递率曲线在104.6Hz附近具有第二峰。这与后面的实际实验结果一致,同样对应于结构的第二模式频率。

[0206] (b)质量M_1的影响

[0207] 应该注意的是,质量M_1用于模拟施加在结构手柄上的向下力。质量M_1越大,则向下力越大,因此对结构的压缩就越多。在使用如前面相同的结构参数的情况下,质量M_1被分别选择为15.7和9.85,加速度传递率T_a的曲线如图5B所示。

[0208] 可以看出,增加质量M_1减小了对结构手柄处的振动抑制来说特别重要的峰值频率;然而,第二峰基本上没有改变,因为其仅取决于路面破碎机的材料和结构。这与之前在图4C中的理论分析一致。

[0209] 因此,结构上的向下力对于振动抑制是关键的。如前所述,向下力将导致传统弹簧系统中的刚度增加,从而导致更差的振动抑制。然而,本披露的结构提供了优异的非线性刚度特性,这由于增加的向下力而可同时呈现更高的振动抑制和更高的拆除效率。

[0210] (c)细长构件装配角度θ的影响

[0211] 在其他参数与先前相同并且调节装配角度θ的情况下,针对不同装配角度的T_a曲线如图5C所示。

[0212] 可以看出,当减小装配角度时,两个峰的频率都变小;这是由于结构的结构刚度降低。

[0213] 这表明随着角度θ的减小,隔振性能变得更好,趋于成为如所讨论的准零刚度特性。这与图4D中的理论分析一致。

[0214] 因此,结构中的细长构件的装配角度是减小振动频率的关键参数,其中在20度至

30度之间的装配角度被确定以提供良好的振动抑制性能。

[0215] (d)阻尼D的影响

[0216] 在使用相同的参数设置但不同的阻尼D的情况下,传递率曲线如图5D所示。

[0217] 增加阻尼可以有效地降低谐振峰值。这与图4C中的理论分析结果类似。然而,增加阻尼比率还将使在10Hz至100Hz之间的频率范围内的加速度传递率的幅值增加。

[0218] (e)细长构件材料的影响

[0219] 可以选择细长构件材料以查看FEM分析中的潜在影响。在使用相同的参数设置但为所有细长构件选择不同材料的情况下,加速度传递率的曲线如图5E所示。

[0220] 可以看出,改变材料可以影响振动传递率的曲线,尤其是对于高频振动,铝或镁细长构件由于材料的刚度更小而具有比钢细长构件小得多的传递率。这是一个重要的设计因素,因为不同的材料在实践中还将影响结构的整体重量及其操作舒适性。

[0221] (f)比率L_1/L_2的影响

[0222] 不同的细长构件长度比率可以在FEM分析中自由改变,这将产生不同的不对称结构。在使用相同的参数设置但L_1=100mm并且使用不同的比率L_1/L_2的情况下,T_a曲线如图5F所示。

[0223] 可以看出,随着比率从1.5降低到0.25,第一谐振频率持续增大,而第二谐振频率相应地减小。考虑到手和臂的敏感振动是从6Hz到20Hz的频率,较大的细长构件长度比率明显好于较小的细长构件长度比率。

[0224] (g)层数n的影响

[0225] 在其他参数设置为与之前所设相同但改变不同n的情况下,加速度传递率曲线如图5G所示。

[0226] 很明显,层数也是隔振效应的重要因素,并且两个谐振频率都随着层数的增加而减小,这对隔振性能有很大的帮助。

[0227] 因此,我们可以通过增加层数来提高隔振效应,但增加的层数导致更大的结构尺寸。

[0228] 结构参数的改善设计

[0229] 从以上可以看出,不同的结构参数会影响本披露的减振组合件的振动抑制效应。因此,重要的是改善参数以针对冲击工具的特定大小、重量和振动频率来提高性能。

[0230] 在实践中,本披露的设备/系统的大小和材料通常不会有太多选择,因为特定冲击工具的大小在市场中通常是一致的,具有类似重量和振动频率。然而,可以修改减振组合件的一些参数诸如弹簧刚度、工作角度θ和材料等。

[0231] 因此,在本节中,基于对前几节中的不同参数的比较分析,确定了对于系统而言相对较好的参数设置,这可以在考虑敏感频率范围6-20Hz时实现好得多的振动抑制效应。

[0232] 适当参数的选择

[0233] 考虑到前两个谐振频率对于6-20Hz频率范围内的振动抑制性能是关键的,下面给出了与振动抑制性能有关的各种参数的影响的总结。

[0234] 表2.参数调节所产生的影响的总结

[0235]

	第 1 谐振		第 2 谐振		6-20 Hz 内的传递率
	频率	峰	频率	峰	
M_1↑	↓↓	--	=	=	↓↓
刚度 K↑	↑↑	↑	=	=	↑↑
装配角度 θ↑	↑↑	↑	↑	--	↑↑
长度比率（L_1/L_2）↑ 具有固定的 L_1 = 100 mm	↓↓	--	↑↑	↓	↓↓
层数 n↑	↓↓	↓	↓↓	↓	↓↓
阻尼效应↑	=	↓	=	↓	↑
从钢到铝到镁的材料	↓	↓	↓	↓	↓

[0236] 从表2可以得出以下几点。

[0237] (a)一般而言，所有结构参数对在6Hz至20Hz之间的频率范围(操作员的手和手臂的振动传递的敏感频率范围)内的传递率呈现单调影响；

[0238] (b)长度比率L_1/L_2对于第一和第二谐振频率的影响是不同的，并且两个较小长度比率对于更紧凑的结构是有利的，但是将导致两个谐振峰更接近20Hz，从而导致在敏感频率范围内更差的振动抑制；

[0239] (c)越大的质量M1、越小的刚度K、越小的装配角度θ和越大的层数n都将单调地导致越小的谐振频率，以及因此在敏感频率范围(6-20Hz)内越好的振动抑制；

[0240] (d)挠性材料诸如塑料似乎对于振动抑制来说更好，但横向刚度对于破碎机的处理能力来说会更差。因此，重量较轻的铝似乎是实践中较好的选择。

[0241] 由以上结果可以看出，考虑到高负载容量、较大位移运动以及避免稳定性问题，可以通过调节若干结构参数来设计结构以实现具有较低固有频率的良好振动抑制性能。

[0242] 例如，

[0243] • 为了在不改变现有装置的大小的情况下增加负载容量，应增大细长构件的装配角度和弹簧的刚度；

[0244] • 为了增加压缩工作范围，应该增大细长构件装配角度和减振组合件结构的层数；

[0245] • 为了减小结构的固有频率，应增大长度比率L_1/L_2、质量M_1和减振组合件结构的层数；或者应减小弹簧刚度并且应减小细长构件装配角度。

[0246] 还应该理解的是，虽然所描绘的实例包括两个减振组合件，但是在不脱离本披露的范围的情况下可以使用一个、两个或三个组合件。

[0247] 总体而言，存在可以用来针对实际应用调整振动抑制性能的冗余结构参数，从而为实现一系列结果提供了卓越的灵活性。

[0248] 实例：

[0249] 基于简单优化从而使临界范围内的加权传递率最小化，建议如下具有初始参数设置的减振设备：

[0250] L_1＝100mm、L_2＝200mm、M1＝10kg、M2＝20kg、θ＝π/4、K＝100N/mm、D＝0.01并且细长构件材料是结构钢。

[0251] 为了优化此设备的参数，选择了以下参数：

[0252] L_1＝100mm、L_2＝200mm、M_1＝15kg、M_2＝20kg、θ＝π/6、K＝100N/mm、D＝0.1并且细长构件材料是铝合金。

[0253] 结果示出于图5中，该图指示了经改善或优化的设计与初始设计之间的加速度传递率曲线的比较。

[0254] 可以看出，使用优化参数设置的所有谐振频率(第一频率是3Hz)和峰值都小于最初的那些谐振频率(第一频率是6Hz)和峰值。

[0255] 在振动传递的敏感频率范围内尤其如此。具体地，在6Hz附近的传递率的最大降低是瞩目的，约40dB。

[0256] 比较这两个参数设置，可以看出质量M_1(即，向下推力)和装配角度是用于此性能改进的两个关键设计参数。

[0257] 然而，这两个参数都与结构大小无关，而是操作员在实践中可以控制的因素。这两个参数都与设备中减振组合件的压缩有关。

[0258] 完整模型改善设计的模拟结果

[0259] 对结构的完整模型进行模态分析以提供对实际应用中的结构动力学的洞察。

[0260] 为了比较，首先分析图2B中描绘的一个减振组合件的简化模型，并且模态分析结果在图6A中示出。然后对图2A所示结构的完整模型进行模态分析，其中两个并行的减振组合件使用上面讨论的优化参数。

[0261] 在图6A中可以看出，一阶模式的频率为仅3Hz。固有的振动模式是上下运动。细长构件的角度改变，但细长构件不变形。这对应于图4G或图5中的改善设计的加速度传递率曲线的第一峰。由于垂直方向上的框架限制了动作，所以不考虑第二模式(39Hz)。第三模式的频率约为48Hz，其水平地产生已成形结构的变形。使细长构件长度L_2更小至等于L_1将解决这个问题。

[0262] 对于所有其他较高振动模式，由于频率为大约或大于50Hz并且振动幅值非常小，因此对结构的手柄的影响将非常小。

[0263] 现在参考图6B，示出了图2A所示的结构的完整模型(包括两个减振组合件)的前3个振动模式。对于简化模型，模态结果与图6A中的模态结果基本上相同。在本系统的系统/设备内用于模式2的振动模式仍然具有如在示例性结构中所示的水平弯曲变形，该结构未固定到引导框架。

[0264] 从上面的模态分析可以看出，(a)所获得的模式频率与系统谐振频率的理论分析基本上一致；(b)在参数选择中应考虑低于50Hz的模式频率；然而，由于X形结构具有出色的准零刚度，因此所有高于5Hz的较高频振动都将被显著抑制；(c)所设计的系统在6-20Hz的敏感频率范围内没有特别的低频模式频率，这对于预测的整体振动抑制性能非常有利。

[0265] 有限元模型分析

[0266] 考虑到真实冲击工具诸如路面破碎机通常在拆除时以恒定频率诸如30Hz工作，使用有限元模型对受到单频激发但具有不同输入幅值的系统的动态响应进行研究。

[0267] 所有结构参数与真实原型基本上相同(稍后介绍)。需注意，刚度系统是非线性的(第3节)，因此预计当激发幅值足够大时应看到非线性响应。这种单频激发对于理解后面的实际实验数据很重要。

[0268] 图7A至C示出了在使用不同的输入力2KN、6KN和10KN的情况下，30Hz单频激发下BIAVE系统的时域和相应频域输出响应。

[0269] 在图7A至C中可以清楚地看到

[0270] (a)振动抑制性能明显，其中振动能量减少约80％-90％；这与先前几小节的理论和模拟结果是一致的；

[0271] (b)当激发幅值足够大到6KN时，由于系统中的非线性动力学，输出响应明显复杂化，观察到更多的频率分量而不是30Hz处的单频峰；

[0272] (c)随着激发幅值的增加，出现比输入频率(30Hz)大两倍的频率(60Hz)的超谐波响应，然后输出响应趋于更复杂化；例如，在10KN的激发下，除了30Hz处的输出响应外，还有一些其他的频率分量，包括60Hz左右的频率分量，45Hz左右的较小频率分量和15Hz处的另一个明显频率分量，这些频率分量分别对应于超谐波响应、互调响应和次谐波响应；并且15Hz处的次谐波响应非常强。

[0273] 因此，几乎所有由单频激发引起的非线性动力学都可以观察到具有非常强的次谐波响应，这表明在强激发环境下真实冲击工具的潜在响应可能非常复杂化。

[0274] 应该注意的是，15Hz处的次谐波响应峰正好位于人类操作员的敏感频率范围(6-20Hz)内，并且因此确实需要具有超低谐振频率的振动抑制系统来隔离这种有害振动。

[0275] 本披露的减振组合件的准零刚度恰好满足了此挑战性要求，其具有约3Hz的非常低的谐振频率并且其可以有效地抑制所示出的振动峰。

[0276] 实际实验原型的测得特性

[0277] 将改善的参数设置用于上面讨论的原型。也就是说，L_1＝100mm、L_2＝200mm、M_1＝15kg、M_2＝20kg、θ＝π/6、K＝100N/mm、D＝0.1并且细长构件材料是铝合金。需注意，M_1是向下推力。

[0278] 也就是说，一旦冲击工具(破碎机)运行，原型结构的手柄将被向下推动到所希望的位置，此位置等效于质量M_1，具有装配角度θ＝π/6。质量M_2恰好是实验中使用的冲击式破碎机的质量。

[0279] 整个结构约一米高。

[0280] 在根据本披露的披露内容所生产的具体原型中，存在并行布置的两个4层X形振动抑制结构(图2A)，但应该理解的是，如先前所讨论，具有不同层数的其他布置将是可能的。

[0281] 这两种振动抑制结构都具有由相应的旋转接头接合的1层较大细长构件和3层较小细长构件。连接杆的质量约为0.3kg/100mm。用于使结构在所希望的装配角度下工作的手柄的总体向下力为15kN，这遵循在理论计算和FEM分析中使用的参数设置。在原型中使用的破碎机为20kg，具有的冲击频率为1800次/分钟，即30Hz。

[0282] 一旦破碎机被启动，击中混凝土或橡胶就会垂直地对系统产生单频激发，该单频激发的主频在橡胶上约为30Hz或在混凝土上约为20Hz。可以测量破碎机和原型结构手柄两

者上的振动加速度信号以供进一步分析，该加速度信号分别称为向下的Z和向上的Z。

[0283] 为了评估振动水平，采用针对手和手臂振动的ISO5349标准计算，这是频率加权的加速度能量，如(33)所示。

[0284] $$a_{hw}=\sqrt{\sum_{i=1}^{n}(K_i a_{hi})^2} \qquad (33)$$

[0285] 其中：

[0286] n是频带的总数。

[0287] K_i是第i个频带的加权系数，其值如表3所示。

[0288] a_{hi}是加速度的RMS值，公式如下：

[0289] $$a_{hi}=\sqrt{\frac{1}{T}\int_0^T a^2(t)dt}=\frac{a_0}{\sqrt{2}} \qquad (34)$$

[0290] 其中：

[0291] T是记录时间。

[0292] a_0是振动加速度的最大值。

[0293] ISO 5349提出了包括倍频带在内的频率范围，其中心频率为8至1000Hz，对于1/3倍频带，其中心频率为6.3至1250Hz。加权系数示出于表3中。

[0294]

中心频率(Hz)	K_i	中心频率(Hz)	K_i
6.3	1.0	100	0.16
8.0	1.0	125	0.125
10.0	1.0	160	0.1
12.5	1.0	200	0.08
16	1.0	250	0.063
20	0.8	315	0.05
25	0.63	400	0.04
31.5	0.5	500	0.03
40	0.4	630	0.025
50	0.3	800	0.2
63	0.25	1000	0.016
80	0.2	1250	0.0125

[0295] 表3.在1/3倍频带下加权加速度的加权系数

[0296] 根据上面提及的计算方法，来自实验室中使用冲击在橡胶材料上的破碎机的若干次实验测试的测量数据汇总在表4中。

[0297]

破碎机上的振动--向下		原型结构手柄上的振动--向上	T_a = 向上振动/向下振动	工作条件
仅Z方向	14.014	4.665	0.332898	3个弹簧满负载
	13.85208	*5.13896*	*0.370988*	*4个弹簧无负载*
	15.46943	6.111534	0.395072	4个弹簧满负载
	13.87586	*4.306374*	*0.310350*	*5个弹簧无负载*
	16.61955	5.460997	0.328589	5个弹簧满负载
总体X+Y+Z3个方向	15.58015263	7.386999616	0.474128835	3个弹簧满负载
	15.25346253	*8.101768629*	*0.53114292*	*4个弹簧无负载*
	16.79109472	8.290267939	0.493730044	4个弹簧满负载
	14.71386693	*7.61053066*	*0.517235251*	*5个弹簧无负载*
	17.62365526	8.249783767	0.468108553	5个弹簧满负载

[0298] 表4.在实验室测试中原型结构的频率加权加速度

[0299] 在表4中,应考虑以下参数

[0300] • 不同的弹簧具有不同的刚度系数(K);

[0301] • 无负载意指下推力是原型结构本身的重量;

[0302] • 满负载意指施加理想的15kg的向下力。

[0303] 从表4可以得出以下几点:

[0304] (i)破碎机上的振动约为14m/s^2,而手柄上的振动为仅约5m/s^2。振动减少非常显著(高达70%),并且被抑制的振动水平意指工作人员可以连续工作长达5或8小时,相比之下在没有该结构的情况下工作人员只能工作约30分钟。

[0305] (ii)当施加更多的向下推力时,破碎机上的振动要高得多,这指示更强力的拆除;但原型手柄上的振动水平保持在相对合理的健康水平,其中整体振动类似地减少(尽管增加了向下力,但振动水平并没有明显增加)。

[0306] (iii)尽管手柄上的相应振动水平增加(由于测试过程中冲击表面的变化而不均匀),但在原型系统中增加更多弹簧可以使得能够在相同压缩水平下具有更多的向下推力。

[0307] (iv)由于Z方向的振动占主导,所以所有3个方向的总体振动与Z方向的振动相比没有显著差异并遵循与其相似的趋势。更清楚的是,更多的弹簧导致从破碎机吸收更多的振动能量,而在比较满负荷和无负荷的情况时在每种情况下可以看到较低的振动传递率,

这再次表明了所披露结构的独特的非线性刚度性质。

[0308] 表5汇总了通过计算所测量的振动信号的均方根而获得的不同测试结果。

[0309]

向下的 Z	向上的 Z	T_a = 向上的 Z/向下的 Z	工作条件
279.0656823	45.36138998	0.16254736	3 个弹簧满负载
275.711242	57.50320354	*0.20856314*	*4 个弹簧无负载*
313.633182	64.42959771	0.20542979	4 个弹簧满负载
275.2987827	39.62296868	*0.14392714*	*5 个弹簧无负载*
334.0796643	52.88027545	0.15828642	5 个弹簧满负载

[0310] 表5.实验室测试中加速度信号的RMS

[0311] 表5汇总了对从破碎机传递到原型手柄的振动能量的总体振动抑制。

[0312] 可以清楚地看到，在所有情况下高达80％或更多的振动能量被抑制，并且越多的弹簧导致破碎机上越多的振动能量，这有助于拆除效率，同时在比较满负载和无负载的情况下在每种情况中可以看到类似的振动传递率。这清楚地表明本披露的系统的独特的非线性准零刚度。

[0313] 图9示出了上述测试结果的一些时间和频率响应。

[0314] 结果汇总或示出在表6和图9中。

[0315] 可以看出，主要的激发来自破碎机的振动频率(约30Hz)，并且在30Hz附近存在明显的振动峰。在每个测试情况下，6Hz与20Hz之间的振动抑制非常好。

[0316] 可以观察到复杂化的非线性动态响应正如先前的分析性分析一样，包括超谐波、次谐波和互调。

[0317] 在一些情况下，次谐波响应非常强(约15Hz)，该次谐波响应由于本披露的结构与破碎机之间的耦合动力学而可以在该结构的手柄和破碎机上观察到，但仍然具有明显的抑制。

[0318] 可以看出，在使用该设备的情况下，破碎机上的振动(Z_1)高于在没有该设备的情况下的振动(总体振动能量提高高达75％或加权振动提高高达30％)。本领域的技术人员将其理解为反映了改进的拆除效率。

[0319] 然而，也可以看出，根据ISO手臂振动标准，在使用本披露的设备/结构的情况下，手柄处的振动(Z_2)与传统破碎机Z相比被显著抑制到更健康的水平。

[0320]

	设备 + 破碎机 Z_1	设备手柄 Z_2	传统路面破碎机 Z
频率加权的加速度	17.7296 ± 0.5651	6.8486 ± 0.4495	13.6950 ± 0.2414
均方根	1072.035 ± 11.4868	416.7246 ± 28.4300	612.856 ± 88.0166

[0321] 表6.所披露的结构和传统破碎机的现场振动测试

[0322] 图10A至D示出了一个典型的测试结果，其中，“传统Z”是指不使用所披露的设备和系统的传统冲击工具(在本情况下是路面破碎机)上的振动，而“向下、向上和手”分别是指使用所述设备和系统的情况下工具本体、设备和系统手柄以及操作员的手上的振动。从这些附图中可以看出，由设备和系统所提供的振动抑制性能在总体振动能量和6-20Hz的敏感频率范围内的振动方面非常显著。

[0323] 减振组合件的非线性刚度允许纯粹的被动减振设备和系统。数学建模、FEM分析和实验验证表明，这非常有效地使振动抑制高达70％或以上，并且可以显著减少从冲击工具传递到操作员手柄的振动。本披露的系统和设备成功解决了多年来因手动操作各种施工工具引起的振动问题。

[0324] 非线性刚度特性对被动振动控制非常有益，同时包括以下若干个独特的特征：(1)准零刚度、(2)高负载容量、(3)随着结构的压缩增加而降低的刚度，(4)灵活且易于实施、以及(5)可调节的结构参数。

[0325] 这些特征使得所述设备/系统在施工现场操纵各种冲击式拆除工具期间能够非常有效且高效地抑制传递到操作员的手的过度振动，而不会影响操作舒适性。与此同时，由于显著减少了传递到操作员的振动(在不同情况下高达70％或90％)，所以该系统可以提高拆除效率(在加权振动能量方面高达30％)。

[0326] 现在参考图11A，描绘了图1A中所示的减振设备的分解图。在此实施例中，手柄40以两个部件40a和40b形成，从而允许调节框架38的引导构件48a与48b之间的间隔。类似地，接纳手提钻或往复式工具60的底部构件由多个长度可调节构件58a和58b以及中央接纳部分52一起构成。现在参考图11B，可以看出，此图描绘了横向延伸构件50的分解图，该横向延伸构件将引导杆38a、38b保持在间隔开的方向。

[0327] 有利地，构件50由附接构件50a和50b组成，附接构件50a和50b附接到引导装置38a、38b以及减振组合件20。有利地，横向延伸构件50的中心部分由夹具组成，该夹具由夹持部件52a和52b形成。这些夹持部件接纳往复式工具诸如手提钻或路面破碎机或冲击钻。应理解的是，所描绘的布置仅是示例性的，并且有可能其他布置也可以将冲击往复式工具保持在所希望的方向中。如图所示，还可能存在接合装置，该接合装置在沿着引导框架的一个或多个点处可滑动地附接振动组合件。

[0328] 现在参考图11C，描绘了图1A的减振设备的另一个实施例。有利的是，可以看出，手柄40由部件40a和40b组成，该部件40a和40b可以相对于彼此移动以调节引导构件38a与38b

之间的间隔。手柄支撑在引导构件38a上，使得手柄可以在偏置装置或弹簧39上在引导构件上移动。弹簧支撑在止动件41上，该止动件限定所允许的手柄40的最大行程量。

[0329] 有利的是，出于安全原因，手柄可以如图所示成形为具有向上延伸的引导件，该引导件包含引导装置的端部以避免刺到操作员。

[0330] 还可以看到，附接手提钻或路面破碎机60以使得工具的往复运动轴线与引导装置38a、38b大致对齐。通常，这些参数的长度在50-120cm之间并且宽度在30-80cm之间，但是这些参数当然可以根据约束在其中的往复式工具来调节。

[0331] 在图12C所描绘的实施例中，减振组合件20的偏置装置或弹簧24a、24b在细长构件的端部之间横向延伸。存在在往复运动轴线的方向上对齐的附加弹簧26，该弹簧可以提供某种有限的阻尼。

[0332] 如本领域的技术人员将理解的，为了操作本披露的减振设备，操作员将向手柄40施加负载。此负载压缩手柄弹簧39，直到该手柄弹簧到达止动件41。与此同时，在操作过程中，由冲击工具(支撑在引导框架38a和38b上的手提钻60)产生往复运动。

[0333] 由操作员提供的力通过振动组合件20向下传递，然后通过与横向构件50的接合而到达工具60的端部或某一点。

[0334] 如先前已经详细论述，减振设备在负载下的非线性刚度特性有利地将已经放置在手柄上的操作员的手与预定振动范围内的大量振动隔离，可以如所讨论的针对所述预定振动范围定制设备的各种参数。

[0335] 以上实施例仅通过实例来描述。在不脱离如所附权利要求中定义的本披露的范围的情况下，许多变化情况是可能的。

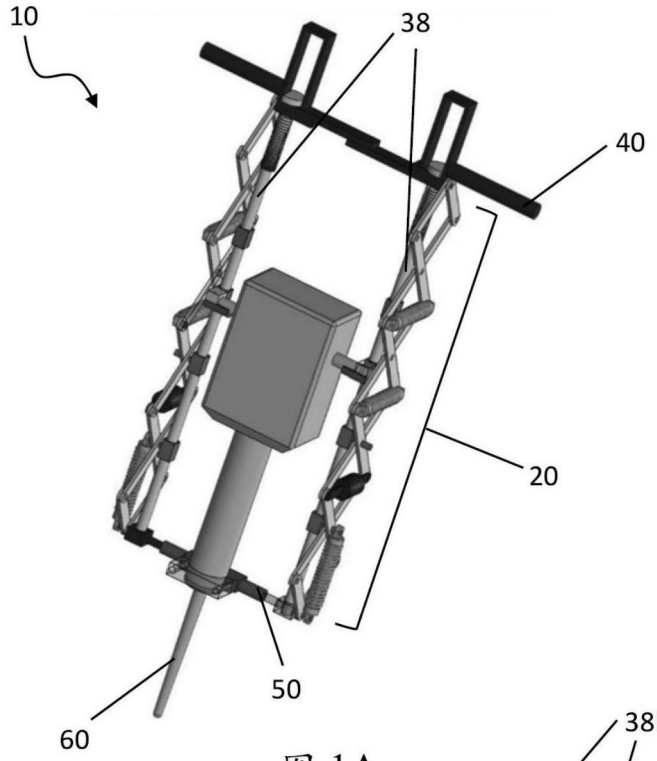

图 1A

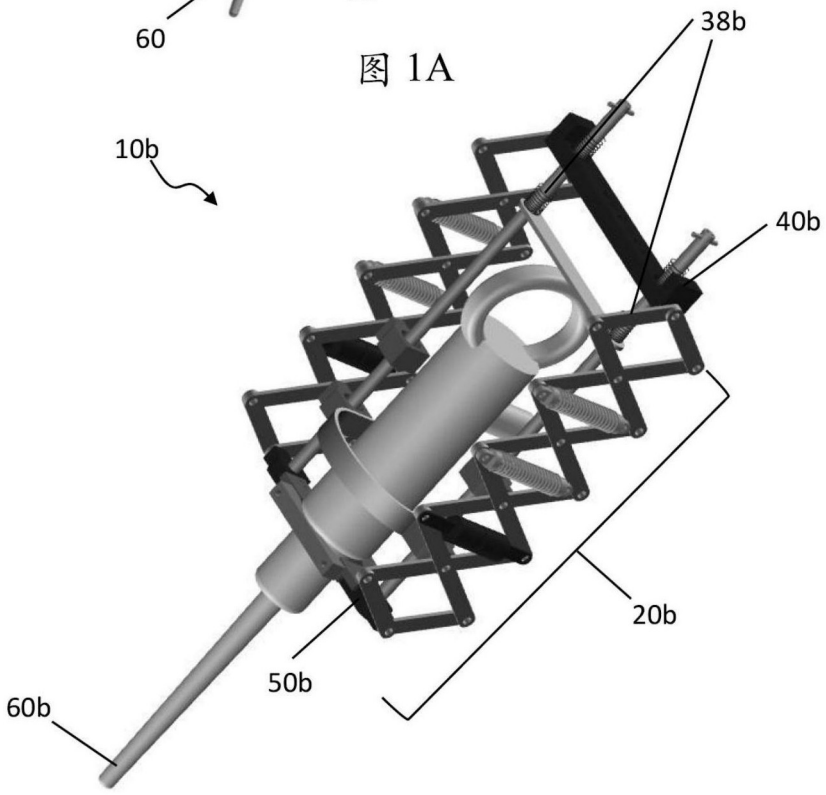

图 1B

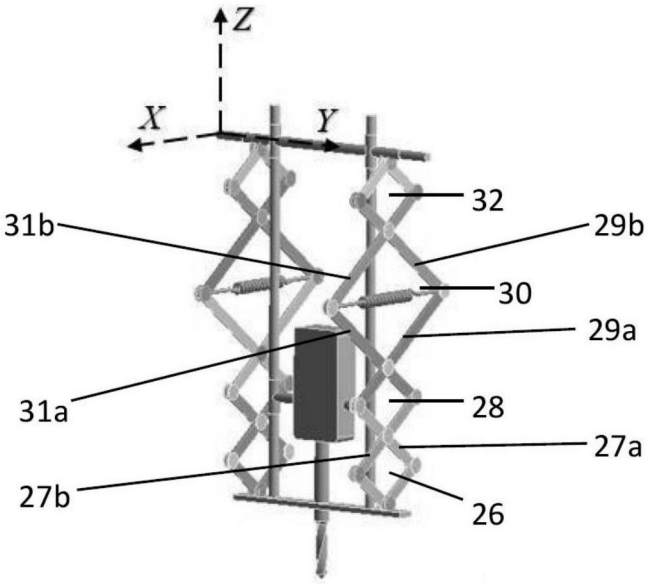

图2A

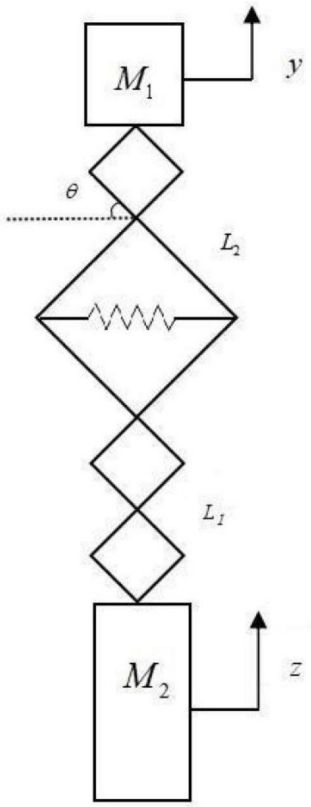

图2B

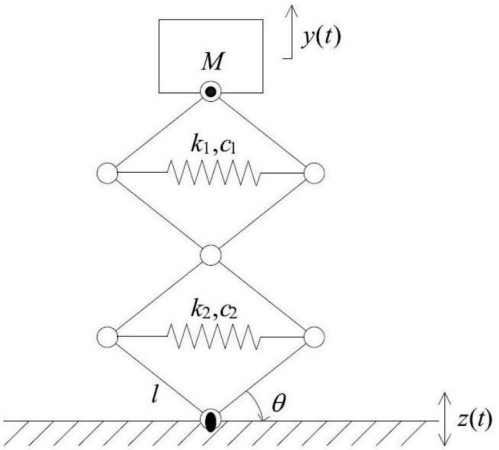

图2C

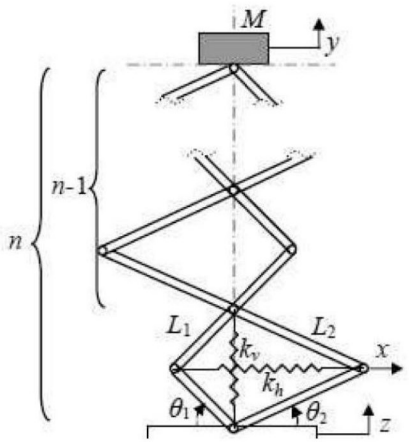

图2D

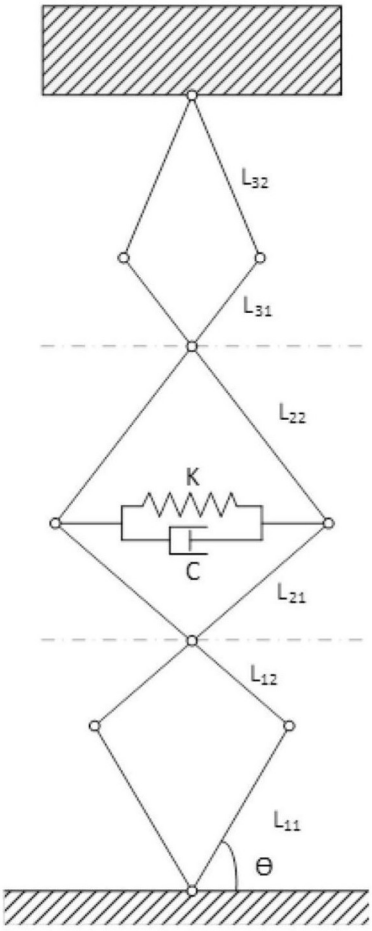

图2E

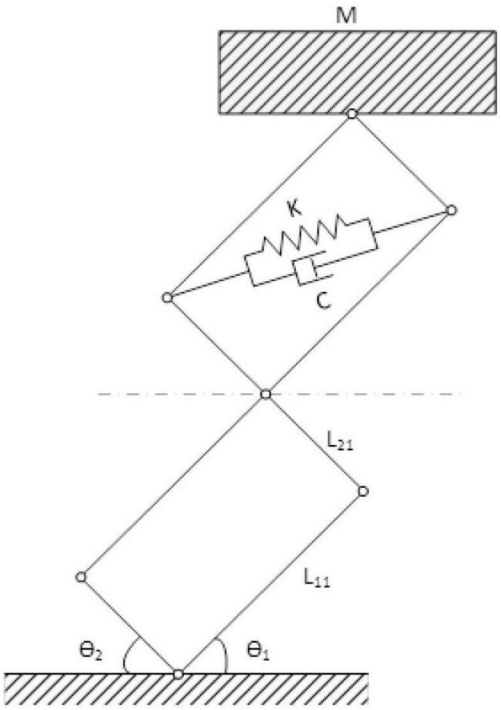

图2F

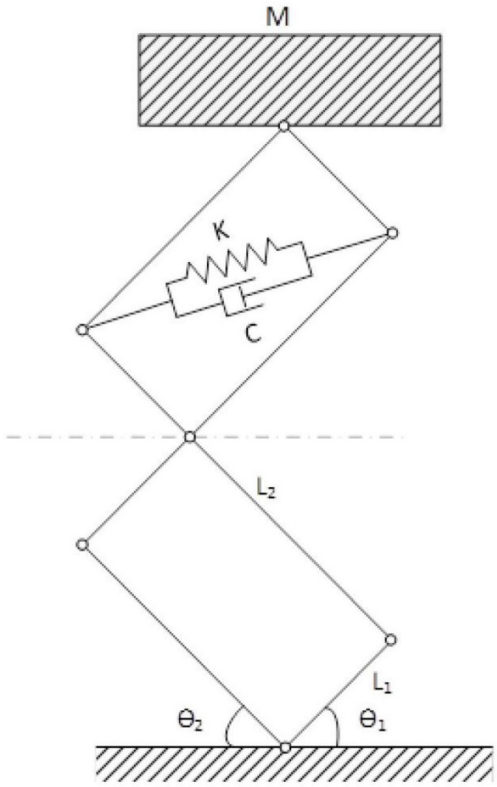

图2G

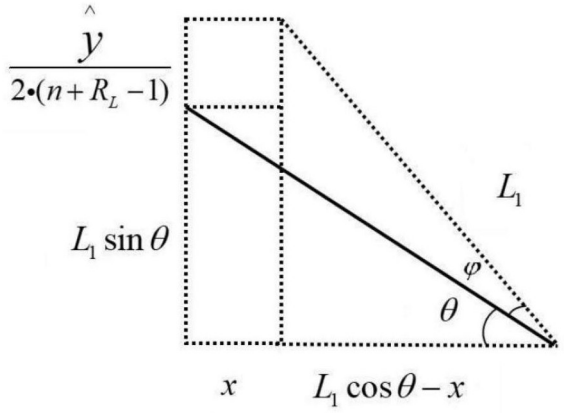
$\frac{\hat{y}}{2\bullet(n+R_L-1)}$
L_1
$L_1\sin\theta$
φ
θ
x
$L_1\cos\theta-x$

图2H

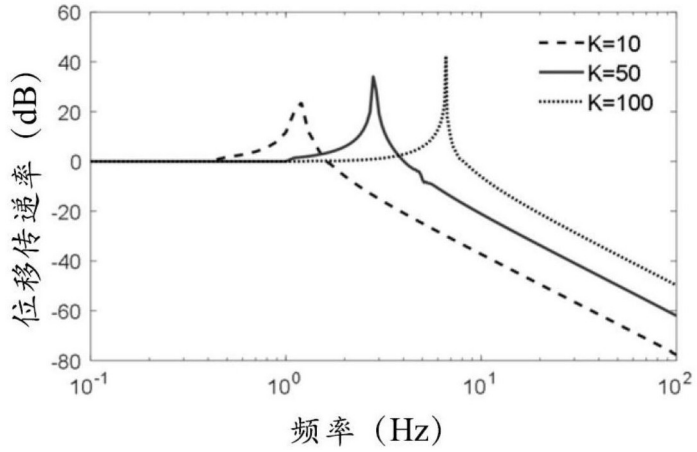
K=10
K=50
K=100
位移传递率（dB）
频率（Hz）

图3A

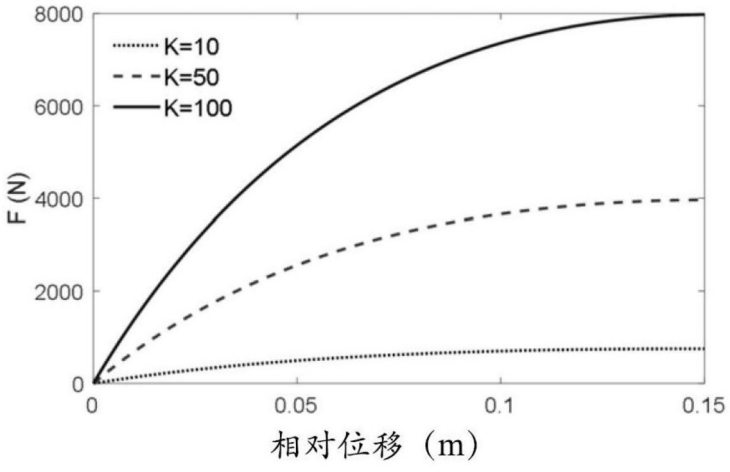
K=10
K=50
K=100
F (N)
相对位移（m）

图3B

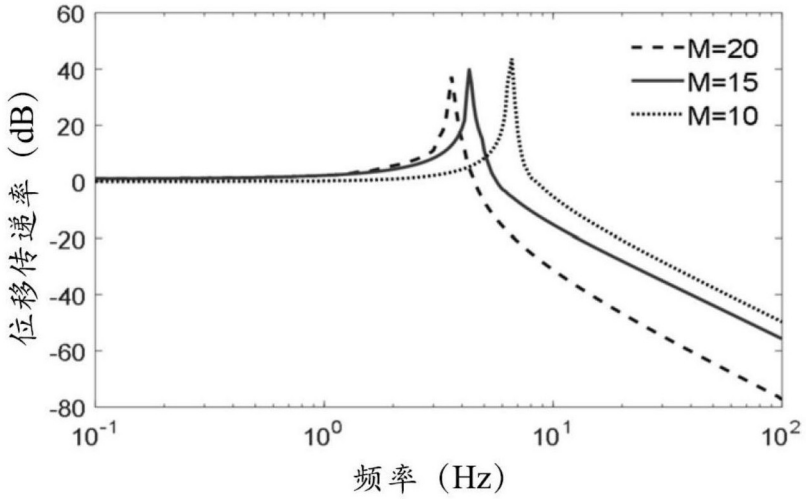
M=20
M=15
M=10
位移传递率（dB）
频率（Hz）
60
40
20
0
-20
-40
-60
-80
10^-1
10^0
10^1
10^2

图3C

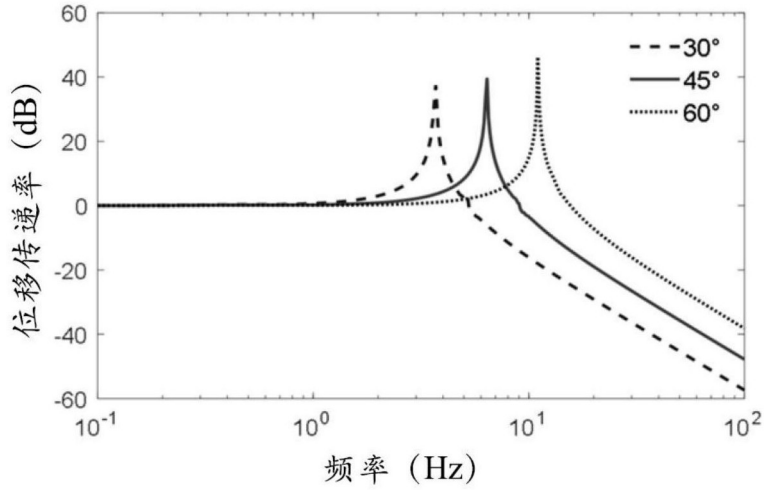
30°
45°
60°
位移传递率（dB）
频率（Hz）
60
40
20
0
-20
-40
-60
10^-1
10^0
10^1
10^2

图3D

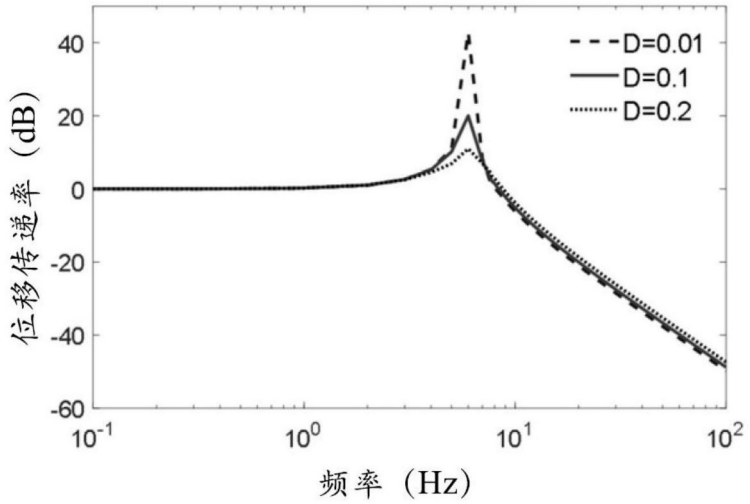
D=0.01
D=0.1
D=0.2
位移传递率（dB）
40
20
0
-20
-40
-60
10^{-1}
10^{0}
10^{1}
10^{2}
频率（Hz）

图3E

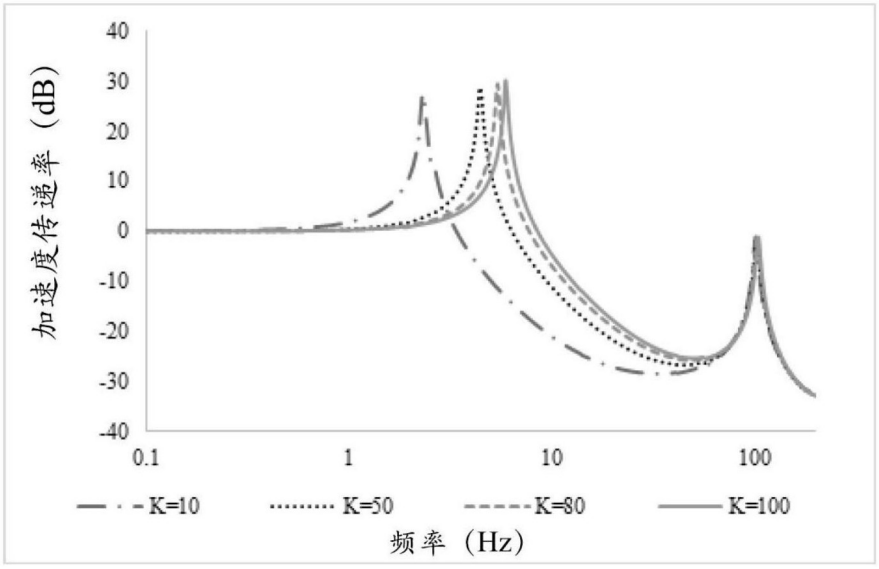
加速度传递率（dB）
40
30
20
10
0
-10
-20
-30
-40
0.1
1
10
100
K=10
K=50
K=80
K=100
频率（Hz）

图4A

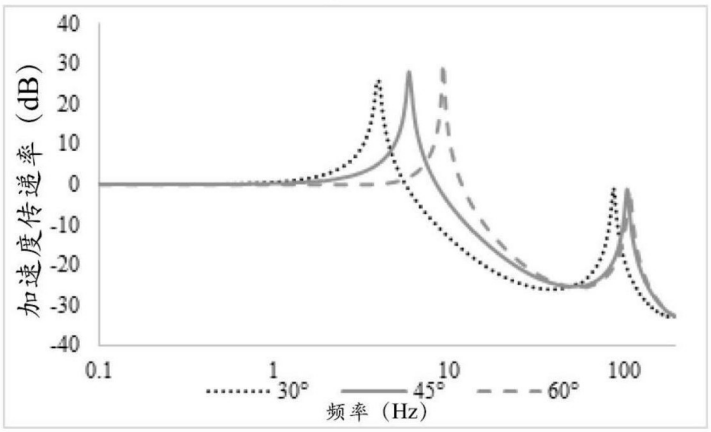
加速度传递率（dB）
40
30
20
10
0
-10
-20
-30
-40
0.1
1
10
100
30°
45°
60°
频率（Hz）

图4B

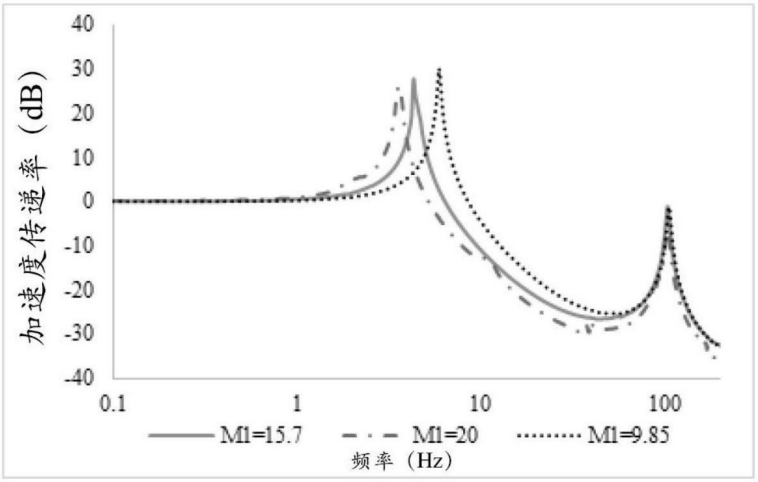
加速度传递率（dB）
40
30
20
10
0
-10
-20
-30
-40
0.1
1
10
100
M1=15.7
M1=20
M1=9.85
频率（Hz）

图4C

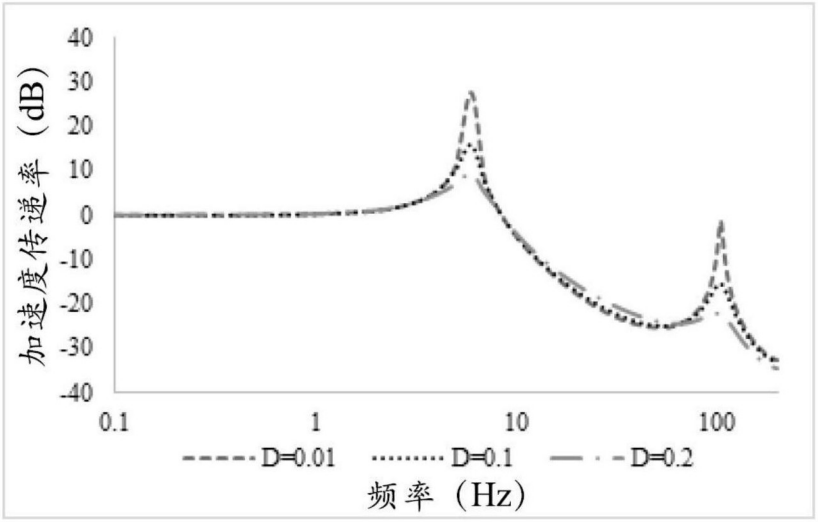
加速度传递率（dB）
40
30
20
10
0
-10
-20
-30
-40
0.1
1
10
100
D=0.01
D=0.1
D=0.2
频率（Hz）

图4D

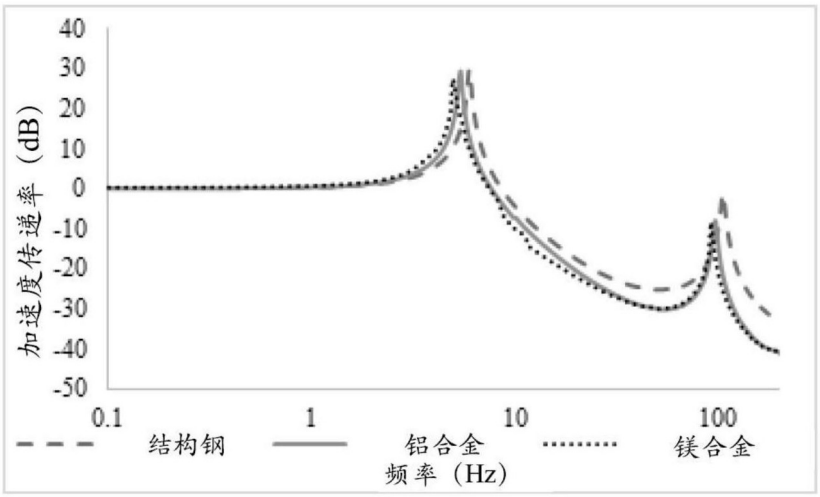
加速度传递率（dB）
40
30
20
10
0
-10
-20
-30
-40
-50
0.1
1
10
100
结构钢
铝合金
镁合金
频率（Hz）

图4E

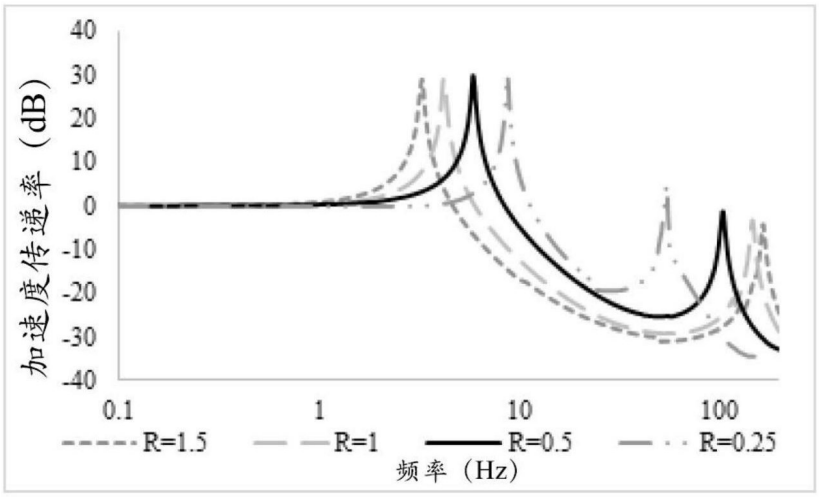
加速度传递率（dB）
40
30
20
10
0
-10
-20
-30
-40
0.1
1
10
100
R=1.5
R=1
R=0.5
R=0.25
频率（Hz）

图4F

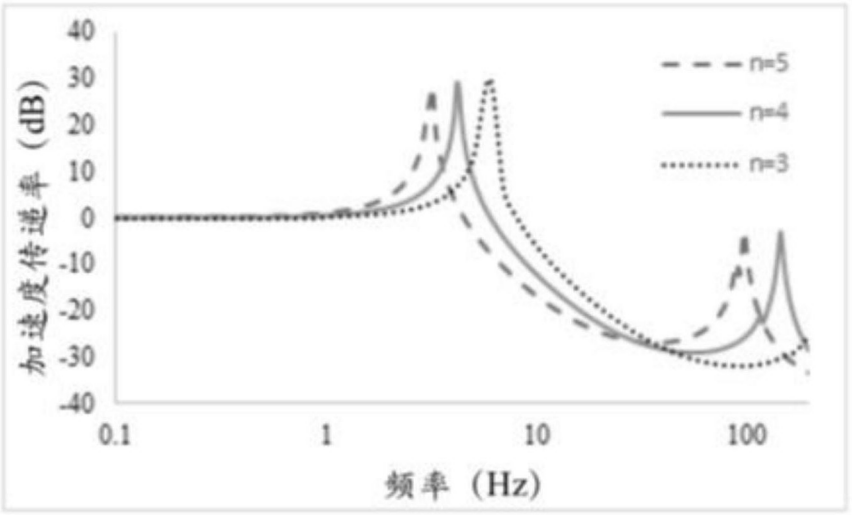
加速度传递率（dB）
40
30
20
10
0
-10
-20
-30
-40
0.1
1
10
100
n=5
n=4
n=3
频率（Hz）

图4G

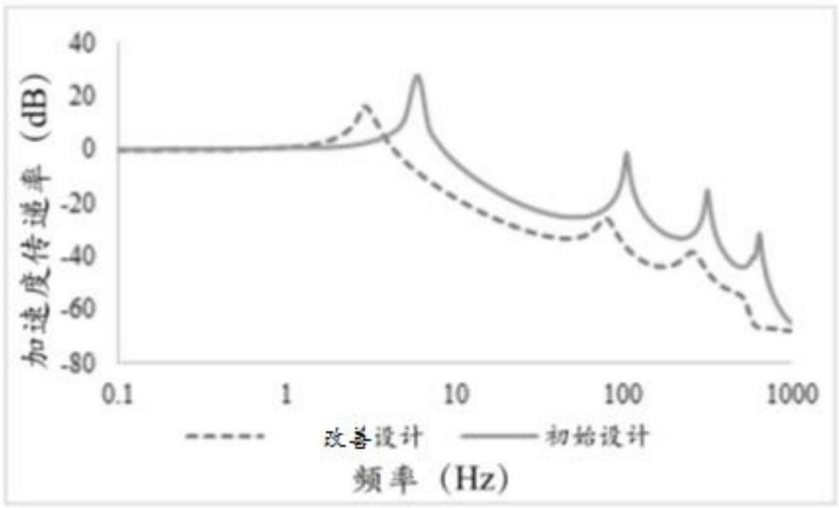
加速度传递率（dB）
40
20
0
-20
-40
-60
-80
0.1
1
10
100
1000
改善设计
初始设计
频率（Hz）

图5

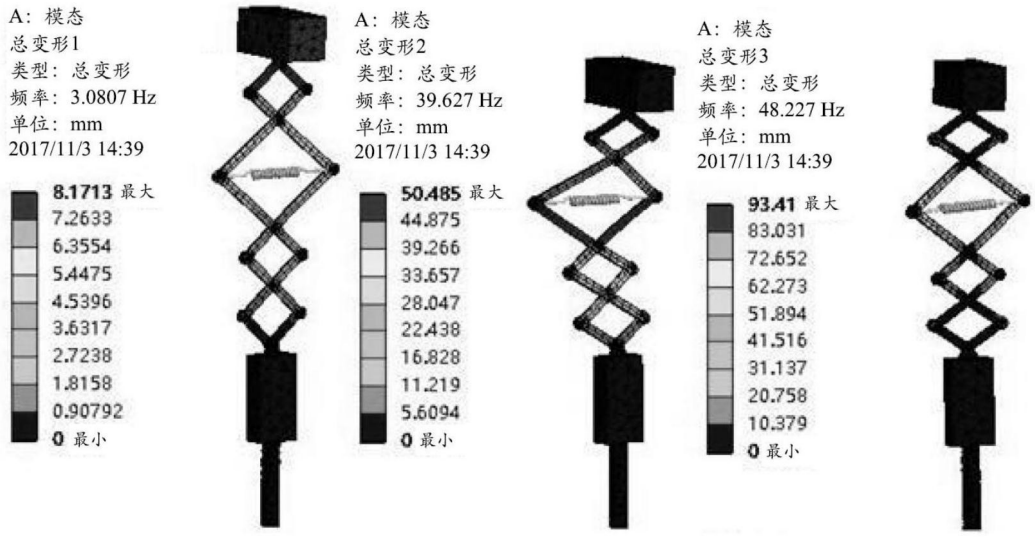
A：模态
总变形1
类型：总变形
频率：3.0807 Hz
单位：mm
2017/11/3 14:39
8.1713 最大
7.2633
6.3554
5.4475
4.5396
3.6317
2.7238
1.8158
0.90792
0 最小
A：模态
总变形2
类型：总变形
频率：39.627 Hz
单位：mm
2017/11/3 14:39
50.485 最大
44.875
39.266
33.657
28.047
22.438
16.828
11.219
5.6094
0 最小
A：模态
总变形3
类型：总变形
频率：48.227 Hz
单位：mm
2017/11/3 14:39
93.41 最大
83.031
72.652
62.273
51.894
41.516
31.137
20.758
10.379
0 最小

图6A

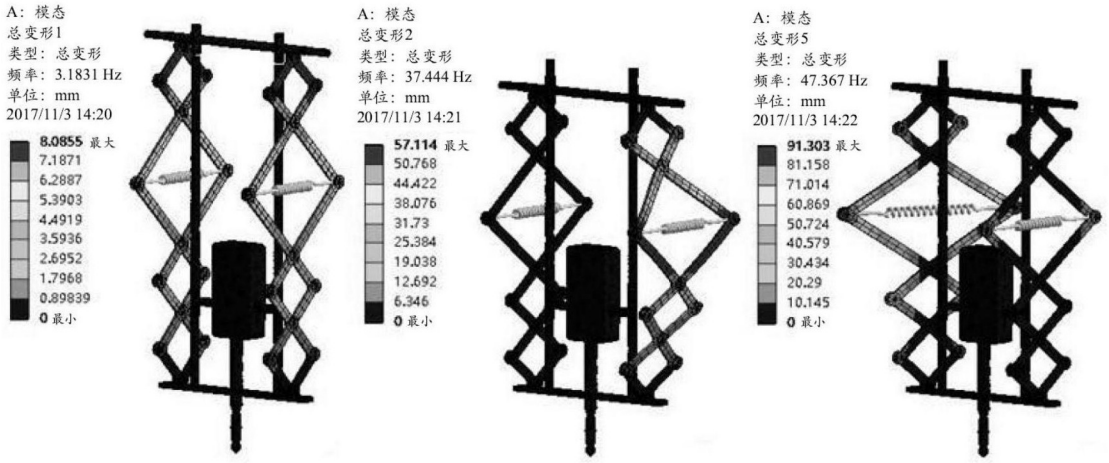
A：模态
总变形1
类型：总变形
频率：3.1831 Hz
单位：mm
2017/11/3 14:20
8.0855 最大
7.1871
6.2887
5.3903
4.4919
3.5936
2.6952
1.7968
0.89839
0 最小
A：模态
总变形2
类型：总变形
频率：37.444 Hz
单位：mm
2017/11/3 14:21
57.114 最大
50.768
44.422
38.076
31.73
25.384
19.038
12.692
6.346
0 最小
A：模态
总变形5
类型：总变形
频率：47.367 Hz
单位：mm
2017/11/3 14:22
91.303 最大
81.158
71.014
60.869
50.724
40.579
30.434
20.29
10.145
0 最小

图6B

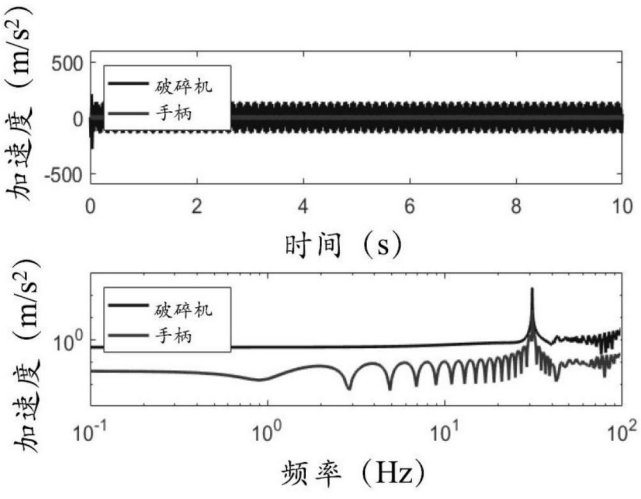

（a）2 *KN*输入力

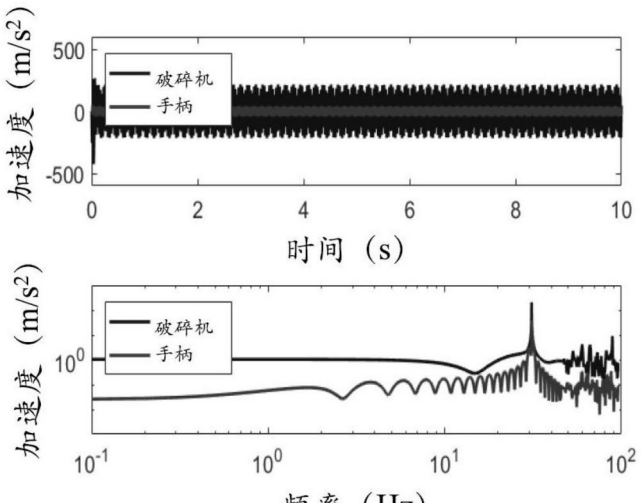

（b）6 *KN*输入力

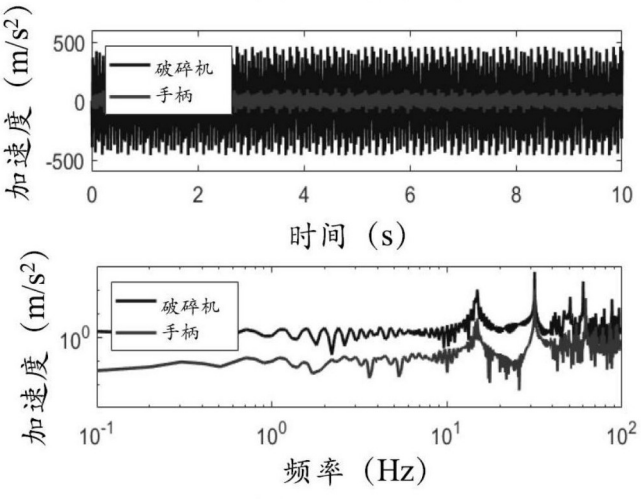

（c）10 *KN*输入力

图7

图8A

图8B

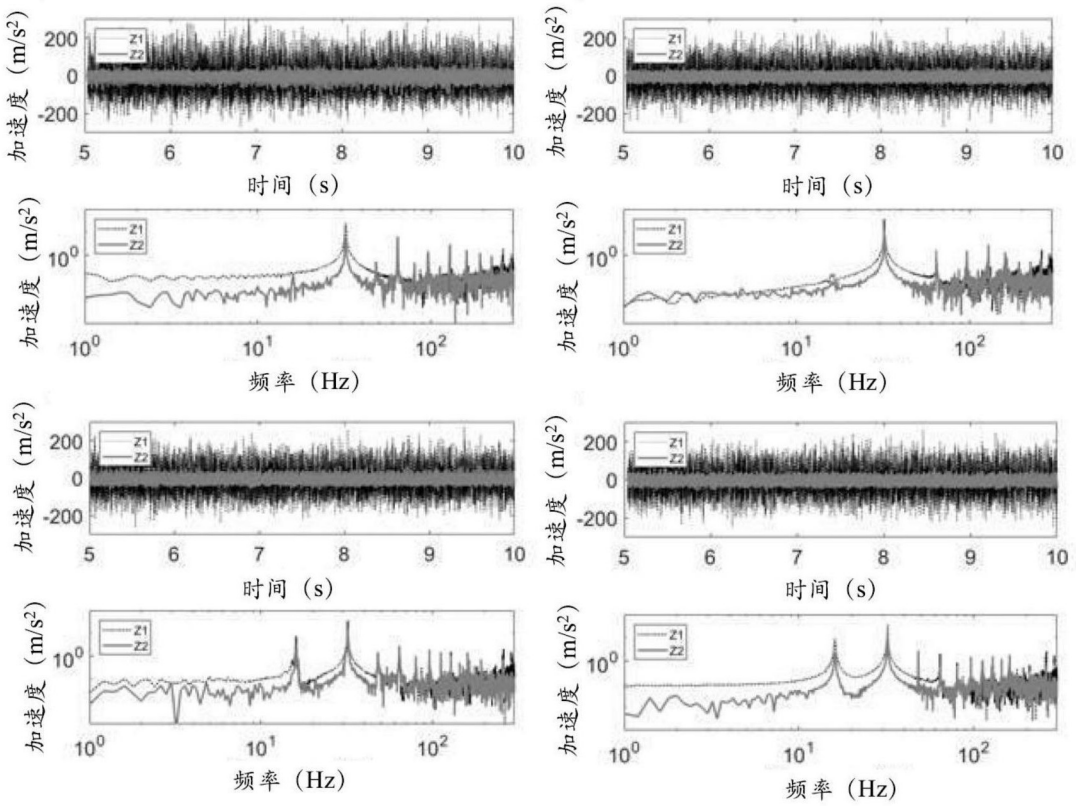

图9

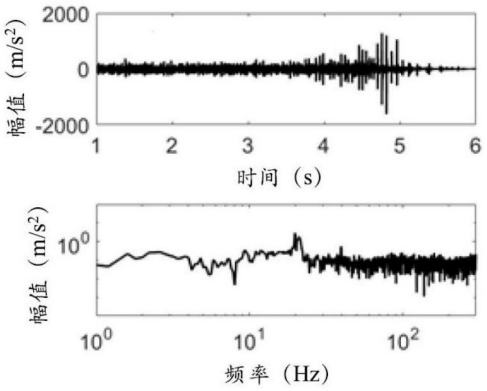

图10A

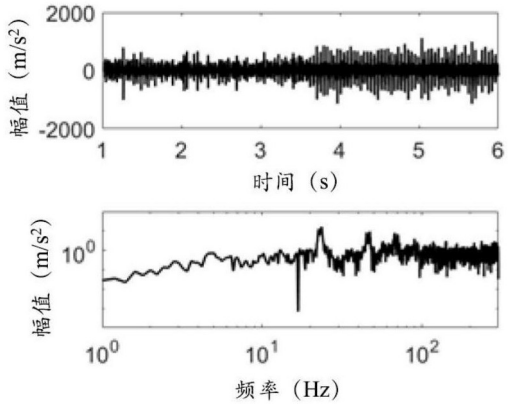

图10B

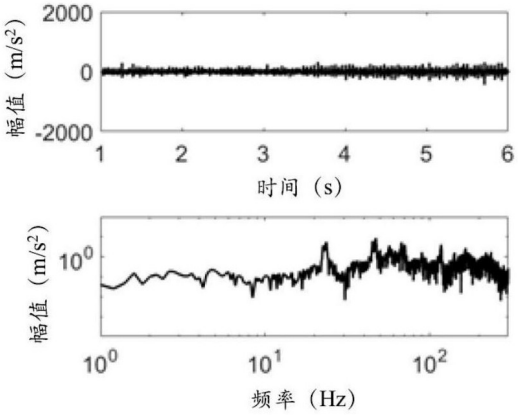

图10C

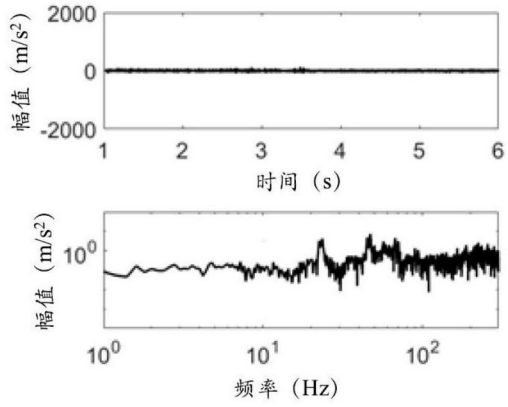

图10D

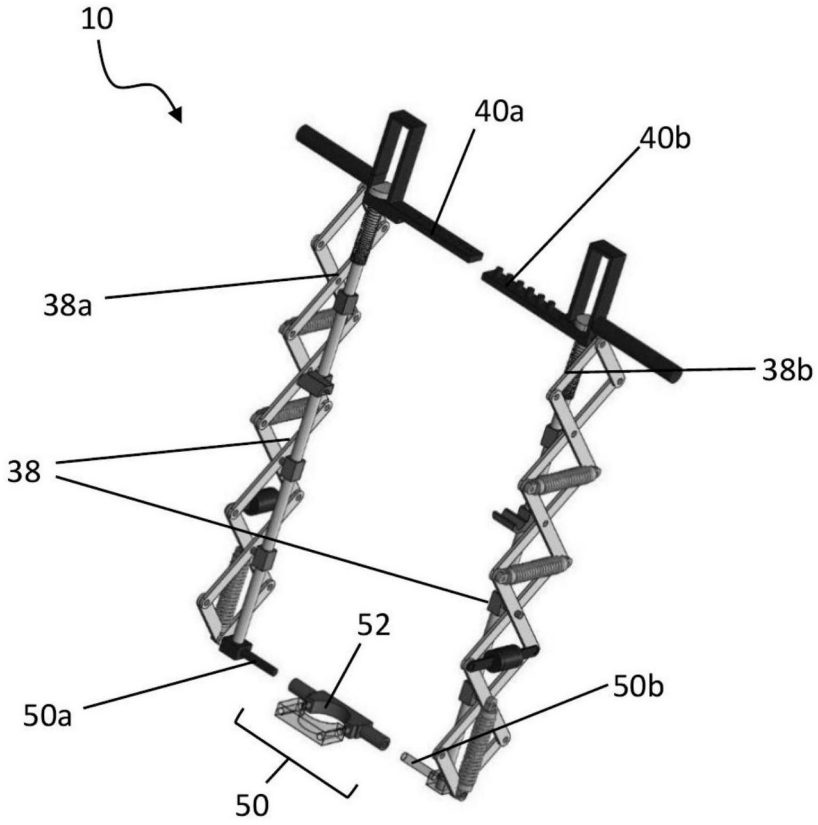
10
40a
40b
38a
38b
38
52
50a
50b
50

图11A

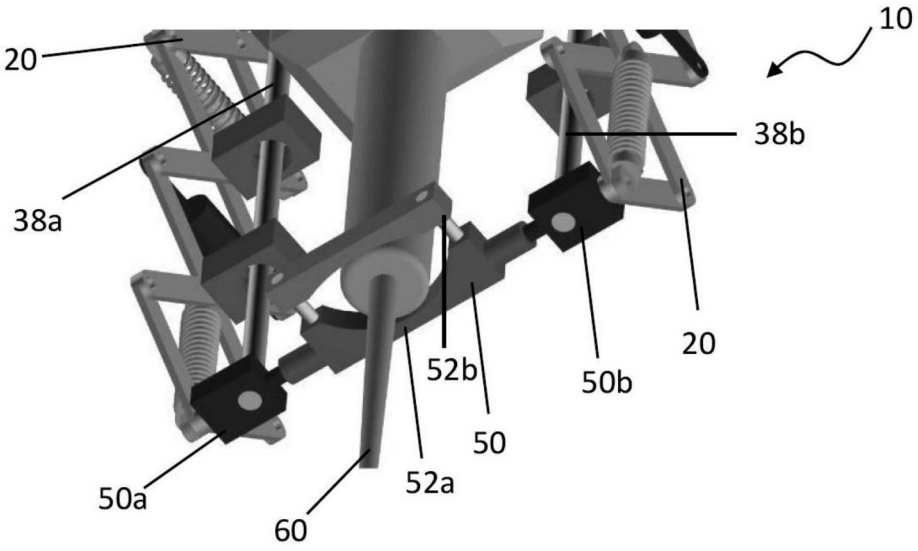
10
20
38b
38a
20
52b
50b
50
52a
50a
60

图11B

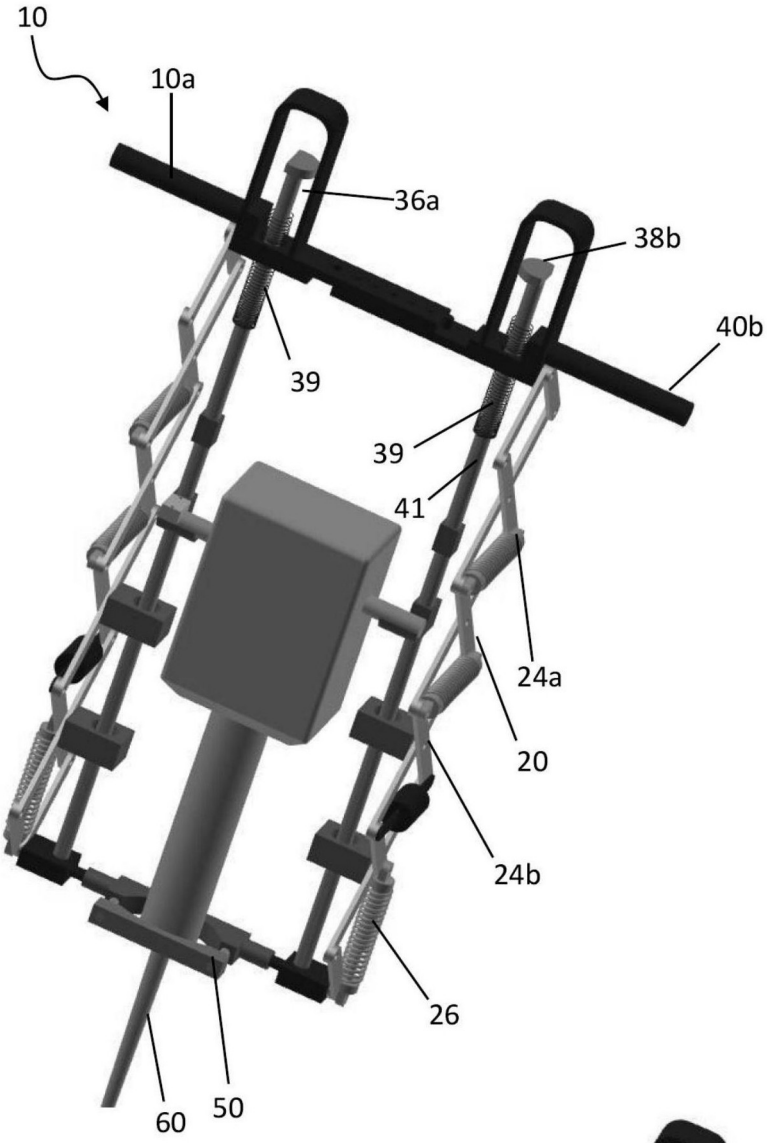

图 11C

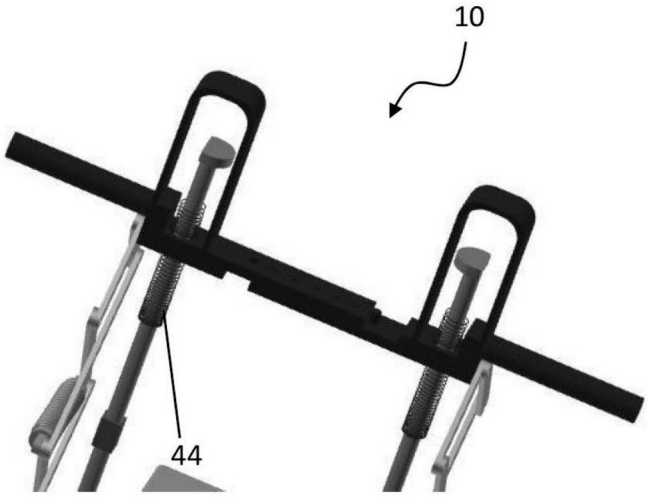

图 11D